

Alma Mater Studiorum – Università di Bologna

**DOTTORATO DI RICERCA IN
Scienze Biomediche e Neuromotorie**

Ciclo XXXII

Settore Concorsuale: 06/D6

Settore Scientifico Disciplinare: MED/26

**EFFECT OF HOST GENOTYPE AND PRION STRAIN ON THE
PHENOTYPIC HETEROGENEITY OF CREUTZFELDT-JAKOB DISEASE:
THE PERIPHERAL NERVOUS SYSTEM INVOLVEMENT AND THE
SPECTRUM OF THE GENETIC FORM**

Presentata da: Dott. Simone Baiardi

Coordinatore Dottorato

Prof. Pietro Cortelli

Supervisore

Prof. Piero Parchi

Esame finale anno 2019

INDEX

Introduction

1.1 Prion disease: general introduction.....	1
1.2 Brief overview of PrP ^C and PrP ^{Sc}	2
1.3 PrP ^C - PrP ^{Sc} conversion and in vitro amplification techniques.....	6
1.4 Phenotypic spectrum and classification of human disease subtypes.....	8
1.4.1 Sporadic CJD.....	8
1.4.2 Familial CJD.....	15
1.5 Prion strains.....	19
1.5.1 Strain M1.....	19
1.5.2 Strain V2.....	20
1.5.3 Other CJD strains: M2T, M2C and V1.....	20

List of PhD projects

Prion-related neuropathy in CJD

2.1 Background.....	23
2.2 Material and methods.....	23
2.2.1 Study population	23
2.2.2 Clinical and neurophysiological analysis.....	24
2.2.3 PrP investigation in peripheral nerves.....	25
2.2.4 Statistical analysis	26
2.3 Results.....	26
2.3.1 Clinical findings in the whole cohort.....	28
2.3.2 Neurophysiological findings.....	29
2.3.2 PrP ^{Sc} detection in peripheral nerve.....	30
2.4 Discussion.....	33

Phenotypic heterogeneity of genetic CJD

3.1 Background.....	35
3.2 Material and methods.....	35
3.2.1 Case selection and clinical data.....	35
3.2.2 Neuropathological analysis.....	36
3.2.3 Molecular genetic analysis.....	37
3.2.4 Protein studies.....	37
3.2.5 CJD classification.....	37
3.3 Results.....	39

Index

3.3.1 Demographic findings, age at onset and disease duration.....	39
3.3.2 Clinical findings.....	41
3.3.3 Neuropathological findings.....	47
3.3.4 PrP ^{Sc} typing.....	53
3.3.5 Mixed phenotypes in gCJD.....	54
3.4 Discussion.....	55
References.....	59

INTRODUCTION

1.1 Prion disease: general introduction

Prion diseases, also known as transmissible spongiform encephalopathies (TSEs) are invariably fatal neurodegenerative disorders of humans and other mammals, characterized by aggregation and tissue deposition of a structurally modified isoform of the prion protein (PrP). In this pathological process, the physiological cellular PrP (PrP^C) converts into abnormal, partially protease-resistant and aggregation-prone isoform, commonly identified as scrapie PrP (PrP^{Sc}) through posttranslational events leading to an increased β -sheet secondary conformation (Prusiner, 1998). Once formed, PrP^{Sc} replicates itself by a seeded-conversion mechanism where PrP^{Sc} binds PrP^C and mediates its conversion to PrP^{Sc}. Newly converted PrP^{Sc} then propagates and accumulates preferentially, but not exclusively, in the central nervous system (Caughey *et al.*, 2009).

Notably, aberrant protein folding leading to amyloid fibril formation does not exclusively involve prion disease, but it has been linked to a rapidly expanding list of pathologies, gathered together under the definition of protein misfolding neurodegenerative disorders. As a remarkable example, a similar prion-like seeded-polymerization mechanism is responsible for the formation of protein aggregates involving α -synuclein, amyloid-beta, tau and transactive response DNA binding protein 43 kDa (TDP-43) in Parkinson's disease, Alzheimer's disease, primary tauopathies and sporadic forms of amyotrophic lateral sclerosis (Walker and Jucker, 2015).

To date, prion disease uniquely includes disease subtypes proven to be transmissible from one individual to another by exposure to affected tissues via ingestion, injection or transplantation. Given the property to propagate after inoculation into susceptible hosts, the experimental transmission of human and animal prions led to the isolation and characterization of different prion strains, a term which has been borrowed from microbiology to underline the similarities between viral and prion (i.e. PRoteinaceous Infectious ONly particle) strains. These were initially defined as animal or human "isolates" that, after injection into syngeneic hosts, cause diseases with distinctive characteristics, such as the incubation period, the pattern of PrP^{Sc} distribution and regional severity of neuropathological changes (Bruce, 2003).

Results from experimental transmissions of the disease raised some questions about the use of the term TSEs. Indeed, not all prion disorders show spongiform change, while some forms do not genuinely propagate the disease from host-to-host but only transmit pathological changes (Rossi *et al.*, 2019a). Strictly speaking, these variants would better fit the definition of prion-like disorders (or prionoids), the terms currently used for transmissible but not-infectious neurodegenerative disorders characterized by protein misfolding, aggregation and seeded polymerization (e.g., synucleinopathies, tauopathies) (Scheckel and Aguzzi, 2018).

Although rare, prion disease includes a broad spectrum of clinicopathological phenotypes. Animal prion diseases include scrapie in sheep, bovine spongiform encephalopathy (BSE) in cattle, chronic wasting disease in cervids, transmissible mink encephalopathy, while more recently, a novel prion disease of camels has been recognized in Algeria (Babelhadj *et al.*, 2018; Houston and Andréoletti, 2019).

The clinicopathological spectrum of human prion disease is traditionally classified in three major disease groups, which include Creutzfeldt-Jakob disease (CJD), fatal insomnia (FI), Gerstmann-Sträussler-Scheinker disease (GSS), to which recently a fourth disorder, namely variably protease-sensitive prionopathy (VPSPr), has been added. Nevertheless, apart from FI, which truly represents a distinctive disease subtype linked to a specific prion strain, all the others represent heterogeneous groups, including multiple distinct disease phenotypes or subtypes.

Introduction

Human prion diseases can be also classified according to their etiology. More than 80% of all cases of prion disease occur as sporadic (or idiopathic) disease probably caused by spontaneous, unknown stochastic cellular events leading to PrP^C conversion into PrP^{Sc}. The genetic form (also called inherited or familial prion disease) is linked to mutations in the prion protein gene (*PRNP*), encoding for PrP^C, and accounts for about 10% of cases. Finally, the acquired form may originate from accidental human-to-human transmission as in iatrogenic CJD (iCJD) or ritual cannibalism as in kuru, or from ingestion or inoculation of BSE-derived prions as in variant CJD (vCJD) (Baiardi *et al.*, 2018c) (Table 1).

Table 1. Classification of human prion disease according to etiology.

Etiology	
<i>Sporadic / Idiopathic</i>	
Sporadic Creutzfeldt-Jakob disease	Unknown
Sporadic fatal insomnia	Unknown
Variably protease-sensitive prionopathy	Unknown
<i>Familial / Genetic</i>	
Familial Creutzfeldt-Jakob disease	Several <i>PRNP</i> mutations
Fatal familial insomnia	<i>PRNP</i> mutation p.D178N (129 Met)
Gerstmann-Sträussler-Scheinker disease	Several <i>PRNP</i> mutations
<i>Acquired</i>	
Iatrogenic Creutzfeldt-Jakob disease	Accidental prion transmission through treatment with prion-contaminated preparations of human growth hormone, dura mater and corneal grafts, surgical instrument
Kuru	Infection through ritualistic cannibalism in the Fore population in Papua New Guinea
Variant Creutzfeldt-Jakob disease	Oral exposure to food contaminated with material from bovine spongiform encephalopathy (BSE)-affected cattle

1.2 Brief overview of PrP^C and PrP^{Sc}

PrP^C is a cell surface protein encoded by *PRNP*, a highly conserved gene, which in humans is located on the short arm of chromosome 20. PrP^C is expressed in a variety of different organs and tissues, but with highest levels in the central nervous system where it is detected in most neural cell types, including neurons, astrocytes, and to a lesser extent in oligodendrocytes and microglia. Within the nervous system, PrP^C has also been found in the dorsal and ventral root ganglia of the spinal cord, sensory and motor axons, and Schwann cells (i.e. peripheral nervous system). Additionally PrP^C is expressed in the spleen, liver, heart, pancreas, bowel, kidneys and by cells of the immune system, including T lymphocytes, natural killer cells, and mast cells (Gill and Castle, 2018).

The physiological function of PrP^C is still largely unknown. Since transgenic mice devoid of PrP^C are resistant to scrapie infection (Büeler *et al.*, 1993), PrP^C confers predisposition to develop prion disease. Nevertheless, some sort of beneficial function is indirectly suggested by its marked evolutionary conservation (Wopfner *et al.*, 1999; Calzolari *et al.*, 2005). Moreover, *PRNP* is not particularly polymorphic, suggesting that PrP^C may have been under evolutionary

Introduction

pressure to resist changes to its sequence (Watts *et al.*, 2018). PrP^C function has been extensively studied in PrP knockout mice, showing some neuroprotective attributes against stress and myelin maintenance in peripheral nerves (Bremer *et al.*, 2010). Other possible functions include protection against oxidative stress, cellular differentiation, signal transduction, sleep regulation and maintenance of synaptic plasticity (Peggion *et al.*, 2017).

Human PrP^C is initially synthesized as a 253-aminoacid precursor and incorporates both N- and C-terminal signal peptides. This protein precursor is trimmed to a 209 amino acid fragment following the removal of N- and C-terminal peptides in the endoplasmic reticulum (Wulf *et al.*, 2017). Before being transported to the cell membrane, PrP^C undergoes the attachment of a glycosylphosphatidylinositol (GPI) moiety at the C-terminus, that mediates the tethering to the outer leaflet, and up to two N-linked glycans at position 181 and 197. Based on glycan site occupation, three main PrP isoforms can be distinguished: diglycosylated (i.e. the predominant PrP^C isoform), monoglycosylated and unglycosylated.

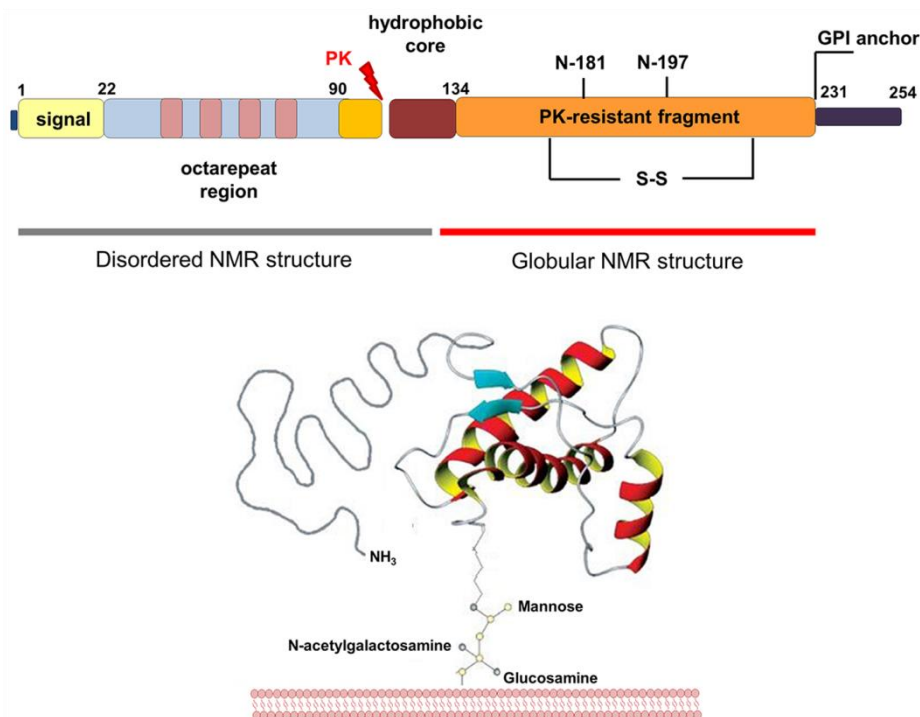


Figure 1. Structural features of PrP^C. Primary and tertiary structure as predicted by NMR spectroscopy.

The mature protein (residues 23–230/231 of the precursor protein) is composed of two major domains of similar size:

- the N-terminal intrinsically disordered domain;
- the globular domain that includes the flexible C-terminal region (229-230/231).

Moreover, between the N- and C-terminal domains the protein comprises a 20-residue trait of hydrophobic amino acids that is significantly conserved from fish to humans.

The N-terminal domain includes four highly conserved octapeptide (PHGGGWGQ) repeats and six histidines (H) with high affinity for divalent metal cations such as Cu²⁺ and Zn²⁺. This positively charged region has crucial relevance for the endocytosis of PrP^C.

The globular domain consists of three α -helices and two short β -strands; its tertiary structure is sustained mostly by non-covalent interactions, such as hydrogen bonds and hydrophobic interactions, between residues which are close during the folding process. As the only exception, a single disulfide bridge (covalent interaction) links the cysteine

Introduction

residues 179 and 214 (helices 2 and 3, respectively) (Capellari *et al.*, 2011). Finally, this region includes the above mentioned GPI anchor and the glycosylation sites at position Asn 181 and Asn 197. Notably, since each N-glycan can carry up to five negatively charged sialic acid residues, at physiological pH PrP^C molecules display a dramatic range of different electric charges, which contribute to PrP^C heterogeneity (Baskakov *et al.*, 2018).

PrP^{Sc} is the hallmark of prion disease and, therefore, its detection represents operatively a diagnostic marker for this group of disorders. Notably, according to Prusiner's "protein-only hypothesis" of prion propagation, it is widely believed that PrP^{Sc} itself is infectious and carries, within its conformation, all information necessary to initiate (i.e., propagate) prion disease when administered to naïve individuals (Prusiner, 1998).

As previously stated, PrP^{Sc} originates from PrP^C misfolding. In this process, the secondary structure of PrP^C shifts from a predominant α -helical conformation to a predominant β -sheet (from 3% up to 40%) structure in PrP^{Sc} (Caughey and Raymond, 1991; Safar *et al.*, 1993). This conformational change is associated with a modification of the physicochemical properties of the protein. In particular, at variance with PrP^C, PrP^{Sc} is partially resistant to protease digestion, insoluble in non-denaturing detergents, and prone to aggregation. As a consequence of these changes, PrP^{Sc} is also prone to deposits in the form of aggregates in diseased tissues (Prusiner, 1998).

Among these properties, the resistance to protease digestion has been largely used with diagnostic purposes. Indeed, while PrP^C is completely digested after treatment with proteinase K (PK), abnormal PrP^{Sc} can be unravelled by the presence of protease-resistant fragments at Western blotting. The latter ones originate from the C-terminal domain, while, on the contrary, the N-terminal region is completely degraded. Since the C-terminal domain includes the glycosylation sites, PK-resistant PrP^{Sc} in CJD comprises diglycosylated, monoglycosylated and unglycosylated forms, as shown by the typical 3-bands detected by Western blotting. Interestingly, while PrP^C tends to be primarily diglycosylated, PrP^{Sc} contains larger amounts of monoglycosylated and unglycosylated species. This observation has raised the hypothesis that the levels of N-glycan site occupancy may be involved in initiating the misfolding process and/or in defining strain-specific structures related to the disease phenotypes (Baskakov *et al.*, 2018).

Although PrP^{Sc} resistance to PK digestion represents the diagnostic hallmark of prion disease, some prion disorders are characterized by high sensitivity to protease digestion (e.g. GSS and VPSPr in human, Nor98 in sheep). In these disease variants, PrP^{Sc} is detectable only with modified Western blot protocols and through the use of very low concentrations of PK. Notably, even different subtypes within the same prion disorder may show variable proteolytic resistance as exemplified by the findings across the phenotypic spectrum of sCJD (Saverioni *et al.*, 2013).

Another controversial and largely unsolved issue concerns the so-called PK-sensitive form of PrP^{Sc} (sPrP^{Sc}), which has been defined as an isoform of PrP^{Sc} characterized by a degree of protease-resistance comparable to that of PrP^C (Safar *et al.*, 2005). sPrP^{Sc} has not been exclusively found in highly PK-sensitive prion diseases, but also coexists with PrP^{Sc} in typical prion disease (i.e. those biochemically defined by PrP^{Sc} detection after proteolytic digestion). Since a standardized test/protocol allowing the detection of sPrP^{Sc} does not exist, the application of various detection techniques in different studies led to the findings of variable sPrP^{Sc} levels ranging from 10% up to 80% (Safar *et al.*, 2005; Choi *et al.*, 2011; Saverioni *et al.*, 2013). A detailed report of these divergent results and their possible explanations can be found in Rossi *et al.*, 2019a.

The GPI anchor may play a role in the pathogenesis of prion diseases. Notably, transgenic mice expressing heterozygosity for PrP^C without a GPI anchor (GPI^{-/-}) do not succumb to prion disease after scrapie inoculation, but accumulate PrP^{Sc} as amyloid plaques, rather than the usual nonamyloid form of PrP^{Sc} (Chesebro *et al.*, 2005). Distinguishing anchored from anchorless forms of PrP^C has considerable relevance since they differ not only for structural features but also for biochemical and biological (e.g. toxicity, infectivity, etc.) properties, which are

Introduction

ultimately accountable for distinct phenotypes in human prion diseases. In vitro studies demonstrated that anchorless PrP is neither tethered to the cell membrane nor recycled within the endosomal compartment, but is secreted from the cells (Campana *et al.*, 2007). The development of experimental models based on transgenic mice expressing anchorless PrP^C promoted new interesting findings: following its extracellular secretion, anchorless PrP spreads through the drainage system either to the brain's interstitial fluid or to cerebral and peripheral perivascular areas (Chesebro *et al.*, 2010, Rangel *et al.*, 2013a, b), and accumulates in peripheral tissues such as spleen, muscle, kidney, eyes, pancreas, heart and bowel after scrapie infection (Trifilo *et al.*, 2006; Lee *et al.*, 2011). By using the same experimental model, toxicity and neuroinvasive potential were found to be reduced in mice expressing anchorless PrP compared to those expressing anchored PrP, suggesting that the GPI moiety may influence all these properties. Interestingly, scrapie infection failed to induce clinical disease in heterozygous GPI^{+/-} mice, while caused a slowly progressive fatal disease in homozygous GPI^{-/-} mice, which expressed two-fold more anchorless PrP, underpinning a dose-dependent pathogenic effect of anchorless PrP accumulation (Chesebro *et al.*, 2010). In both GPI^{+/-} and GPI^{-/-} mice, histopathology revealed amyloid PrP^{Sc} deposits, with preferential accumulation near or within the basement membranes of endothelial cells, smooth muscle cell and pericytes, without grey matter spongiform change which conversely is the hallmark of prion diseases in mice with anchored PrP (Chesebro *et al.*, 2005, 2010). Finally, mice overexpressing anchorless PrP^C develop a late onset neurologic dysfunction characterized by widespread deposition of short PrP^{Sc} fragment in the form of amyloid plaques, even in the absence of scrapie inoculation, indicating that the GPI moiety prevents the intrinsic propensity of PrP to form fibrillary aggregates (Stöhr *et al.*, 2011).

The mechanisms underpinning PrP^{Sc} neurotoxicity are largely unexplained. An important clue to this unsolved question is the observation that PrP^C knockout neurons are relatively resistant to the toxic effects of PrP^{Sc} (Brandner *et al.*, 1996; Mallucci *et al.*, 2003). This finding suggests that a critical neurotoxic signal is mediated by PrP^C and likely generated during the process by which endogenous cell-surface PrP^C is converted into PrP^{Sc}. Similarly, the attachment to the plasma membrane seems to be critical for PrP^C functioning/signalling, given that scrapie-infected GPI^{-/-} mice develop some neuropathological abnormalities (Chesebro *et al.*, 2005). Recently, experimental studies focused on early synaptic dysfunction in the pathogenesis of prion disorders. A model based on hippocampal neuronal culture to study the synaptotoxic effect of exposure to exogenous PrP^{Sc} demonstrated the early activation of NMDA and AMPA receptors, stimulation of p38 MAPK phosphorylation and collapse of the actin cytoskeleton in dendritic spines (Le *et al.*, 2019). Other studies, based on PrP^C manipulation in cellular and murine models, revealed that the toxic cellular effect of PrP is mediated by the flexible N-terminal domain through an intramolecular interaction with the C-terminal globular domain (Le *et al.*, 2019). Notably, while a large body of evidence indicates that the misfolded protein aggregates are the cause of the neurodegeneration, the role of intermediated structures, such as oligomers and fibrils, is still discussed (Caughey and Lansbury, 2003). On the one hand, evidence suggests that pre-fibrillary, oligomeric PrP is toxic for neurons (Simoneau *et al.*, 2007); on the other hand, fibrillary PrP is believed to have a protective role mediated by oligomer sequestration (Douglas *et al.*, 2008). Although apparently in contrast, it cannot be excluded that inert fibrils of certain morphologies can be detached from small, highly toxic oligomers, which are ultimately responsible for the cytotoxic effect. Finally, PrP^{Sc} toxicity could be mediated, at least partially, by microglial activation. Experimental evidence supports the idea of a dual role of microglia in prion disease pathogenesis. In the early disease stages, microglia has a protective role by increasing the phagocytosis of PrP^{Sc} aggregates, whereas during disease progression, both the accumulation of PrP^{Sc} and the neuronal damage contribute to switching microglia to a proinflammatory phenotype contributing to brain toxicity. In support of this hypothesis, early microglial cell activation and proliferation have been demonstrated in CJD brains along with a co-localization of microgliosis with PrP^{Sc} deposits (Franceschini *et*

Introduction

al., 2018). Moreover, pro- and anti-inflammatory cytokines, members of the complement system, regulatory proteins involved in microglial proliferation and key regulators of inflammation COX-1/2 and PGE₂, are all elevated in brains of CJD (Deininger *et al.*, 2003; Llorens *et al.*, 2014).

1.3 PrP^C- PrP^{Sc} conversion and in vitro amplification techniques

According to Prusiner's hypothesis, the basic molecular premise of prion disease pathogenesis is based on the assumption that PrP^{Sc} acts as a template upon which PrP^C misfolds, thereby setting the basis for the propagation of PrP^{Sc} structure (Prusiner, 1998). This hypothesis assumes that either a direct or indirect physical interaction between PrP^{Sc} and PrP^C is the prerequisite for conformational conversion and propagation of disease (Horiuchi and Caughey, 1999; Baron *et al.*, 2002). Lipid raft sited on the plasmatic membrane and/or intracellular vesicle, such as endosome, lysosome and endoplasmic reticulum, are critical structures for this interaction between the two isoforms (Poggiolini *et al.*, 2013). The process of PrP^C-PrP^{Sc} conversion provided the basis for the development of prion amplification techniques, such as the protein misfolding cyclic amplification assay (PMCA) and the real-time quaking-induced conversion (RT-QuIC) method, which mimic in vitro the process of PrP^{Sc} replication thought to occur in vivo. The application of these novel techniques led, on the one hand, to the successful detection of PrP^{Sc} in tissues and fluids containing a minute amount of the abnormal protein (e.g. blood, urine, cerebrospinal fluid), and on the other, to a better understanding of the molecular mechanisms of prion replication (Rossi *et al.*, 2019a). Experimental evidence demonstrated that the efficiency of in vitro PrP^C-PrP^{Sc} conversion (and likely of that occurring in vivo) is modulated (promoted and/or inhibited) by molecular cofactors. Among those acting as chaperones, lipids, nucleic acids, metals and polyanions have been implicated, although their precise mechanism of action remains unclear (Poggiolini *et al.*, 2013). Starting from Prusiner's theoretical model, two distinct molecular mechanisms for PrP^C-PrP^{Sc} conversion/propagation have been proposed (Aguzzi, 2001). The first postulates that the interconversion between PrP^C and PrP^{Sc} is separated by a large energy barrier and cannot take place spontaneously: an interaction between spontaneously generated or exogenously introduced PrP^{Sc} and endogenous PrP^C may induce directly its transformation into further PrP^{Sc} ("refolding" or template assistance model). The high energy barrier between the two isoforms prevents the spontaneous conversion of PrP^C into PrP^{Sc}. On the contrary, the second postulates that PrP^C and PrP^{Sc} are in a reversible thermodynamic equilibrium that is heavily in favor of the PrP^C conformation. In this condition, PrP^{Sc} monomers are highly unstable and cannot trigger a stable PrP^C misfolding, which instead may occur when several monomeric PrP^{Sc} molecules are assembled into a highly ordered seed ("seeding" or nucleation-polymerization model). In both models, the fragmentation of PrP^{Sc} aggregates increases the number of seeding nuclei, allowing the recruitment of further PrP^{Sc} monomers.

In human prion disease PrP^{Sc} may 1) originate from a rare, stochastic event (sporadic/idiopathic forms), 2) have an exogenous origin (acquired forms), 3) be favoured by genetic mutation conferring instability to PrP^C and increasing the misfolding opportunity.

Among the above mentioned in vitro amplification techniques, PMCA fosters PrP^{Sc} amplification through a series of alternating sonication and rest cycles which promote the fragmentation of prion aggregates and the emergence of new nucleation sites. Depending on the protocol, the PrP^C substrate is provided by normal brain or peripheral tissues homogenates (Soto *et al.*, 2005; Concha-Marambio *et al.*, 2016), plasma (Bougard *et al.*, 2016), human platelets (Jones *et al.*, 2007), cultured cells (Yokoyama *et al.*, 2011), or recombinant PrP (rPrP) (Atarashi *et al.*, 2007).

Introduction

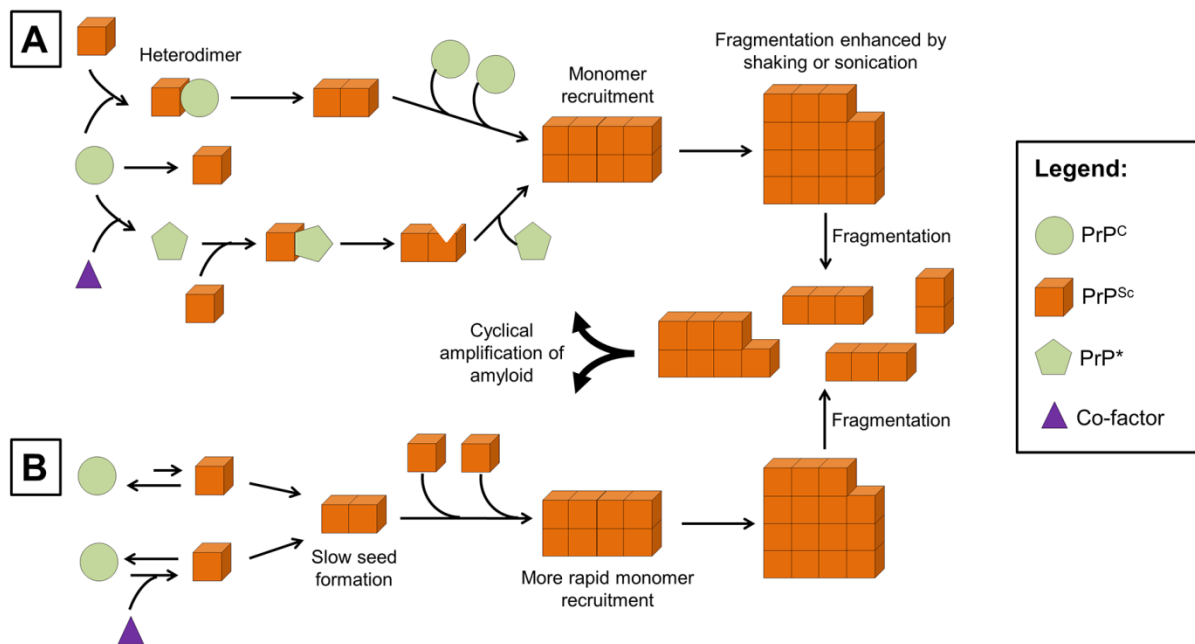


Figure 2. Models of PrP^C-PrP^{Sc} conversion and propagation. (A) "Refolding" or template assistance model. (B) "Seeding" or nucleation-polymerization model. PrP* represents an intermediate state (partial misfolding) between PrP^C and PrP^{Sc}.

At variance with PMCA, RT-QuIC exclusively uses rPrP as substrate and the sonication step is replaced by shaking at a relatively high temperature. Moreover, the reaction can be monitored in real time by including Thioflavin T (ThT) in the reaction which binds the aggregated PrP^{Sc} causing a change in the ThT emission spectrum.

RT-QuIC has ultimately gained more interest than PMCA as detection technique with diagnostic applicability since it is less affected by the potential drawbacks of PMCA such as the time taken, the complexity of the substrate and the reliance on sonication, which is difficult to standardize (Atarashi *et al.*, 2011). Accordingly, the application of RT-QuIC successfully provided a robust and reproducible assay with high sensitivity and specificity for the clinical diagnosis of CJD. Diagnostic RT-QuIC for CJD uses cerebrospinal fluid (CSF) or olfactory mucosa (OM) as seeds (Orrú *et al.*, 2014; McGuire *et al.*, 2016) and various sources of rPrP as substrate, the latter being the main factor affecting the diagnostic performance of RT-QuIC. As the most significant example in humans, the use of truncated (90-231) hamster rPrP instead of full-length (23-231) hamster rPrP, in the so-called second generation RT-QuIC, significantly improved the diagnostic sensitivity of the assay without affecting its specificity (Franceschini *et al.*, 2017). Results obtained in several laboratories with the first generation of this assay demonstrated a 79-86% sensitivity and a 99-100% specificity (Atarashi *et al.*, 2011; McGuire *et al.*, 2012; Cramm *et al.*, 2015; Lattanzio *et al.*, 2017), while the diagnostic sensitivity with the RT-QuIC of the second generation rose to 95-97% (Bongianni *et al.*, 2017; Foutz *et al.*, 2017; Franceschini *et al.*, 2017).

1.4 Phenotypic spectrum and classification of human disease subtypes

From a molecular standpoint, human prion diseases can be divided into two major groups according to the dominant PrP^{Sc} form that accumulates within the brain. In CJD and FI PrP^{Sc} accumulates as full-length or N-terminally truncated fragments retaining the GPI membrane anchor (also known as PrP27-30), while in GSS and other PrP-amyloidoses PrP^{Sc} mainly deposits in the extracellular space as unglycosylated anchorless fragments. The following paragraphs examine in-depth the phenotypical heterogeneity of sporadic and genetic prion disorders linked to PrP27-30, while acquired forms (variant and iatrogenic CJD, kuru) and GSS are not discussed further.

1.4.1 Sporadic CJD

Sporadic CJD (sCJD) is by far the most common human prion disease and is responsible for 85-90% of all CJD cases (Parchi *et al.*, 2011). Its estimated prevalence is of about 1.5 cases per million (Ladogana *et al.*, 2005b). The origin is unknown but it is thought to depend on a stochastic event inducing PrP^C conversion into PrP^{Sc}, although some environmental contribution cannot be definitely ruled out. The disease is clinically characterized by a progressive neurological syndrome usually with predominant dementia, ataxia and visual symptoms, and pathologically by a widespread brain deposition of PrP^{Sc} leading to spongiform change, microglial activation, synaptic and neuronal loss, and astrocytic gliosis of variable severity and regional distribution. In about 10% of cases, PrP-amyloid plaques are also present (Baiardi *et al.*, 2018c).

The current classification of sCJD subtypes is based on the convincing evidence of a very strong correlation between, on the one hand, the clinico-pathological phenotype and, on the other hand, genetic and molecular features. More specifically, sCJD phenotype is largely determined by the combination between the genotype at polymorphic *PRNP* codon 129 and the type of PrP^{Sc} accumulating in the affected tissues.

In the general population, *PRNP* codon 129 presents a methionine (ATG=M)/valine (GTG=V) polymorphism, leading to three possible combinations, that are homozygosity for methionine (MM) or valine (VV) and heterozygosity (MV). This polymorphism not only modulates the disease phenotype, but also determines the susceptibility to disease, being methionine homozygosity the most susceptible genotype to sCJD and heterozygosity the less susceptible (Palmer *et al.*, 1991; Laplanche *et al.*, 1994; Salvatore *et al.*, 1994; Windl *et al.*, 1996). In a large study representative of sCJD cases and controls from the USA and Europe the overall distribution showed a higher prevalence of MV (51%) followed by MM (37%) and VV (12%), whereas considering only the sCJD group 71.6% of patients were MM, 16.7% were VV and only 11.7% MV (Parchi *et al.*, 1999), indirectly suggesting that *PRNP* 129MM predispose to the development of disease.

In CJD, as well as FI, the proteolytic cleavage of PrP^{Sc} aggregates by PK generates two major core fragments, named types 1 and 2, and a variable amount of less represented shorter N-terminally truncated fragments. PrP^{Sc} type 1 primarily originates by PK cleavage at residue 82 and has a relative molecular mass of 21 kDa, while the type 2 has a molecular mass of 19 kDa and is primarily cleaved at residue 97 (Parchi *et al.*, 1997, 2000).

The combination between *PRNP* codon 129 and PrP^{Sc} is not entirely casual: indeed, PrP^{Sc} type 1 is preferentially found to be associated with methionine at codon 129 whereas the type 2 with valine. The possible combinations between host codon 129 genotype and PrP^{Sc} type specify the six sCJD clinicopathological subtypes recognized by current disease classification with only a few exceptions (Parchi *et al.*, 1999, 2009b, 2012) (Table 1).

Table 1. Distinctive clinical (early) and pathological features of sCJD subtypes.

Fr	Disease subtype	Mean age at onset, years (range)	Mean duration, months (range)	Common early clinical signs/symptoms	Regional pattern of distribution	Distinctive histopathological features
65%	MM(V)1 (typical CJD)	68 (31-86)	4 (1-24)	Cognitive or visual impairment, ataxia, psychiatric	Neocortex (especially in occipital lobe), striatum, thalamus, and cerebellum constantly affected	Small vacuoles and “synaptic type” PrP staining
15-20%	VV2 (ataxic/cerebellar variant)	64 (40-83)	6.5 (3-18)	Ataxia, diplopia	Prominent subcortical and cerebellar pathology, late cortical involvement (occipital lobe least affected)	Laminar intracortical distribution of spongiform change (i.e. predominant involvement of deep layers), plaque-like and perineuronal PrP staining
10%	MV2K (kuru-plaque variant)	65 (36-83)	17 (4-48)	Ataxia, cognitive impairment, extrapyramidal	Similar to VV2 with more consistent involvement of the cerebral cortex	Amyloid-kuru plaques in the cerebellum, and consistent plaque-like and focal PrP deposits
	MM2T (thalamic variant or sFI)	52 (26-71)	26 (7-96)	Ataxia, diplopia, psychiatric signs, sleep loss	Atrophy of the thalamus and inferior olive, patchy spongiosis limited to the cerebral cortex and limbic regions	
	MM2C (cortical variant)	64 (49-77)	16 (9-36)	Cognitive impairment	Spongiosis in all cortices with sparing of the cerebellum	Large confluent vacuoles and coarse/perivacuolar PrP staining
	VV1 (cortico-striatal variant)	44 (19-55)	21 (17-42)	Cognitive impairment	Severe pathology in the cerebral cortex and striatum with sparing of the brainstem nuclei and cerebellum	Intermediate vacuoles

Abbreviation: Fr=relative frequency

On the one hand, cases belonging to MM1 and MV1 groups have been merged into a single subtype MM(V)1 because of their striking similarities; on the other hand, the MM2 cases may belong to two subtypes with distinctive histopathological features and topographical distribution of lesions mainly affecting the cerebral cortex (MM2-Cortical or MM2C) or the thalamus (MM2-Thalamic or MM2T). Finally, the MV2 subtype characterized by amyloid plaques of the kuru type (most frequent) has nosologically been designated as MV2K to distinguish it from rare MV2C cases resembling MM2C. A further peculiarity of MV2 group is the association of PrP^{Sc} type 2 with a further fragment presenting an electrophoretic mobility of approximately 20 kDa intermediate molecular between types 1 and 2, and designated as PrP^{Sc} “i”. Consequently, in MV2 cases the profile of unglycosylated PrP^{Sc} isoforms appears as a “doublet” at Western blot.

Introduction

As stated above, different codon 129 genotype/PrP^{Sc} type combinations influence numerous variables including the age at onset, the clinical presentation, and disease duration, type of spongiform change, morphology of PrP^{Sc} aggregates and their topographic distribution within the brain (Table 1). Remarkably, from a clinical standpoint, the results of diagnostic investigations, such as cerebrospinal fluid biomarkers and PrP assays, electroencephalography and brain magnetic resonance imaging, may vary throughout the sCJD subtypes. Nevertheless, the current diagnostic criteria for sCJD updated in January 2017, have been developed irrespectively of subtype-specific differences (Table 2).

Table 2. Diagnostic criteria for sCJD (http://www.cjd.ed.ac.uk/sites/default/files/criteria_0.pdf).

<p><u>DEFINITE sCJD</u> Progressive neurological syndrome AND neuropathologically or immunocytochemically or biochemically confirmed</p> <p><u>PROBABLE sCJD</u> I + two of II + typical EEG [generalized periodic complexes]</p> <p>OR I + two of II + typical MRI [high signal in caudate/putamen or at least in two cortical regions (temporal, parietal, occipital) either on DWI or FLAIR]</p> <p>OR I + two of II + positive 14-3-3</p> <p>OR Progressive neurological syndrome + positive RT-QuIC in CSF or other tissues</p> <p><u>POSSIBLE sCJD</u> I + two of II + duration < 2 years</p>
<p>I. Rapidly progressive cognitive impairment</p> <p>II. (A) myoclonus, (B) visual or cerebellar problems, (C) pyramidal or extrapyramidal features, (D) akinetic mutism</p>

MM(V)1 subtype. It is the most frequent subtype (about 65% of all sCJD cases) and is characterized by a rapidly progressive neurological syndrome with prominent cognitive decline (2/3 of cases), ataxia (1/3 of cases), language difficulties, visual disturbances, myoclonus and other involuntary movements (i.e. typical sCJD phenotype) (Zerr and Parchi, 2018). Notably, a subgroup of MM(V)1 cases presents exclusively with visual symptoms of cortical origin, which have been related to an early and quite selective involvement of the occipital lobe (Heidenhain variant) (Baiardi *et al.*, 2016). Among sCJD subtypes, the shortest disease duration (mean 4 months, range 1-24). Pathologically, MM(V)1 is characterized by spongiform change with small (2–10 mm) round to oval vacuoles, predominantly located in the neuropil and distributed throughout the cerebral cortices, basal ganglia, thalamus and molecular layer of cerebellum, while hippocampus and brainstem appear largely spared. Immunocytochemistry for PrP shows a “synaptic” pattern of deposition (Parchi *et al.*, 1999). MM(V)1 is also associated with the higher occurrence of periodic sharp-waves complexes (PSWCs) among sCJD subtypes (70-75% of cases (Collins *et al.*, 2006; Franceschini *et al.*, 2017)). Brain magnetic resonance imaging (MRI) shows typical signal hyperintensities in fluid attenuated inversion recovery and/or diffusion weighted sequences in 82.8% of cases, while CSF 14-3-3 protein is positive in 95.3% of case and total

Introduction

(t)-tau protein levels are >1250 pg/ml in 95.2% of cases (Franceschini *et al.*, 2017). Prion detection through RT-QuIC has good sensitivity with both first generation assays using full-length (23-231) hamster recombinant PrP (82.5%) and second generation ones using truncated 90-231 hamster recombinant PrP (96.8%) (Parchi's lab, unpublished data).

VV2 subtype. It is the second most frequent subtype. It is clinically characterized by a predominant cerebellar/brainstem involvement and “ascending” progression of histopathological changes from subcortical areas to the cerebral cortex (Baiardi *et al.*, 2017). The disease usually presents with unsteadiness of gait and in a minority of cases with oculomotor disturbances, behavioral changes, isolated memory loss, but not dementia (Baiardi *et al.*, 2017). The disease duration is slightly longer than in the MM(V)1 subtype (mean 6 months, range 3-18). Pathologically, the VV2 subtype is characterized by spongiform change in the grey matter of limbic structures, striatum, thalamus, hypothalamus, cerebellum, and brainstem, whereas the neocortex is relatively spared, especially in cases with a rapid course. Typically, spongiosis in the cerebral cortex involves only the deep layers (i.e. laminar pattern). Immunostaining for PrP is characterized by focal plaque-like deposits and “perineuronal” immunoreactivity, that is a strong reaction around neuronal perikarya (Parchi *et al.*, 1999, 2012). Among diagnostic investigations brain MRI and CSF surrogate biomarkers of neurodegeneration 14-3-3 and t-tau have a sensitivity of 87.5%, 100.0% and 100.0% respectively (Franceschini *et al.*, 2017). Both first and second generation RT-QuIC assays have an optimal sensitivity (94.7% and 100% respectively) (Parchi's lab, unpublished data). On the contrary, PSWCs are detectable on electroencephalography only in 13.3% of cases (Franceschini *et al.*, 2017), mostly in late disease stages (Baiardi *et al.*, 2017).

MV2K subtype. This subtype accounts for about 10% of sCJD cases and is characterized by a longer duration than the previously described subtypes (mean 17 months, range 4-48). Despite some striking pathologic and molecular similarities with VV2, this subtype may present either with dementia (50% of cases) or ataxia or extrapyramidal signs (Zerr and Parchi, 2018). The histopathological hallmark of MV2K is the presence of PrP^{Sc} deposits in the form of cerebellar amyloid-kuru plaques. PrP^{Sc} accumulates also as plaque-like deposits (Parchi *et al.*, 1999). Together with the slow progression rate that clinically differentiates the MV2K phenotype from “typical” sCJD, the suboptimal sensitivity of some diagnostic investigations complicates the diagnosis of sCJD in vivo. Indeed, electroencephalography presents the typical PSWCs only in 13.0% of cases, and CSF 14-3-3 protein is positive only in 56.0%, while CSF-t-tau levels are increased >1250 pg/ml in 79.2% of cases (Franceschini *et al.*, 2017). First generation RT-QuIC assay shows also a poor sensitivity (75.0%), which has significantly increased up to 100.0% by second generation ones (Parchi's lab, unpublished data). Brain MRI also discloses a good diagnostic performance in this subtype (sensitivity = 87.5%) (Franceschini *et al.*, 2017).

MM2C subtype. The cortical variant of MM2 subtype is characterized by a relatively long duration (mean 16 months, 9-36) and clinically by progressive impairment of higher cognitive functions, mimicking other most common forms of dementia such as Alzheimer's disease. Spongiform change determined by large and confluent vacuoles is predominantly localized in cerebral cortices, followed by basal ganglia and thalamus. Cerebellum and limbic structures are largely spared, except for cases with very long duration. Coarse PrP^{Sc} deposits are localized at the rim of the vacuoles (i.e. “perivacuolar” pattern) (Parchi *et al.*, 1999, 2012). PSWCs are detected on electroencephalography only in 33.3% of cases, and CSF 14-3-3 and t-tau (>1250 pg/ml) proteins are positive in 25% and 28.6% (Franceschini *et al.*, 2017). Brain MRI shows typical abnormalities in 87.5% of cases (Franceschini *et al.*, 2017). CSF prion RT-QuIC has a sensitivity of 75.0% and 100.0% using first and second generation assays (Parchi's lab, unpublished data).

MM2T subtype. It is also known as the sporadic form of FFI and to date about 50 cases have been reported worldwide. In a large European cohort the mean age of onset was 43 years and the mean disease duration 30 months (Abu-Rumeileh *et al.*, 2018). Interestingly, at variance with most neurodegenerative disorders occurring in both

Introduction

sporadic and genetic forms, sCJD MM2T patients are younger than the FFI ones. Early clinical findings include a various combination of psychiatric symptoms, oculomotor and sleep disturbances. The latter include severe reduction of total sleep time and/or disorganized sleep with loss of physiological sleep figures. Less frequently cognitive impairment and postural instability are observed in early disease stages. Notably, at variance with FFI, the autonomic failure is not a prominent feature of sCJD MM2T. The clinical investigations included in the diagnostic criteria (EEG, MRI, CSF surrogate biomarkers of neurodegeneration) are often unravelling. In a small number of cases tested, prion CSF RT-QuIC assay showed a sensitivity of 60% (Abu-Rumeileh *et al.*, 2018). Fluorodeoxyglucose positron emission tomography reveals severe thalamic hypometabolism in about 70% of cases (Abu-Rumeileh *et al.*, 2018). Pathologically, the mediodorsal and anterior nuclei of the thalamus, and the inferior olivary nuclei are constantly affected by neuronal loss and gliosis but not spongiosis (Parchi *et al.*, 1999). Mild to moderate patchy spongiform change may be observed in the cerebral cortex. Striatum and hippocampus are usually spared, although the former may present spongiform change in the cases of longest course (Abu-Rumeileh *et al.*, 2018). PrP immunohistochemistry is characterized by patchy deposits of synaptic or small granular type mostly in the superficial layer of the cerebral cortex (Parchi *et al.*, 1999).

VV1 subtype. It is a rare subtype (~1 of all sCJD cases). With the only exception of MM2T, this subtype occurs in younger subjects (mean age at onset 44 years, range 19-55) in comparison with the most frequent ones. The mean disease duration is 21.0 months. The clinical onset is usually dominated by cognitive and psychiatric symptoms at onset, while parkinsonism and cerebellar signs appear during the disease course (Zerr and Parchi, 2018). Neuropathological change affects mainly the cerebral cortices (frontal and temporal lobes more than occipital lobe) and the basal ganglia, from which the definition con “cortico-striatal” variant, while the cerebellum is generally spared. Immunostaining for PrP discloses faint punctate/synaptic deposits (Parchi *et al.*, 1999) (Figure 3).

Beside the typical presentations described above for each subtype, a number of other “unusual” clinical manifestations may characterize the early stages of the disease (Table 3). Unusual presentations include not only the rare symptoms, but also typical symptoms when they occur isolated such as visual disturbances in the Heidenhain variant of CJD (Baiardi *et al.*, 2018a) or with abrupt appearance such as the stroke like-presentation. Interestingly, they are sometimes exclusively or predominantly associated with a specific subtype. The recognition of these atypical presentations has clinical relevance because of the diagnostic challenge which may ultimately lead to possible diagnostic delay. Moreover, according to the updated diagnostic criteria, even a single dysfunctional neurologic domain associated with a positive prion RT-QuIC result is sufficient for the diagnosis of probable sCJD, overcoming the need of full blown neurologic manifestations of the previous criteria (‘WHO | WHO infection control guidelines for transmissible spongiform encephalopathies. Report of a WHO consultation, Geneva, Switzerland, 23-26 March 1999’, n.d.; Zerr *et al.*, 2009).

Table 3. Main clinical features of unusual presentations and relation with CJD subtypes.

Onset	Main clinical features	sCJD subtype
<i>Visual</i>	Reduced visual acuity, blurred vision, spatial/form/color misperception, alexia, visual field restriction, visual agnosia	MM(V)1, MM2C (rare)
<i>Auditory</i>	Hearing loss variably associated to tinnitus, gurgling noises, aural fullness	Unknown
<i>Seizures</i>	Epilepsia partialis continua, focal or generalized non-convulsive status epilepticus	MM(V)1
<i>Psychiatric</i>	Psychosis, mood disorder	MM(V)1, MV2K, VV2 (rare)
<i>Corticobasal syndrome</i>	Alien limb, focal dystonia, unilateral myoclonus and hyperreflexia, cortical sensory loss	MM(V)1, MV2K
<i>PSP-syndrome</i>	Vertical gaze palsy, falls, axial rigidity, global bradykinesia	MM2T, MM2C, VV2
<i>Pseudobulbar palsy</i>	Dysarthria, dysphagia, labile affect	MM(V)1
<i>Involuntary movements</i>	Dystonia, blepharospasm, myoclonus, chorea (often unilateral)	MM(V)1
<i>Neuropathy</i>	Walking difficulties, numbness and tingling of limb extremities	MV2K, VV2
<i>Aphasia</i>	Difficulty in naming, reduced verbal fluency, paraphasias, word recall deficit, agrammatism	MM(V)1, MM2C, MV2K
<i>Stroke-like</i>	Visual field deficit, unilateral paresis, aphasia	MM(V)1

Finally, an intriguing and mostly unexplained event, which is likely relevant for the understanding of pathogenesis of prion diseases, is the co-occurrence of PrP^{Sc} types 1 and 2 in about 35% of sCJD cases (Parchi *et al.*, 2009b). Although the co-occurrence of PrP^{Sc} types 1 and 2 characterizes all codon 129 genotypes, the two abnormal PrP^{Sc} isoforms coexist more frequently in MM (43%) than in MV (23%) or VV (15%) subjects (Parchi *et al.*, 2009b). More rarely, mixed phenotypes are characterized by the coexistence of subtypes linked to the same PrP^{Sc} type (e.g., MV2K+2C). Moreover, the co-occurrence of subtypes linked to the same PrP^{Sc} type only affects subjects carrying MM (MM2T+2C) or MV (MV2K+2C). In these “mixed” subtypes, the pathological features are the same described for the “pure” subtypes but with a predominance of the traits reflecting the most prevalent PrP^{Sc} type in the brain (Parchi *et al.*, 2009b). Interestingly, the association between CJD subtypes in mixed phenotypes is not random, but seems to follow some rules as demonstrated by the fact that certain subtype combinations have never been observed and from a quantitative standpoint VV2, MV2K and MM2T subtypes contribute invariably to the mixed phenotype as “dominant” subtypes, VV1 as “not-dominant” subtype, while MM(V)1 and MM2C can manifest either as dominant or “not-dominant” subtypes.

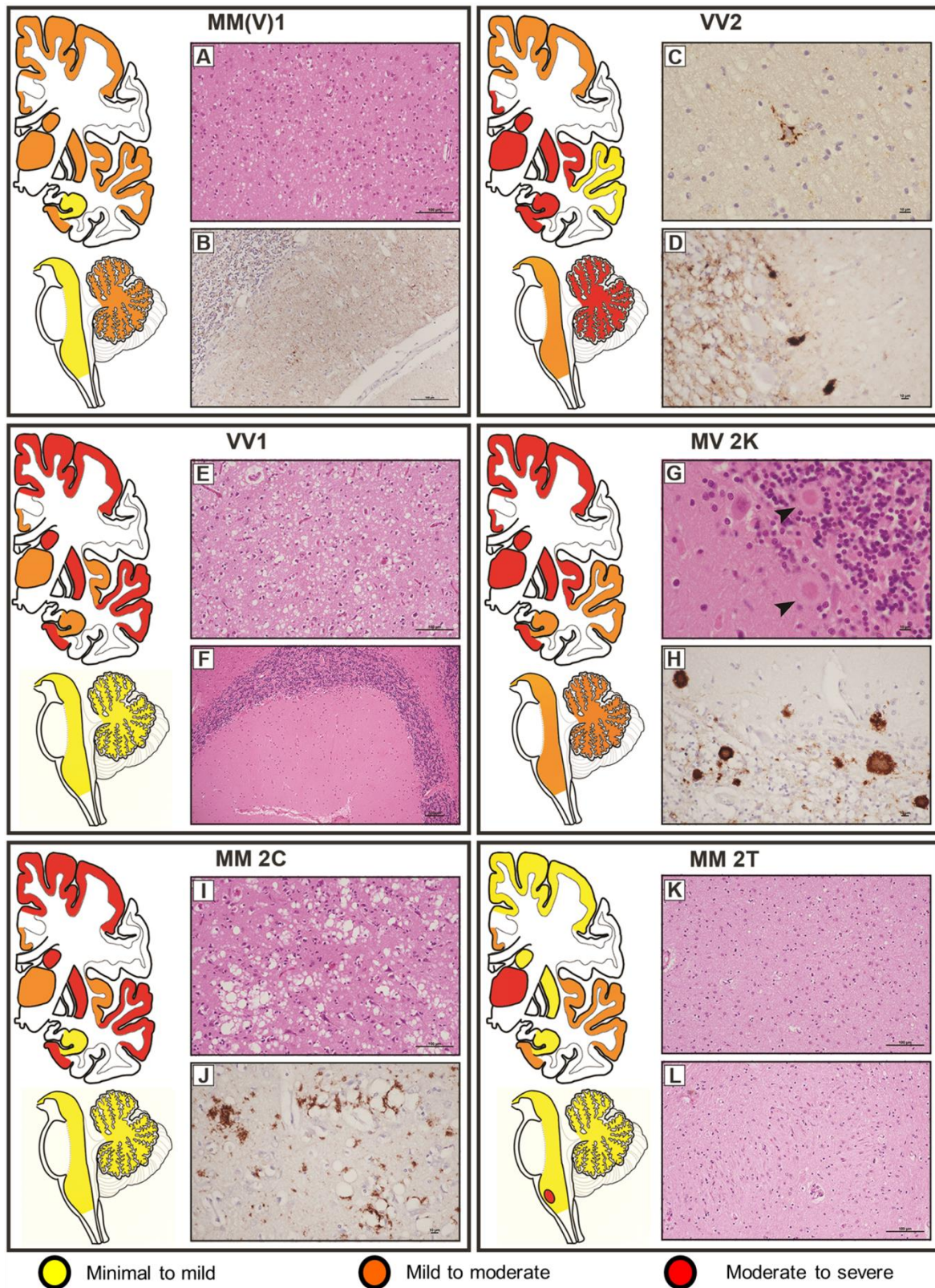


Figure 3. Lesion profiles and histopathological hallmarks of sporadic Creutzfeldt-Jakob subtypes.

Analyzed brain regions have been highlighted in yellow, orange and red according to the degree of neuropathological change. Distinctive histopathological features of sCJD subtypes. (A) Spongiform change characterized by small, fine, microvacuoles in the neuropil, and (B) synaptic pattern of PrP^{Sc} deposition in the molecular and granular layers of the cerebellum in sCJD MM(V)1. PrP staining is punctate and diffuse in the molecular layer, while it stands out the cerebellar glomeruli in the granular cell layers. (C) Perineuronal PrP staining in deep layers of the frontal cortex and (D) plaque-like PrP^{Sc} deposits at the transition between the molecular and the granular cell layers of the cerebellum in sCJD VV2. (E) Spongiform change

Introduction

characterized by non-confluent vacuoles of “intermediate” size, relatively larger than those observed in sCJD MM(V)1, but overall smaller than those of sCJD MM2C, in the occipital cortex, and (F) Minimal/mild pathological changes in the cerebellum of sCJD VV1. (G, H) Unicentric kuru amyloid plaques at the transition between the molecular and the granular cell layers of the cerebellum in sCJD MV2K. (I) Spongiform change characterized by large, confluent vacuoles and (J) coarse, dense PrP^{Sc} deposits with perivacuolar distribution in the temporal cortex of sCJD MM2C. (K, L) Severe neuronal loss and reactive gliosis in the absence of significant spongiform change in the medial-dorsal thalamic nucleus (K) and inferior olive (L) of sCJD MM2T. Legend: H&E, hematoxylin and eosin stain (A, E-G, I, K, L); IHC, PrP immunohistochemistry with primary Ab 3F4 (B-D, H, J). Magnification: x100, F, x200, A, I, K, L; x400, B, D, H, J; x600, C, G. Adapted from (Baiardi *et al.*, 2018c).

1.4.2 Familial CJD

About 10% of CJD cases occurs in an inherited, often familial, form linked to pathogenic mutations in *PRNP*, however, given the increasing number of cases suspected to have sCJD (i.e. absence of positive familial history) in which *PRNP* variants were identified, the term genetic CJD (gCJD) is preferred instead of familial CJD (Kovács *et al.*, 2005). Genetic CJD forms are inherited with an autosomal dominant pattern with variable penetrance. The *PRNP* mutations associated with gCJD consist of point mutations or insertion of octapeptide repeats (OPRIs) in the N-terminal region (Capellari *et al.*, 2011).

Epidemiology of gCJD reveals a variable incidence from country to country (Ladogana *et al.*, 2005a), which depends either on the different genetic background or on the specific *PRNP* mutations. The former explains the different distribution of some variants between Caucasian and East Asian races (Jeong and Kim, 2014), while the latter account for the founder effect associated with some mutations (e.g. E200K) (Lee *et al.*, 1999; Colombo, 2000). In Italy, the overall incidence of CJD cases is higher than that calculated worldwide because of the occurrence of two genetic clusters linked to E200K and V210I mutations (D’Alessandro *et al.*, 1998, Ladogana *et al.*, 2005b). Other geographical or ethnic clusters regarding the E200K and D178N variants have been found in Israel, Slovakia, Chile and Spain (Chapman *et al.*, 1994; Mitrová and Belay, 2002; Rodríguez-Martínez *et al.*, 2005).

For surveillance purposes, genetic TSE (including gCJD) are classified as “definite” when a patient with definite TSE has either a first degree relative with probable/definite TSE or a pathogenic *PRNP* mutation (http://www.cjd.ed.ac.uk/sites/default/files/criteria_0.pdf). The *PRNP* mutations associated with CJD neuropathological phenotype are the following: D178N-129V, V180I, V180I+M232R, T183A, T188A, E196K, E200K, V203I, R208H, V210I, E211Q, M232R, 4 OPRIs, 5 OPRIs, 6 OPRIs, 2 OPRs deletion. “Probable” genetic TSE is defined by the presence of a progressive neuropsychiatric disorder associated with either a first degree relative with probable/definite TSE or a pathogenic *PRNP* mutation.

Similarly to the sporadic form, gCJD shows remarkable phenotypic heterogeneity which is only in part explained by the variety of *PRNP* mutations. Indeed, different genetic variants have been found with a similar clinical and pathological phenotype, while different phenotypes can be observed in patients carrying the same mutation. Evidence indicates that the polymorphism at *PRNP* codon 129 influences both the susceptibility to develop the disease and its phenotypic expression. However, at variance with sCJD, in gCJD it mainly acts in *cis* with the mutation, while its role in the normal allele is less significant or even absent. The most striking evidence of codon 129 effect on phenotypic variability is the mutation D178N which is associated with two different prion disorders depending on whether the mutation co-segregates with methionine (FFI) or valine (gCJD) (Goldfarb *et al.*, 1992b). From a clinical standpoint, it is fundamental defining the 129 genotype in *cis* with the mutation to characterize subjects carrying D178N and

Introduction

heterozygosity methionine/valine at codon 129 which, despite the apparent similar genetic background, present with divergent clinico-pathological phenotypes. Therefore, in gCJD it is more appropriate to identify each disease-associated *PRNP* genotype through the haplotype, which is given by the combination of the mutation and the amino acid present at codon 129 in the mutant allele (e.g. D178N-129M or D178N-129V) (Capellari *et al.*, 2011). The increased susceptibility to develop the disease is indirectly suggested by the younger age of clinical onset observed in some cases, especially carrying mutations in *cis* with M at codon 129 (Ladogana and Kovacs, 2018).

Depending on the *PRNP* mutation, the conversion of PrP into the pathological isoform PrP^{Sc} may be limited to the mutant allele (e.g. D178N-129M, D178N-129V, E200K-129M, E200K-129V) or involve both the mutant and the normal allele (e.g. V210I-129M, R208H-129M, OPRI-129M) (Capellari *et al.*, 2011). In vitro models indicate that most *PRNP* mutations act primarily disrupting the metabolism and the trafficking of the mutant PrP allele. Structural alterations include changes of the affinity to bond ions (OPRIs), surface charges (E200K), disruption of hydrogen bonds (D178N, T183A) and salt bridges (R208H), abnormal folding (V180I, V210I) and stability of β -sheets (D178N) (Capellari *et al.*, 2011). The most frequent biochemical modifications associated with the *PRNP* mutation are increased insolubility in detergents and resistance to PK digestion and modification in the glycosylation pattern (see below).

Similarly to sCJD, PrP²⁷⁻³⁰ accumulates also within the brain of gCJD patients in the form of PrP^{Sc} type 1 and 2. Nevertheless, in contrast to the uniform glycosylation pattern characterizing sCJD cases in which the monoglycosylated isoform is predominant, different glycoform ratios have been observed in gCJD. Notably, the glycosylation pattern seems to be influenced mostly by the mutation regardless of the PrP^{Sc} type and the codon 129 genotype. According to the glycoform ratio, *PRNP* mutations may be divided into three major groups:

- I. Predominance of the monoglycosylated isoform (= sCJD): G114V, R148H, T188K, R208H, V210I, and OPRI.
- II. Predominance of the diglycosylated isoform and marked underrepresentation of the unglycosylated one: D178N and E200K.
- III. Marked underrepresentation (G114V, T183A) or lack of the diglycosylated isoform (V180I).

As stated above, for some of these mutations of the first group (e.g. V210I, R208H and OPRI) the PrP^{Sc} derives from the conversion of the normal allele and, therefore, the effect of the mutation on the glycosylation might be masked. The mutations belonging to the second group act destabilizing the mutant PrP allele which is retained, especially the unglycosylated isoform, in the intracellular compartment being less available to pathological conversion (Capellari *et al.*, 2000a). In the third group, the 183 mutant residue (T183A) affects the first N-glycosylation site of PrP^C (Capellari *et al.*, 2000b), while on the contrary the analysis of V180I-PrP^C in Chinese hamster ovary cells reveals a normal diglycosylated isoform (Chasseigneaux *et al.*, 2006).

Literature data on the clinical and pathological features of gCJD according to *PRNP* haplotype analysed in the experimental dissertation are summarized in the Table 4.

Introduction

Table 4. Clinical and pathological phenotypes of gCJD according to *PRNP* haplotype.

<i>PRNP</i> haplotype	Age at onset, range (years)	Disease duration, range (months)	Clinical phenotype	EEG PSWCs	CSF 14-3-3 protein	Typical brain MRI	Pathological phenotype
R148H-129M	53-82	2-18	Similar to sCJD MM(V)1 in codon 129 MM and to sCJD MV2K in codon 129MV. Symptoms: gait impairment, rapid cognitive deterioration, psychiatric, myoclonus.	1/3	1/3	2/3	Similar to MM(V)1 or MV2K. The latter case shows cerebellar kuru plaques.
D178N-129V	26-73	2-51	Similar to sCJD VV1. Symptoms: in early stage cognitive and behavioural/psychiatric; later myoclonus, cerebellar, extrapyramidal, pyramidal, visual (rare).	7/53	8/14	7/10	Most cases similar to VV1 with predominant involvement of cerebral cortex and basal ganglia, and relative sparing of cerebellum and brainstem. Panencephalopathic phenotype in 1 case.
T183A-129M	37-49	24-108	Onset with behavioural disturbances and memory deficit. Later dementia, parkinsonism.	0/7	0/1	0/2	Most significant involvement of cerebral cortex and basal ganglia. Plaque-like PrP deposits in putamen, synaptic in cerebellum.
T188K-129M	40-80	2-13	Similar to sCJD MM(V)1. Symptoms: dementia, ataxia, myoclonus, pyramidal, extrapyramidal, visual.	5/17	14/18	12/19	Similar to sCJD MM(V)1 (only 1 autopsy).
E196K-129M	64-80	2-18	Onset with psychiatric and cognitive symptoms. Later myoclonus, cerebellar, pyramidal, extrapyramidal.	1/10	9/10	4/7	Similar to sCJD MM(V)1 (only 3 autopsy).
E196K-129V	65, 71	3.5, 9	Psychiatric, cerebellar at onset. Later pyramidal, extrapyramidal, myoclonus.	0/2	2/2	0/1	Similar to sCJD VV2.

Continued

Introduction

Continued

E200K-129M	31-84	1-111	Similar to sCJD MM(V)1. Atypical presentations: peripheral neuropathy, supranuclear gaze palsy, sleep disturbance, corticobasal syndrome.	232/308	273/320	115/160	Similar to MM(V)1 . Granular “dense” PrP deposits in the molecular layer of cerebellum in many cases.
E200K-129V	67-67	3.5-6	Early ataxia, rapidly progressive dementia, late appearance of myoclonus.	-	4/4	-	Similar to VV2. The MV cases do not show kuru plaques.
V203I-129M	48-80	1-52	Similar to sCJD MM(V)1.	11/13	11/11	8/8	Synaptic, somatosynaptic and perineuronal PrP deposits.
R208H-129M	45-74	2-28	Similar to sCJD MM(V)1.	7/11	5/9	4/9	Similar to sCJD MM(V)1.
R208H-129V	62-67	7-30	Similar to sCJD VV2. Frequent psychiatric presentation. One case with supranuclear palsy at onset.	2/4	2/4	3/4	Similar to sCJD VV2, but with cerebellar kuru plaques (n=2)
V210I-129M	39-82	2-34	Similar to sCJD MM(V)1.	65/87	94/101	10/54	Similar to sCJD MM(V)1.
E211Q-129M	41-81	3-32	Similar to sCJD MM(V)1.	5/6	3/3	-	Similar to sCJD MM(V)1.
3-4OPRIs-129M	39-85	2-77	Similar to sCJD MM(V)1.	7/10	3/8	6/15	Similar to sCJD MM(V)1.
5-6OPRIs-129M	20-63	4-252	Onset with behavioural/psychiatric and cognitive symptoms. Later ataxia, myoclonus, pyramidal, extrapyramidal, seizure.	4/40	2/8	0/22	Pathologic change usually mild despite the long duration mainly involving the cerebral cortices. PrP patches in the molecular layer of the cerebellum.
6OPRIs-129V	33-51	3-180	Early cognitive, ataxia, sensory.	0/5	-	0/5	Not reported.

1.5 Prion strains

Prion strains are operationally defined as infectious isolates that, when transmitted to syngeneic hosts, under fixed and controlled conditions, exhibit distinct prion-disease phenotypes (Bartz, 2016). The strain-associated phenotypic traits include incubation times, histopathological lesion profiles, pattern of electrophoretic mobility, glycosylation and PK-resistance, which, although not invariably, usually persist upon serial transmission (Aguzzi *et al.*, 2007; Morales, 2017).

Historically, the existence of disease strains was firstly characterized in scrapie in the early 60s, while the characterization of strains in human prion disease started much later after the molecular-phenotypical classification of sporadic Creutzfeldt-Jakob disease. This delay has various explanations: firstly, early transmission studies were focused on the assessment of the infectious potential of the disease and not to its phenotypic features; second, the cross-species transmission of disease to wild-type hosts was often problematic because of a “species barrier”. Since the 90s, the latter problem has been overcome by the development of transgenic (Tg) animal models expressing the human *PRNP* sequence.

To date, the experimental transmission of human prion disease “isolates” has led to the identification of five different CJD strains, named M1, V2, M2C, M2T and V1 according to the combination of the *PRNP* codon 129 genotype that is most susceptible to PrP^C conversion and the PrP^{Sc} type (1 or 2) accumulating in the brain. Remarkably, the same or highly similar strains characterize sporadic, genetic and iatrogenic CJD as well as kuru, indicating that they are not modulated by etiology.

1.5.1 Strain M1

Although the first successful transmission of sCJDMM(V)1 (in non-human primates) must be reasonably attributed to Gajdusek’s group, Prusiner’s lab first characterized the phenotype of experimentally transmitted sCJDMM(V)1 in Tg mouse lines overexpressing a chimeric mouse-human prion protein (MHu2M) (Korth *et al.*, 2003). The comparison of histopathological and biochemical PrP^{Sc} features in affected mice revealed a consistent pattern of PrP^{Sc} deposition, distribution of vacuolation and electrophoretic mobility of PrP^{Sc} unglycosylated fragment (21 kDa, type 1) compatible with a single strain, designated as M1.

In full agreement with the disease epidemiology in humans, the sCJDMM1 inoculum showed a faster transmission in mice expressing human PrP transgene encoding methionine at codon 129 (Tg(HuPrP,M129)) than in the homologous mouse line with valine at the same codon (Tg(HuPrP,V129)) (Korth *et al.*, 2003), identifying codon 129 MM as the most susceptible genotype to this strain. The same results have been obtained by transmission of sCJDMM(V)1 to transgenic and knock-in mouse lines expressing human PrP^C (Bishop *et al.*, 2010; Kobayashi *et al.*, 2010, 2013; Notari *et al.*, 2014; Watts *et al.*, 2015; Jaumain *et al.*, 2016), bank voles (Nonno *et al.*, 2006) and four species of non-human primates.

The inoculation of brain homogenates from gCJD carrying the E200K-129M mutation into Tg(HuPrP,M129) and Tg(MHu2M,M165V,E167Q) showed an incubation time and a size of PrP^{Sc} fragments (type 1) comparable to those obtained with sCJDMM1 (Korth *et al.*, 2003). Similar results were obtained in bank voles inoculated with gCJD linked to E200K-129M and V210I-129M mutations, and in squirrel monkeys with gCJD E200K-MM1 (Parchi *et al.*, 2010). Finally, the inoculation of gCJD linked to a six octarepeat insertion in cis with M at codon 129 and PrP^{Sc} type 1 in 129VV Tg152 mice also gave results closely resembling that of the sCJDMM(V)1 isolates with a 100% attack rate (Mead *et al.*, 2006).

Introduction

Taken together, the results from transmission studies indicate that the same M1 prion strain is responsible for all cases of CJDMM(V)1, independently of the supposedly different etiology.

1.5.2 Strain V2

The experimental transmissions of sCJD VV2 and MV2K revealed a convergence to a single propagating phenotype, indicating that a common strain, designated as V2, is linked to both subtypes (Bishop *et al.*, 2010; Parchi *et al.*, 2010). Consequently, the host codon 129 genotype is the main responsible for the phenotypic differences between these subtypes in humans. The transmission of the VV2 and MV2K subtypes to Tg mice and non-human primates showed a lower incubation time and a higher attack rate in host expressing VV at codon 129 (Bishop *et al.*, 2010; Parchi *et al.*, 2010), representing the genotype/agent combination with the shortest incubation time in mice expressing physiological PrP levels within the spectrum of human prions. Notably, since MV2K transmits more efficiently in Tg HuVV than in Tg HuMV, the strain tropism for the valine allele is more critical than the genotypic homology between the inoculum and the host for prion replication efficiency (Bishop *et al.*, 2010).

A single gCJD E200K-129V inoculum showing PrP^{Sc} type 2 has been transmitted to Tg152 expressing human PrP 129V with 100% attack rate, short incubation period and plaque-like focal deposits (Asante *et al.*, 2009), paralleling the results obtained with sCJD VV2 and MV2K inocula. Remarkably, when inoculated in Tg mice overexpressing human PrP with E200K-129M, the same case showed a marked increase of the incubation time, reduced attack rate and less abundant PrP-plaque at neuropathological evaluation (Asante *et al.*, 2009). Overall, these results demonstrate that, as for the M1 isolate, the V2 strain is responsible for sporadic and genetic, highlighting, once again, the fact that the strain-specific properties of CJD prions are mainly encoded by PrP^{Sc} properties that are independent of the presence of specific *PRNP* mutations and the disease etiology.

1.5.3 Other CJD strains: M2T, M2C and V1

FFI was successfully transmitted (in both wild type (Tateishi *et al.*, 1995) and Tg mice overexpressing human PrP (Collinge *et al.*, 1995; Telling *et al.*, 1996) earlier than sFI (sCJDMM2T) (into Tg mice expressing a chimeric mouse-human PrP (Mastrianni *et al.*, 1999). Neuropathological findings and PrP^{Sc} properties in affected mice showed striking similarities between FFI and MM2T inocula, which is consistent with a common strain (M2T) (Mastrianni *et al.*, 1999). Data from subsequent transmissions in murine lines either overexpressing human PrP (Korth *et al.*, 2003) or expressing normal PrP levels (Moda *et al.*, 2012) corroborated the conclusion further.

Among the sCJD subtypes, MM2C (strain M2C) is the only one that did not successfully transmit to knock-in mice expressing human PrP at physiological levels (Bishop *et al.*, 2010; Moda *et al.*, 2012; Kobayashi *et al.*, 2013). However, the disease propagated successfully in transgenic and knock-in murine lines overexpressing human PrP with 129M (Korth *et al.*, 2003; Notari *et al.*, 2014; Chapuis *et al.*, 2016; Jaumain *et al.*, 2016), despite with a remarkably longer incubation time than M1 prions (Korth *et al.*, 2003; Nonno *et al.*, 2006; Notari *et al.*, 2014; Jaumain *et al.*, 2016). Likewise M1 prions, M2C prions transmitted more efficiently in Tg mice expressing 129M than in those carrying 129V (Korth *et al.*, 2003). Taken together these transmission data indicate that the M2C strain has a low transmission efficiency and a reduced infectious potential. Moreover, whether M2C prions are also linked to gCJD, remains to be demonstrated.

VV1 is the last successfully transmitted (into Tg mice expressing physiological levels of PrP^C and VV or MV) among sCJD subtypes (Bishop *et al.*, 2010). Likewise V2 prions, V1 prions preferentially transmit to host expressing at

Introduction

least one 129V allele, although V1 prions showed significantly longer incubation times and a lower attack rate than V2 prions, which indicate a reduced virulence of the former. Likewise for M2C, whether V1 prions are also linked to gCJD, remains to be seen.

LIST OF PhD PROJECTS

During the three years of my PhD I focused my research on CJD to investigate clinical and molecular aspects underlying or contributing to its phenotypical heterogeneity.

Two main aims/projects have guided my work:

- i. To analyse the involvement of the peripheral nervous system in sporadic CJD;
- ii. To characterize the clinical, pathological, and molecular variability associated with genetic CJD.

Both the studies, including molecular characterization and histopathologic analysis, have been performed at the Neuropathology Laboratory (NP Lab) of the Institute of Neurological Sciences of Bologna, Italy.

The CJD cases included in the present studies were referred to the NP Lab at the Institute of Neurological Sciences of Bologna, Italy (i, ii), to the National Prion Pathology Surveillance Center of United States, Cleveland, USA (i, ii), to the German National CJD Surveillance study, Munich, Germany (i, ii), and to the Foundation IRCCS, Carlo Besta Institute of Neurology, Milan, Italy (i).

PRION-RELATED NEUROPATHY IN CJD

2.1 Background

Patients with sCJD usually present with neurological signs of central origin reflecting the predominant PrP^{Sc} accumulation in the CNS, which is not surprising given the higher expression levels of PrP^C within the brain. Recently, however, the application of techniques with improved sensitivity, such as prion RT-QuIC and PMCA, allowed the demonstration of PrP^{Sc} deposits also in peripheral tissues (Glatzel *et al.*, 2003; Peden *et al.*, 2006; Orrú *et al.*, 2017). Furthermore, the detection of PrP^{Sc} in autonomic and dorsal root ganglia (Hainfellner and Budka, 1999; Ishida *et al.*, 2005; Lee *et al.*, 2005), and in trigeminal (Guiroy *et al.*, 1989) and peripheral nerves of sCJD subjects (Favereaux *et al.*, 2004), although limited to isolated cases, specifically suggested a possible peripheral nervous system (PNS) involvement.

Despite this progress, studies specifically addressing the prevalence and type of peripheral signs in sCJD secondary to the PNS involvement are lacking. Neuropathy has been to date only anecdotally reported as a presenting clinical feature in sCJD (Esiri *et al.*, 1997; Samman *et al.*, 1999; Kovács *et al.*, 2002; Zéphir *et al.*, 2009).

These findings, together with the observation of some sCJD cases belonging to the VV2 and MV2K subtypes, misdiagnosed with neuropathy at disease onset, stimulated to investigate whether and to what extent PNS involvement features in the phenotypic spectrum of sCJD VV2 and MV2K. Remarkably, these subtypes share prions associated with VV2 and MV2K behave as a unique prion strain, i.e. the V2 strain, and share distinctive clinical and pathological features including a predominant involvement of subcortical structures in the early course and an “ascending” pattern of progression to the cerebral cortex, which is especially striking in the sCJD VV2 subtype (Baiardi *et al.*, 2017). Intriguingly, the same pattern of spreading is observed in peripherally acquired forms of human prion disease linked to the V2 strain (e.g. kuru and iatrogenic CJD secondary to subcutaneous injection of contaminated growth hormone). Furthermore, whether peripheral nerves from sCJD patients accumulate significant amounts of PrP^{Sc} and/or prion seeding activity has been investigated.

2.2 Materials and methods

This study was approved by the Ethics Committee, AUSL of Bologna (n. 16184/CE). Written informed consent on retained tissues was given by the patients during life or their next of kin after death.

2.2.1 Study population

The medical charts and analyzed clinical and neurophysiological data of 209 sCJD patients were reviewed. One hundred-seventy-eight of them received a “definite” diagnosis of sCJD VV2 (n=104) or MV2K (n=74) according to histopathological and molecular consensus criteria (Parchi *et al.*, 2009b, a, 2012), while the remaining 31 cases fulfilled the current diagnostic criteria for “probable” sCJD (Zerr *et al.*, 2009) and carried the genotype VV at codon 129 of *PRNP*. In all cases, the screening of *PRNP* open-reading frame ruled out pathogenic variants (Ferrer *et al.*, 2007).

Inclusion criteria comprised: a) the availability of comprehensive medical records including at least one hospitalization in a Neurology Department, b) the lack of pathogenic mutations in *PRNP* coding region, and c) the absence of metabolic, paraneoplastic, infectious, and inflammatory causes of neuropathy. Accordingly, 16 cases lacking sufficient clinical information and 6 cases with concomitant causes of neuropathy (diabetes, n=2; monoclonal

gammopathy, n=1; exposure to chemotherapeutic agents for cancer treatment, n=2; vitamin B₁₂ deficiency, n=1) were excluded. Furthermore, three probable sCJD cases with clinical features highly suggestive for the very rare VV1 subtype, including an age of onset ≤36 years, a disease duration ≥17 months and the predominant cortical symptoms/signs without ataxia, were excluded. After selection, the cohort analysed for PNS involvement included 184 patients (Figure 4).

Of these 184 patients, 100 were referred to the Laboratory of Neuropathology (NP lab), University of Bologna, Italy (from 2000 to 2017), 39 to the Foundation IRCCS, Carlo Besta Institute of Neurology, Milan, Italy (from 1994 to 2016), and the remaining 45 were part of a previously published case series (Parchi *et al.*, 1999).

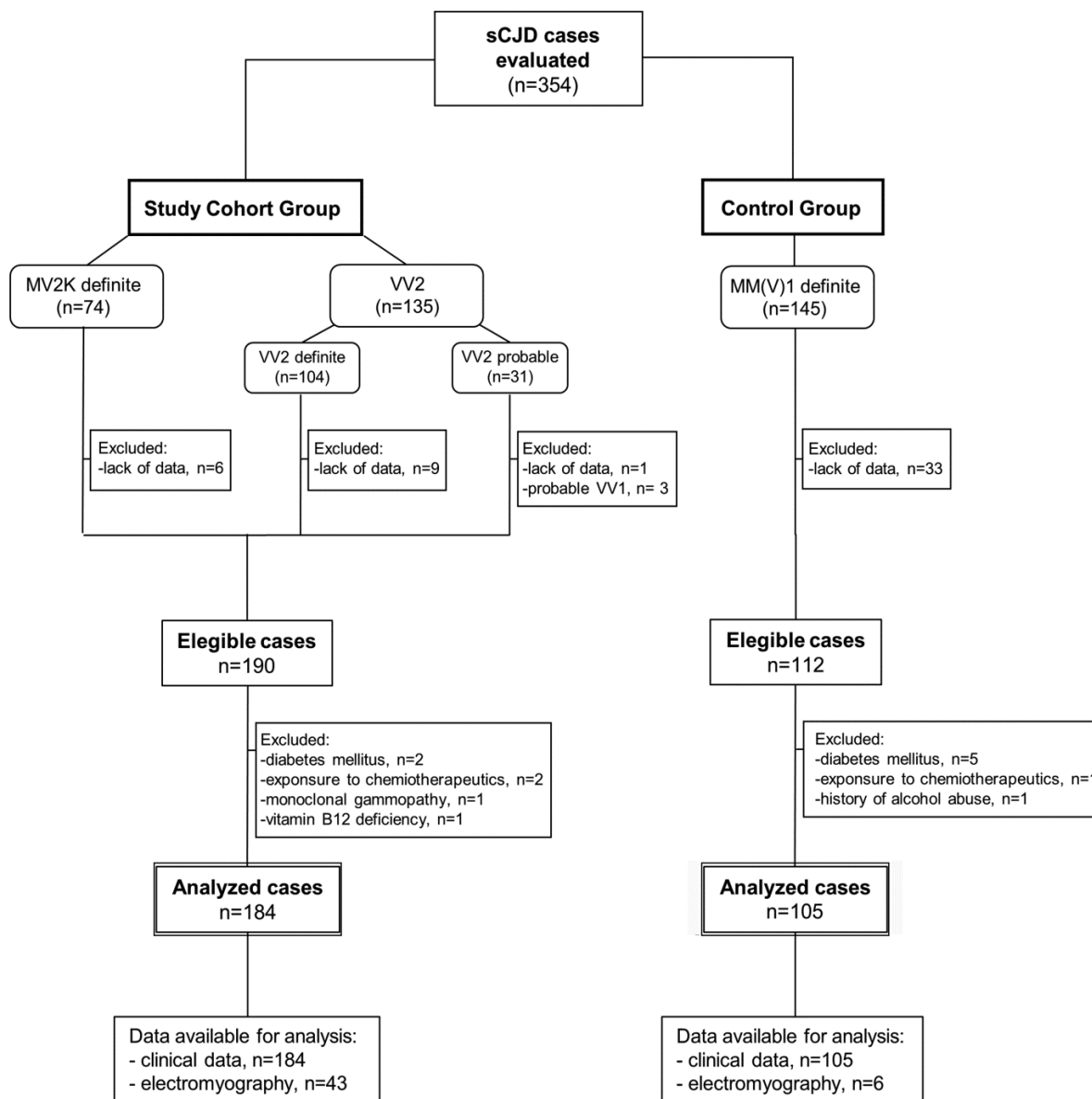


Figure 4. Study flow-chart (patient selection).

2.2.2 Clinical and neurophysiological analysis

The clinical findings indicative of PNS or spinal cord involvement as indicated in the clinical reports by the examining neurologists were recorded. In addition, the results of neurophysiological tests, such as electromyography

Prion-related neuropathy in CJD

(EMG), motor and somatosensory evoked potentials (MEPs, SEPs), and of nerve biopsy were evaluated, when performed.

To verify whether the PNS involvement is a peculiar finding of V2 strain-related subtype, clinical data from VV2 and MV2K patients were compared with those from a consecutive series of definite MM(V)1 cases referred to the NP lab, University of Bologna from 2009 to 2017 (n=105) (Figure 4).

Three representative cases, suffering from sensory symptoms/signs at onset and with abnormalities at neurophysiological studies are reported in detail.

2.2.3 PrP investigations in peripheral nerves

Patients and tissues

A total of 18 frozen peripheral nerve and 3 cranial nerve post-mortem samples from 11 sCJD patients (VV2, n=5; MV2K, n=1; MM(V)1, n=4, MM2C n=1), one case of genetic CJD V210I-129M, and 2 non-CJD (frontotemporal dementia) controls were included. The samples were from the following nerves: sciatic (intrapelvic, n=7), femoral (n=1), sural (n=6), common peroneal (n=1), tibial (n=1), trigeminal (n=2), vagus (n=1) and lumbosacral roots (n=2). Among these cases, 2 sCJD VV2 and 1 MV2K (cases #8, #9 and #10 in the result section) were not included in the clinical study cohort due to the lack of detailed clinical information, whereas cases #1 and #2 had clinical and neurophysiological evidence of peripheral neuropathy.

PrP^{Sc} purification and sample preparation for Western blotting

Purification of PrP^{Sc} was obtained from 150-200 mg of peripheral nerve according to a previously reported protocol (Saverioni *et al.*, 2013), with minor modifications. Briefly, tissues were homogenized in 2 ml of 2X TEND (20 mM Tris, pH 8.3, 1 mM EDTA, 130 mM NaCl, 1 mM dithiothreitol) with a gentleMACS Octo Dissociator (Miltenyi BioTec), using the Protein 1 setting. After the addition of 2 ml of 20% Sarkosyl and three cycles of freezing and thawing by sonication the homogenate was exposed to three ultracentrifuge steps in a Beckman rotor SW55Ti (16000 rpm, 25 min at 4 °C; 45000 rpm, 143 min at 4 °C; and 45000 rpm for 143 min at 18 °C, the latter after resuspension in 2.5 ml 1X TEND, 10% NaCl, and 1% Sarkosyl). The final pellet (P3) was resuspended in 100 µl of lysis buffer (100 mM NaCl, 10 mM EDTA, 0.5% Nonidet P-40, 0.5% sodium deoxycholate, 100 mM Tris, pH 6.9), sonicated and frozen at -80 °C.

P3s were then digested with proteinase K (PK) (Roche Diagnostics) at a final concentration of 4 U/ml for 1 h at 37 °C. To maximize the sensitivity of detection, PK-digested P3s were concentrated by protein precipitation in 8 volumes of methanol overnight at -20 °C. After centrifugation at 14000 rpm for 45 min at 4 °C, the supernatant was discarded and the pellet resuspended in 20 µl of sample buffer (3% SDS, 4% β-mercaptoethanol, 10% glycerol, 2 mM EDTA, 62.5 mM Tris).

PrP deglycosylation

N-linked glycans were removed by using a peptide-Nglycosidase F kit (New England Biolabs) according to the manufacturer's instructions.

Western blot analysis

Western blot analysis was performed according to previously published procedures (Rossi *et al.*, 2017). An equivalent of 75-100 mg of peripheral nerve wet tissue was loaded on 13% SDS-PAGE gels and transferred to Immobilon-P membranes (Millipore). The monoclonal antibody 3F4 (epitope at PrP residues 108–111, 1:30000

Prion-related neuropathy in CJD

working dilution) was used as primary antibody. The immunoreactive signal was detected by ultrasensitive enhanced chemiluminescence (SuperSignal™ West Femto, Thermo Fisher Scientific) on a LAS 3000 camera (Fujifilm). Densitometric analysis was performed using the software AIDA (Image Data Analyzer v.4.15, Raytest GmbH).

Prion real-time quaking induced conversion assay (RT-QuIC)

For RT-QuIC analysis samples were homogenized 10% (w/v) in cold QuIC buffer [phosphate buffered saline (PBS) containing 150 mM NaCl, 1.0% Triton X-100, 4 mM EDTA, and a Protease Inhibitor Mixture (Roche)] with a gentleMACS Octo Dissociator (Miltenyi BioTec) at Protein 1 setting and stored at -80°C. Before analysis, samples were serially diluted (up to 1000 fold) in N2 buffer [0.1% SDS in PBS supplemented with N2 media (Gibco)] (Orrú *et al.*, 2009). Peripheral nerve samples (diluted 1000 fold) were analyzed by the RT-QuIC assay as described (Franceschini *et al.*, 2017), with minor modifications. The RT-QuIC reaction mix contained 10 mM phosphate buffer at pH 7.4, 300 mM NaCl, 1 mM EDTA at pH 8.0, 10 µM thioflavin-T (ThT), and 0.1 mg/ml of Syrian hamster recombinant truncated form of prion protein (Ha rPrP 90–231). After sealing, the plate was incubated in a FLUOstar OMEGA reader (BMG Labtech, Germany) at 55 °C, over a period of 60 hours with intermittent cycles of shaking (60 s, 700 rpm, double-orbital) and rest (60 s). The fluorescence intensity of ThT-positive PrP^{Sc}-seeded aggregates, expressed as relative fluorescence units (RFU), was taken every 45 minutes using 450±10 nm (excitation) and 480±10 nm (emission) wave-lengths, with a bottom read and a gain of 1000. A sample was considered prion positive if at least two out four sample replicates gave a fluorescence signal higher than the threshold cut-off value, representing the mean RFU values of negative samples plus at least 10 standard deviations.

2.2.4 Statistical analysis

RT-QuIC relative fluorescence responses were analyzed and plotted using the Sigma Plot software (Systat Software Inc, Chicago, IL, USA). The Mann-Whitney test was used to test differences between two groups, while the one-way ANOVA (followed by Tukey's or Bonferroni's post hoc test) was applied for multiple group comparisons. P-values <0.05 are considered statistically significant. Unless otherwise stated, data are expressed as mean with standard error of the mean (SEM).

2.3 Results

Case 1. A 67-year-old man started complaining of numbness and tingling in the fingertips and in the feet. He was hospitalized with the suspicion of neuropathy four months after clinical onset. His medical record was negative for common types of hereditary polyneuropathies, diabetes, viral infections or toxic exposure. The neurological examination showed stocking-like hypoesthesia, apallescsthesia, ataxic gait, weak deep tendon reflexes in lower limbs and positive Romberg's test. Blood tests including a panel of antiganglioside and onconeural antibodies as well as standard CSF were unremarkable. EMG was consistent with a predominant axonal neuropathy, showing marginal slowing of nerve conduction velocities, bilaterally reduced amplitudes of tibial and peroneal nerve compound muscle action potential (CMAP), and bilaterally unobtainable sensory action potentials (SAPs) in the sural nerve. MEPs and SEPs showed a prolonged central conduction time when elicited from lower limbs. Spinal cord MRI did not show any pathological findings. Assuming a distal acquired inflammatory neuropathy, a variant of chronic inflammatory demyelinating polyneuropathy, IV Methylprednisolone 500 mg for 4 days was administered, without any benefit. Sural nerve biopsy, performed two months later, showed marked fibre loss with some admixed demyelination and occasional onion bulbs, but no inflammatory infiltrates (Figure 5A). Teased fibres showed predominantly axonal damage, but also

occasional segmental demyelination according to Dyck's classification (Figure 5B-C). The ultrastructural analysis confirmed the predominant axonal pathology and revealed the accumulation of undetermined electron-dense material in the adaxonal space (Figure 5D-F).

Eight months from onset the patient's ataxia had markedly worsened and spasticity, bradykinesia, resting tremor, limb rigidity and hypophonia became apparent with bilaterally Babinski sign. Because of the concomitance of rapidly progressive cognitive impairment and behavioural abnormalities, CSF analyses were repeated to measure neurodegenerative biomarkers, which revealed positive 14-3-3 protein and increased total-tau levels (1789 pg/ml). Moreover, a brain MRI showed bilateral hyperintensity of basal ganglia on diffusion-weighted (DW) sequences consistent with CJD. The patient's neurologic status steadily deteriorated until death, which occurred 12 months after clinical onset. Histopathological and molecular analyses determined the diagnosis of sCJD MV2K.

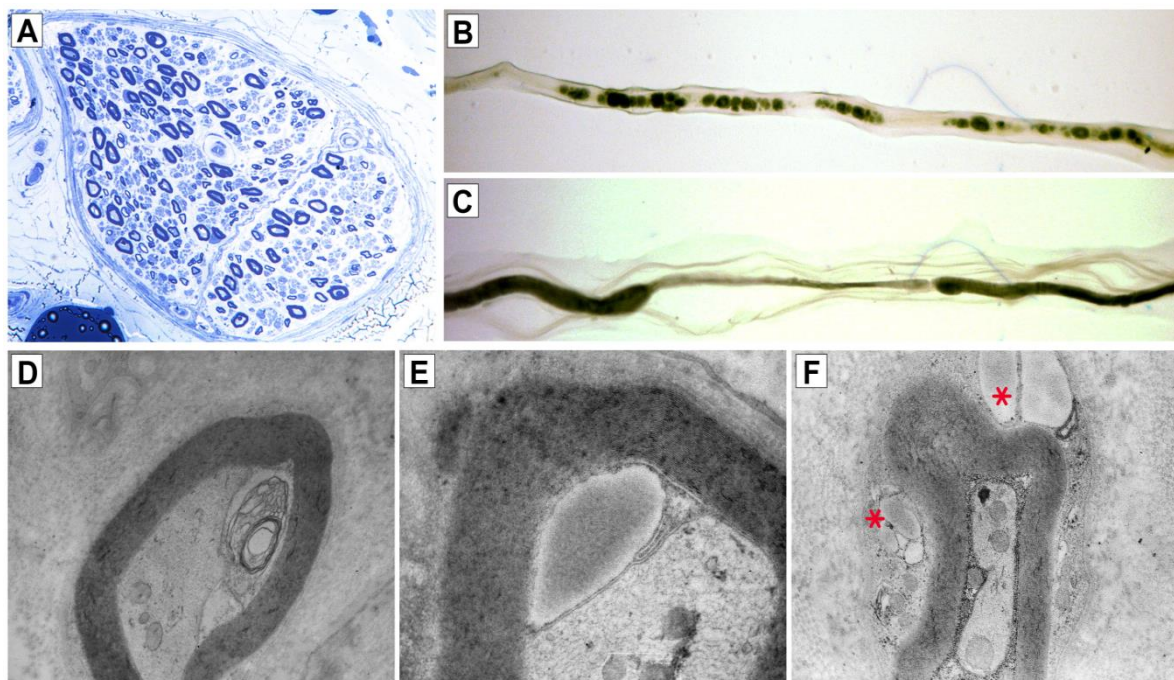


Figure 5. Sural nerve biopsy findings in a patient with sCJD MV2K (case 1). Marked loss of fibers (A, toluidine-blue-stained plastic sections 400x) [fiber density=1200 ff/mm²; normal range=4800 ff/mm²]. Teased fibers analysis showing predominant signs of axonal damage with wallerian degeneration (“myelin balls”; B, 200x) and segmental demyelination (C, 200x). Electronic microscopy of large myelinated fibers showing vacuolation of uncompact myelin in the adaxonal space (D, 12000x) and accumulation of electron-dense material with a fibrillary structure (E, 20000x), slightly resembling amyloid fibrils. Electron-dense cytoplasmic deposits in Schwann cells (F, 12000x). Adapted from (Baiardi *et al.*, 2018b).

Case 2. A 62-year-old man presented with an 11-month history of sensory symptoms, gait instability and behavioural disturbances. The patient's first complaint was a sense of imbalance, although his wife also noted a concomitant change in his behaviour (i.e. he feared being alone and began to lock himself into his house). In the following 10 months, the patient complained of feet paraesthesia and developed unsteady gait with falls and disinhibition with sexual hyperactivity. Neurological examination revealed dysarthria, intention tremor, trunk and limb ataxia, myoclonus, bilateral weak deep tendon reflexes in the lower limbs, and a symmetric loss of tactile, pain and thermal sense in the feet. Two months later, the symptoms significantly worsened: the patient complained of burning feet and was unable to walk without assistance. At this time, peripheral neurological examination revealed glove-and-stockings sensory deficit and all deep tendon reflexes. In the next two months, he rapidly developed a full-blown

Prion-related neuropathy in CJD

dementia. CSF evaluation revealed a positive 14-3-3 test and high levels of total-tau protein (1474 pg/ml). Electroneurographic studies performed 11 and 13 months after onset, revealed a progressive sensorimotor polyneuropathy. In particular, the first exam showed a prolonged distal latency (DL) in both tibial nerves associated with slowing of motor conduction velocity (MCV) in the same nerves and in the right peroneal nerve, as well as amplitude diminution, prolonged DL and MCV slowing in the sural nerves. The second examination showed absence of SAPs in both sural nerves, a further diminution of amplitude and slowing of CV as well as an absence or evident prolongation of F wave latency in all examined motor nerves. Moreover, the needle EMG showed fasciculations in right tibialis anterior and left vastus medialis muscles. A biopsy of the left sural nerve was performed after the second EMG and microscopic examination showed a moderate loss of large myelinated fibres with signs of regeneration, without evidence of cellular infiltration. The patient died 17 months after clinical onset. The molecular and neuropathological features led to the diagnosis of sCJD MV2K.

Case 3. A 75-year-old woman with unremarkable medical history developed unsteadiness of gait, asthenia and intermittent diplopia over a few weeks. The first neurological examination, one month after clinical onset, revealed ataxic gait, positive Romberg, absence of deep tendon reflexes in the lower limbs and postural tremor in the upper limbs. A subacute polyneuropathy was suspected and confirmed by EMG. The latter showed a sensorimotor axonal polyneuropathy characterized by prolonged DL in the median, ulnar, common peroneal and tibial nerves; a reduced amplitude of SAPs in the median and ulnar nerves and a prolongation of F waves latency in all the examined motor nerves. In the following three months, the gait disturbance further worsened, and the patient developed severe cognitive impairment and dysphagia. At this time, a CSF analysis revealed a positive 14-3-3 protein assay and markedly elevated total-tau protein levels (17600 pg/ml), while a brain DW-MRI showed a hyperintensity of basal ganglia. The patient died 6 months after the disease onset. Molecular and histopathological examinations determined the diagnosis of sCJD VV2 subtype.

2.3.1 Clinical findings in the whole cohort

In the study cohort, neurological symptoms suggestive of PNS involvement occurred at onset in 17 patients (9 VV2, 7.6% and 8 MV2K, 12.1%) and as isolated features in six. All four patients with isolated peripheral signs for whom detailed early clinical information was available received an initial diagnosis of peripheral neuropathy. At first neurological assessment, none of these patients was considered a case of possible CJD.

In patients presenting with peripheral neurological symptoms, the most frequent complaints were limb paraesthesia (n=5), dysesthesia (n=1), numbness (n=1) and weakness (n=2) in the MV2K group and limb weakness (n=5, 4.2%) and paraesthesia (n=3, 2.5%) in the VV2s. Peripheral symptoms at onset involved symmetrically the lower extremities in all but one MV2K patient who also had paraesthesia in the hands.

Overall, 50 (42.4%) VV2 patients and 30 (45.4%) MV2Ks suffered from symptoms and/or signs suggestive for PNS and/or spinal cord dysfunction sometimes during the course of the disease (Table 5). Furthermore, 9 (7.6%) VV2 patients presented cranial nerve dysfunction of peripheral origin affecting the oculomotor (n=1), trigeminal (n=1), abducens (n=3) and facial (n=4) nerves.

Remarkably, 47 patients had objective signs indicative of neuropathy, eventually confirmed by neurophysiological studies, in absence of any subjective complaint.

Within the MM(V)1 control group only 11 (10.5%) patients showed PNS or spinal cord symptoms/signs and limb paresthesia was reported at onset by only one patient. Overall, both symptoms and signs of peripheral origin were much less frequent in the MM(V)1 group than in the VV2 and MV2K groups (Table 5).

Table 5. PNS/spinal cord symptoms and signs in the study cohort and control group.

	VV2 n=118 (%)	MV2K n=66 (%)	Study group [VV2+MV2K] n=184 (%)	Control group [MM(V)1] n=105 (%)
Symptoms (n, %)				
Limb weakness*	10 (8.5)	8 (12.1)	18 (9.8)	-
Numbness	1 (0.8)	2 (3.0)	3 (1.6)	-
Paraesthesia (tingling)	3 (2.5)	7 (10.6)	10 (5.4)	2 (1.9)
Dysesthesia (burning, painful)	5 (4.2)	4 (6.1)	9 (4.9)	-
Cramps/myalgia	1 (0.8)	1 (1.5)	2 (1.1)	1 (0.9)
Signs (n, %)				
Absent or reduced deep tendon reflexes	37 (31.3)	19 (28.8)	56 (30.4)	5 (4.8)
Absent or reduced vibratory sense	10 (8.5)	4 (6.1)	14 (7.6)	-
Absent or reduced touch, thermic or pick sense	3 (2.5)	5 (7.6)	8 (4.3)	1 (0.9)
Positive Romberg's test	8 (6.8)	6 (9.1)	14 (7.6)	1 (0.9)
Sensory ataxia	1 (0.81)	1 (1.5)	2 (1.1)	1 (0.9)
Fasciculation	12 (10.2)	4 (6.1)	16 (8.7)	1 (0.9)
Muscular atrophy	3 (2.5)	5 (7.6)	8 (4.3)	-

*Without pyramidal signs

2.3.2 Neurophysiological findings

Forty-three patients of the study cohort (VV2 and MV2K) and only six of the control group [MM(V)1] received at least one electromyography, performed on average 2.6 ± 1.7 and 0.6 ± 0.5 months from clinical onset in the study cohort and control group, respectively. In the study cohort, neurophysiological studies revealed signs of neuropathy in 14 cases, with either sensorimotor (n=7) or pure motor (n=4) or sensory (n=3) impairment. In addition, polyradiculoneuropathy was documented in one case, a focal neuropathy involving the ulnar and median nerves (n=1) or the peroneal nerve (n=2) in other three patients, and a not better-specified neuropathy in two subjects (Table 6). Nerve conduction studies were unremarkable in the remaining 13 (29.5%) patients. Needle EMG documented a spontaneous muscle fiber activity in 14 patients, associated with signs of subacute or chronic denervation in 9. Interestingly, nerve conduction studies were unremarkable in most of these cases (n=9). The latter finding was significantly more frequent in VV2 than in MV2K patients (Table 6).

Table 6. Results of neurophysiological studies in sCJD MV2K and VV2 patients.

	MV2K (n=10)	VV2 (n=21)
Nerve conduction studies		
Sensorimotor axonal polyneuropathy	3	2
Sensorimotor demyelinating polyneuropathy with conduction block	1	-
Sensory axonal and demyelinating polyneuropathy	-	1
Sensory axonal polyneuropathy	1	-
Sensory polyneuropathy*	1	1
Motor axonal polyneuropathy	-	1
Motor demyelinating polyneuropathy	1	1
Motor polyneuropathy*	-	1
Polyradiculoneuropathy	-	1
Ulnar and median neuropathy	1	-
Peroneal axonal neuropathy	1	1
Unspecified neuropathy	1	1
Needle EMG		
Fasciculation	-	12
Myokymia	1	1
Fibrillation, positive waves	-	1
Subacute denervation signs	-	6
Chronic denervation signs	-	3

*Not specified whether with axonal or demyelinating pattern of damage.

SEPs and MEPs were performed in 12 VV2 and 5 MV2K subjects with clinical and/or neurophysiological evidence of PNS/spinal cord involvement, on average 3.5 ± 0.7 months from clinical onset. Abnormal SEPs and MEPs were reported in five VV2 and two MV2K patients, while they were unremarkable in the remaining 10.

Sural nerve biopsy was performed in two (1.1%) patients (case 1 and 2 reported above).

In the control group, the neurophysiological examination was invariably normal, except for a mild sensorimotor demyelinating neuropathy in one patient. SEPs and MEPs were examined in two control patients and they were normal in both. None of the control patients underwent a nerve biopsy.

2.3.3 PrP^{Sc} detection in peripheral nerve

PrP^{Sc} detection by Western blot

The presence of PK-resistant PrP^{Sc} fragments matching those found in the CNS was demonstrated in two purified (P3) samples of peripheral nerves (VV2, n=1; MV2K, n=1) and in all total homogenates of cranial nerves analyzed (2 trigeminal nerves and 1 vagus from two sCJD VV2 cases) (Figure 6 and Table 7). In contrast, all peripheral nerve total homogenates (n=8) and a few enriched P3 preparations (n=3) from sCJD patients [VV2, n=4; MM(V)1, n=3] yielded negative results as the non-CJD controls.

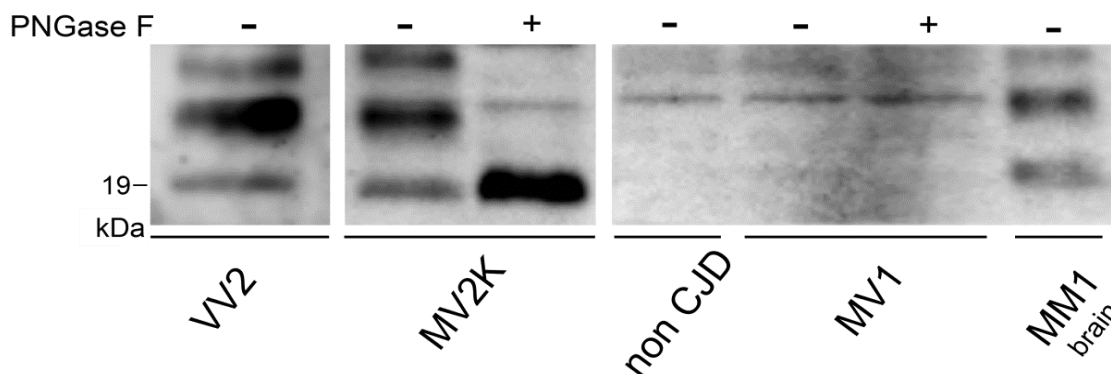


Figure 6. PrP^{Sc} detection and typing in peripheral nerves by Western blotting. Samples were resolved in 7 cm long gels and probed with the primary antibody 3F4. Relative molecular masses are in kDa. From left to right: PrP^{Sc} type 2 was detected in sciatic nerves of sCJD VV2 and MV2K cases. Immunoblotting was negative in both sCJD MV1 (sciatic nerve) and non-CJD (lumbosacral roots) cases. A cortical sample from a sCJD MM1 case (P3 diluted 1:500) was included as positive control. For deglycosylation samples were treated with PNGase F. Adapted from (Baiardi *et al.*, 2018b).

By serial dilution and densitometric analysis of WB signals, the amount of PrP^{Sc} in peripheral nerves was approximately 10^{-4} fold lower than that found in the frontal cortex of a sCJD VV2 patient with typical disease duration (data not shown). Conversely, the signal intensity of PrP^{Sc} band observed in cranial nerves, despite some variability (i.e. vagus nerve showed a stronger PrP^{Sc} band than trigeminal nerves), was almost comparable to that of the brain samples.

PrP^{Sc} detection in peripheral nerve by RT-QuIC

All samples from sCJD patients showed a full positive seeding activity in RT-QuIC (all 4 wells for each sample cross the fixed threshold), the genetic CJD case showed a medium positivity (2 wells of 4 passed the threshold); while none of the controls showed any seeding activity (Figure 7 and Table 7).

Table 7. Summary of results of abnormal PrP^{Sc} detection in peripheral nerves.

	Diagnosis	CJD type	Nerve	WB	RT-QuIC
Case #1	sCJD	VV2	trigeminal (CN V)	positive (TH)	positive
			vagus (CN X)	positive (TH)	positive
			femoral	negative (TH)	positive
			sciatic (intrapelvic)		positive
Case #2	sCJD	VV2	trigeminal (CN V)	positive (TH)	positive
			common peroneal	negative (TH)	positive
			sural	negative (TH)	positive
Case #3	sCJD	MM2C	sural		positive
Case #4	sCJD	VV2	sural	negative (P3)	positive
Case #5	gCJD - p.V210I	MV1	sural		positive*
Case #6	sCJD	MV1	sural	negative (TH, P3)	positive
Case #7	sCJD	MV1	sciatic (intrapelvic)	negative (P3)	positive
Case #8	sCJD	VV2	sciatic (intrapelvic)	negative (TH)	positive

Continued

Continued

Case #9	sCJD	VV2	sciatic (intrapelvic)	positive (P3), negative (TH)	positive
Case #10	sCJD	MV2K	sciatic (intrapelvic)	positive (P3), negative (TH)	positive
Case #11	sCJD	MM1	sciatic (intrapelvic)		positive
Case #12	sCJD	MM1	sciatic (intrapelvic)	negative (TH)	positive
Ctrl #1	FTD	non CJD	lumbar roots		negative
			sacral roots	negative (TH, P3)	negative
Ctrl #2	FTD	non CJD	sural		negative
			tibial		negative

*2/4 wells. List of abbreviations: WB: western blot; RT-QuIC: real-time quaking-induced conversion; CN: cranial nerve; TH: total homogenate; P3: pellet 3 (product of purification process); FTD: frontotemporal dementia.

Both VV2 and MV2K samples (V2-strain group, n=8) showed an earlier lag phase [sCJD V2: 12±1; sCJD MM(V)1: 19±5; gCJD V210I-MV1 41] and a higher ThT maximum response (sCJD V2: 2200±90; sCJD MM(V)1: 1840±240; gCJD V210I-MV1: 1078) than the other CJD cases [MM(V)1 n=4, gCJD V210I-MV1 n=1].

In a further analysis, the prion seeding activity of cranial (n=2) and peripheral nerve from inferior limbs (n=8) samples were compared in cases belonging to the V2-strain group. Interestingly, cranial nerves showed a mean earlier lag phase (5.8±1.3 vs 11.9±1.1, p-value=0.03) and a mean higher ThT value (2950±210 vs 2200±90, p-value=0.04) than other peripheral nerves (Figure 7), thus indirectly supporting the WB finding of a larger PrP^{Sc} deposition in cranial nerves than in nerves of inferior limbs.

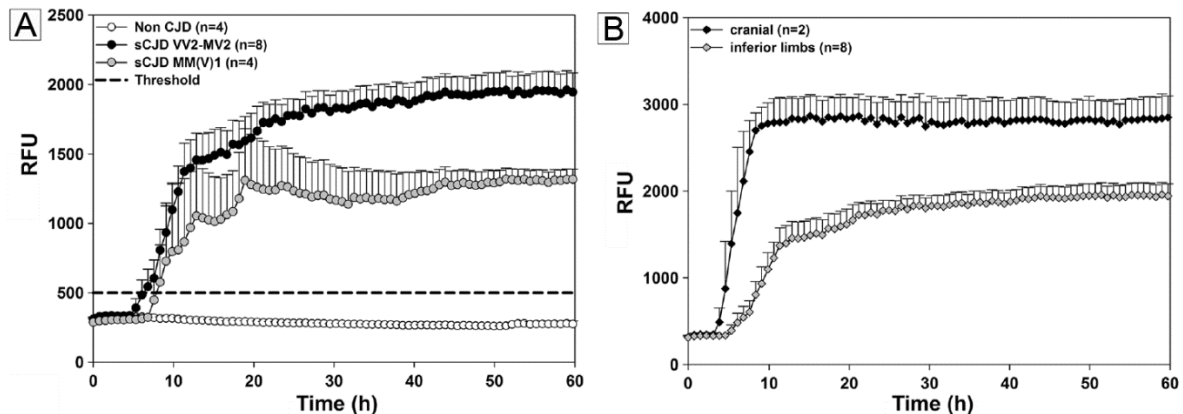


Figure 7. PrP^{Sc} detection in peripheral nerves by RT-QuIC assay. (A) The box shows the ThT fluorescence traces of peripheral nerves from 12 definite sCJD cases and 4 non-CJD cases. sCJD were divided according to the molecular subtype and the strain [e.g. the V2-strain group including VV2 and MV2K subtypes (n=8) and the M1-strain group including MM(V)1 (n=4)]. Threshold was indicated as dot line (500 RFU). (B) Comparison of ThT curves of peripheral nerves from different anatomical sites (cranial vs inferior limbs) in cases belonging to the V2 strain group. Data are expressed as mean ± SEM. Adapted from (Baiardi *et al.*, 2018b).

2.4 Discussion

The results of the present study demonstrate that PNS dysfunction belongs to the phenotypic spectrum of sCJD variants linked to the V2 prion strain. In the present cohort of sCJD VV2 and MV2K cases, the largest analysed to date, the prevalence of peripheral symptoms and/or signs was 43.5% and neuropathy was confirmed by neurophysiological studies in 10.9% of cases. Notably, PNS symptoms and/or signs characterized the onset of disease in 9.2% of cases, leading to frequent misdiagnosis in this subgroup of patients during the early disease stages. These numbers likely underestimate the real prevalence of peripheral neuropathy in sCJD VV2 or MV2K given that EMG is not always performed in CJD patients presenting with PNS symptoms/signs. Results of neurophysiological studies suggest a pattern of peripheral nerve involvement characterized by prominent signs of axonal damage with secondary demyelination and with either sensorimotor or isolated motor or sensory dysfunction.

It is noteworthy that in addition to the peripheral nerve involvement, neurophysiological studies such as needle EMG revealed the occurrence of spontaneous activity, namely fasciculations, fibrillations, positive waves and myokymic discharges in about a third of patients, especially in the VV2 group. These abnormal muscular activities were often associated with other subacute or chronic signs suggesting a lower motor neuron dysfunction (Worrall *et al.*, 2000). Conversely, in a few cases, spontaneous activity occurred in absence of any other sign of denervation, indicating a peripheral nerve hyperexcitability. Although the latter is more commonly associated with autoimmune diseases like Morvan's or Isaacs' syndrome, and serum antibodies to the voltage-gated potassium channel (VGKC) complex have also been anecdotally reported in association with sCJD (Angus-Leppan *et al.*, 2013), a co-morbid condition seems to be unlikely due to the rarity of both sCJD and anti-VGKC-associated disorders. Moreover, the recent report of peripheral nerve hyperexcitability in two other VV2 sCJD patients (Ong *et al.*, 2015) further support a prion-related aetiology of the spontaneous fibre activity.

Similarly, the timing of appearance of neuropathic symptoms/signs in relation to those indicating the CNS involvement, the lack of evidence for other causes of PNS involvement and the collected experimental evidence demonstrating both PrP^{Sc} deposition and presence of prion seeding activity in the peripheral nerve are all in support of a PrP^{Sc}-related aetiology of the peripheral neuropathy. On the other hand, a contribution related to the dysfunction central pathways to the sensory and motor symptoms of presumed peripheral origin cannot be definitely ruled out. In this regard, to focus on PNS involvement more selectively, any sensorimotor sign or complaint with hemibody distribution, which would be more indicative of a CNS origin, was excluded and the analysis was limited to complaints with symmetrical and distal (i.e. "stocking and glove") distribution.

Interestingly, the PNS involvement in sCJD seems to be strongly prion-strain dependent, which is also in support of a prion-related origin of PNS dysfunction in CJD. Indeed, in the control group, including patients with the typical sCJD MM(V)1, peripheral signs/symptoms were significantly less frequent and much more rarely led to a neurophysiological assessment than in the sCJD VV2 or MV2K. However, the faster disease progression and the predominant cognitive symptoms at onset, affecting the ability of these patients to report symptoms and collaborate to neurological examination, might have in part concealed the PNS dysfunction in these cases.

Another issue, which is worth discussing, is the possible implication of these observations on the origin and spread of prions in sCJD. In acquired prion diseases such as vCJD, BSE and other animal forms, prions obligatorily spread from the periphery to the CNS. In these diseases, after oral exposure, the transmissible agent replicates within lymphoid tissues and then spreads centripetally to the CNS. Kimberlin and colleagues demonstrated that invasion of the CNS may occur through sciatic nerves in peripherally injected scrapie mice (Kimberlin *et al.*, 1983). Notably, PrP^{Sc} accumulation

Prion-related neuropathy in CJD

in the PNS has been reported in naturally and experimentally scrapie-affected sheep (Groschup *et al.*, 1996, 1999), hamsters (McBride and Beekes, 1999), BSE-affected cattle (Masujin *et al.*, 2007; Franz *et al.*, 2012), and vCJD (Head *et al.*, 2004; Lee *et al.*, 2005). In the latter, sensory symptoms such as persistent painful sensory complaints, and/or dysesthesia, are common early features (Zeidler *et al.*, 1997). Although the origin of such symptoms has been mainly attributed to a thalamic dysfunction (Macleod *et al.*, 2002), a contribution from a PNS dysfunction cannot be completely ruled out.

At variance with the above mentioned acquired prion diseases, experimental evidence for a centripetal spread through the PNS of the prion agent in sCJD is lacking. In this regard, the finding of a more frequent PNS involvement in sCJD subtypes related to the V2 strain is intriguing, given the similarities in the pattern of CNS spreading between these sCJD subtypes and the peripherally acquired forms of TSEs. Indeed, PrP^{Sc} accumulation in the CNS of sCJD VV2 is initially limited to subcortical structures in cases with the shortest duration, but show a widespread involvement of the cerebral neocortex in those with the longest course (Baiardi *et al.*, 2017), suggesting an “ascending” pathway of prion spreading. Thus, it is tempting to speculate that in VV2 and MV2K cases characterized by neuropathy at onset, the PNS involvement by the prion agent may occur simultaneously, or even precedes, that of the CNS according to a centripetal pattern of invasion. On the other hand, the present semiquantitative data on PrP^{Sc} deposition in peripheral nerves, demonstrating higher amounts of the abnormal protein in proximity of the CNS than in more distal portions (e.g. proximal cranial nerves > of intrapelvic sciatic nerve > of peroneal and sural nerves) support an anterograde spread of prions along peripheral axons.

Interestingly, PrP^{Sc} deposits in sCJD peripheral nerve fibers appear to be located in the adaxonal position (Hainfellner and Budka, 1999), where PrP^c was shown to play a physiological role in myelin maintenance (Bremer *et al.*, 2010; Küffer *et al.*, 2016). Whether these PrP^{Sc} deposits play a significant pathophysiological role in the development of the peripheral neuropathy as well as in the centripetal spread of the prion agent remains to be determined. In this regard, the lack of sufficient tissue specimens to perform a systematic correlative analysis among amount of PrP^{Sc} deposits in relation to their location along the nerve (i.e. proximal vs. distal) and presence and time of appearance of the peripheral neuropathy represents a limitation in this study.

In conclusion, a peripheral neuropathy, likely related to PrP^{Sc} deposition, may occur in sCJD, even as presenting clinical manifestation of the disease. This unusual, but likely underestimated onset, may represent a significant diagnostic challenge for neurologists, who should be aware of this rare cause of neuropathy. This notion is also of importance for the biosafety and management of peripheral tissue specimens such as nerve and muscle biopsies.

Given the current availability of prion specific CSF assays with high diagnostic accuracy CJD should be considered in the differential diagnosis of patients with a neuropathy of recent onset especially when associated with initial signs of CNS involvement. The finding of a significantly higher prevalence of PNS involvement in sCJD variants related to the V2 strain than in typical MM(V)1 further corroborates the PrP-specific aetiology of the peripheral neuropathy, suggests a variable peripheral tropism among sCJD strains, and raises the issue of the origin of peripheral prions early in the disease course in these patients.

PHENOTYPIC HETEROGENEITY OF GENETIC CJD

3.1 Background

Since the discovery of the first genetic variants linked to familial CJD in 1989 (Goldgaber *et al.*, 1989; Owen *et al.*, 1989), the existence of *PRNP* mutations raised questions about their effects on disease pathogenesis and phenotype.

Genetic linkage analyses provided direct evidence of the pathogenicity of some mutations (Goldfarb *et al.*, 1992a), whereas their high penetrance indirectly supported the pathogenic role of other variants (Minikel *et al.*, 2016). Nevertheless, a significant number of gCJD cases has an unremarkable family history, which indicates either a low penetrance of some specific mutations or even the possibility that some genetic variants are rare polymorphisms without significant pathogenic effect but increasing the susceptibility to the disease (Lloyd *et al.*, 2013).

The role of *PRNP* mutation on the phenotypic heterogeneity of gCJD is also a matter of debate. Indeed, while the *PRNP* primary sequence was originally thought to be the main determinant of the phenotype in gCJD, increasing evidence indicates that gCJD mainly reproduces the spectrum of the sCJD variants. Accordingly, the genotype at *PRNP* codon 129 (i.e. especially the allele in *cis* with the mutation), and the type of PrP^{Sc} accumulating in the brain represent the major determinants of the phenotypic expression also in the genetic form (Capellari *et al.*, 2011). In line with these observations, the initial experimental transmissions of gCJD in mice, monkeys, and bank voles induced disease phenotypes indistinguishable from those determined by sCJD inocula. More specifically, gCJD cases carrying *PRNP* mutations in *cis* with 129M and accumulating PrP^{Sc} type 1 transmitted identically to sCJD MM(V)1, those with variants in *cis* with 129V and PrP^{Sc} type 2 reproduced the sCJD VV2 induced phenotype, while the D178V-129M mutation associated with fatal familial insomnia shared transmission properties with sCJD MM2T (see paragraph 1.5).

Despite this evidence, however, no systematic studies on the phenotypic heterogeneity of gCJD has been carried out to date. Aiming to evaluate in more detail the heterogeneity of gCJD phenotypic expression, its relationship with specific *PRNP* mutations and the possible differences/analogies with the sCJD subtypes, we studied the clinical, histopathological and molecular features of a large cohort of gCJD cases representative of the majority of *PRNP* variants, and compared them to those obtained in sCJD.

3.2 Materials and method

3.2.1 Case selection and clinical data

The study was based on 157 cases with a definite diagnosis of gCJD obtained after clinical, neuropathological, and molecular examination. Probable gCJD cases with evidence of a pathogenic *PRNP* mutation, who did not undergo autopsy or biopsy for biochemical /neuropathological confirmation, were excluded. Thirty-six patients died in the USA, and 121 in Europe (83 in Italy, 31 in Germany, 6 in France, and 1 in the Netherlands).

Only medical records including at least one neurological examination were considered; accordingly clinical data were available in 143 cases. Duration of symptoms was calculated from the time of presentation of neurological signs suggesting an organic cause. Clinical signs were classified “at onset” when observed within the first quarter of the mean duration of symptoms of the group to which the patient belonged (i.e., 1 month if the mean duration was 4). We defined as ‘onset symptom(s)’ the first neurological disturbance(s) complained of by the patient at disease onset, and with ‘early symptoms’ those reported within the first quarter of the mean duration of symptoms of the group to which the patient belonged (i.e., 1 month if the mean duration was 4). Similarly, we designated as ‘early signs’ the abnormalities revealed

Phenotypic heterogeneity of genetic CJD

on neurological examinations within the first quarter of disease duration. Symptoms and signs were categorized according to the following 12 groups: cognitive (including the subcategories aphasia and memory loss), visual, oculomotor, ataxia/cerebellar, myoclonus, other dyskinesia (e.g. dystonia, chorea), parkinsonism, pyramidal, sensory, psychiatric, insomnia, pseudobulbar, seizures. When focal neurological signs occurred unilaterally at onset was also noted. The “cognitive” category included one or more among memory loss, confusion and/or disorientation, intellectual decline. The “visual” group accounted only for symptoms attributable to cortical dysfunction involving the occipital or occipitotemporal or occipito-parietal regions, including visual loss, visual field defect, visual distortion, abnormal color vision, cortical blindness. Finally, the “psychiatric” category included one or more among depression or anxiety of recent onset requiring psychiatric evaluation, delusions, hallucinations, panic attacks, and psychosis.

All available cerebral magnetic resonance imaging (MRI) results, including fluid-attenuated inversion recovery (FLAIR) and/or diffusion-weighted imaging (DWI) sequences, were reviewed, searching for hyperintensities on T2-FLAIR and/or DWI sequences in the temporal, parietal and occipital cortices, and in the striatum (Zerr *et al.*, 2009).

Electroencephalographic (EEG) abnormalities were categorized as follow: diffuse non-specific slowing, paroxysmal discharges (PDs) and periodic sharp-waves complexes (PSWCs).

When available, the results of CSF findings such as the detection of 14-3-3 protein and the dosage of total-tau protein and the search of abnormal PrP by RT-QuIC assay were also collected. In all CSF samples referred to the Laboratory of Neuropathology (NP lab), University of Bologna, Italy, the detection of the 14-3-3 protein was performed according to a standardized procedure, as previously described (Lattanzio *et al.*, 2017). Briefly, 10 µl of CSF were mixed with loading buffer, containing 4 mM EDTA, 6% (w/v) sodium dodecyl sulphate (SDS), 20% glycerol (w/v) and 50 mM Tris-HCl (pH 6.8), heated for 5 min at 100 °C. Proteins were then separated by SDS-PAGE on a 13% gel and transferred to a polyvinylidene fluoride (PVDF) membrane. After blotting, the PVDF membrane was blocked for 60 min with 10% (w/v) non-fat dry milk powder in Tris-buffered saline with 0.1% Tween-20 and incubated overnight at 4 °C with pan-anti-14-3-3 rabbit polyclonal primary antibody sc-629 (1:200, Santa Cruz Biotechnology, Inc.). The membrane was then incubated for 1 h at room temperature with an anti-rabbit horseradish peroxidase-linked secondary immunoglobulin diluted 1:3000. The immunoreactive signal was detected by enhanced chemiluminescence on a LAS 3000 camera, measured by densitometry using AIDA software and compared with two CSF controls with a weak or a strong 14-3-3 signal, respectively. Total tau (t-tau) protein levels were measured by quantitative ELISA (INNOTEST hTAU Ag, Innogenetics) according to the manufacturer’s instructions. The optimal cut-off value (1250pg/mL) was chosen based on receiver operating characteristic curve analysis, as previously described (Lattanzio *et al.*, 2017). Prion CSF RT-QuIC assays were performed using either the full length (23-231) (IQ) or truncated (90-231) (PQ) hamster recombinant PrP as substrate as described in (Franceschini *et al.*, 2017; Lattanzio *et al.*, 2017) (see also the paragraph 2.2.3).

3.2.2 Neuropathological analysis

A brain biopsy was performed in 11 patients, whereas the remaining underwent to autopsy according to a standardized protocol: brains were removed at autopsy and either one half or selected coronal sections of tissue, including all major brain structures and nuclei, were immediately frozen and stored at -80°C. The remaining tissue was fixed in formalin and was used for neuropathological examination and PrP immunohistochemistry.

Phenotypic heterogeneity of genetic CJD

Sampling of fixed tissues was performed in Bologna (Italy), Cleveland (USA), Munich (Germany) and Indianapolis (USA); all these Centers are involved in CJD National surveillance and Brain banking, CJD brains are sampled extensively according to protocols, which included all the areas that were of interest for the present study. Histopathological examination was performed on 7 µm thick sections of formalin-fixed and paraffin-embedded brain tissue blocks. Sections of interest were taken from neocortical areas of each lobe, basal ganglia, thalamus, hippocampus, amygdala, midbrain, pons, medulla oblongata and cerebellum (vermis and hemisphere with and without the dentate nucleus). Semiquantitative evaluation of spongiform change, gliosis, and neuronal loss was performed on hematoxylin and eosin stained sections. Spongiosis was scored on a 0 to 4 scale (not detectable, mild, moderate, severe, and status spongiosus), while astrogliosis on a 0 to 3 scale (not detectable, mild, moderate, and severe). Then, lesion profiles were obtained by averaging the two scores for each brain region examined. For immunocytochemistry, tissue samples were processed by using the monoclonal antibody 3F4 (1:400, Signet Labs, MA, USA). Moreover, the extent of Alzheimer's disease (AD)/primary age related tauopathy (PART) was evaluated in a subgroup of 64 gCJD. In these cases, the antibodies 4G8 (1:5000, Signet Labs, MA, USA) and AT8 (1:100, Innogenetics, Gent, Belgium) were used to assess amyloid-beta (A β) and tau immunoreactivity.

3.2.3 Molecular genetic analysis

Pathogenic mutations were analysed by direct sequencing of *PRNP* open reading frame in all cases (n=157). The codon 129 genotype was examined by digestion with the restriction endonuclease *PvuII* in all subjects.

3.2.4 Protein studies

For biochemical protein analysis, samples of frozen gray matter (50-100 mg) were collected from the following regions: middle frontal gyrus, middle temporal gyrus, occipital cortex (calcarine cortex or lateral occipital gyrus), putamen nucleus, thalamus, and cerebellum (hemisphere or vermis). Regional typing was performed in 125 cases: in 62 of them were analyzed six areas, in 26 five areas, in 5 four areas, in 11 three areas, in 12 two areas, and in 9 one area.

The western blot analysis was carried out as described in paragraph 2.2.3. The immunoblot profile of PrP^{Sc} was classified as type 1 or type 2 based on electrophoretic mobility, migration of the unglycosylated band at 21 kDa or 19 kDa, respectively.

3.2.5 CJD classification

All gCJD cases were classified according to the type of mutation and the genotype at codon 129 in the mutated allele (i.e., *PRNP* haplotype) (Table 8).

Moreover, by analogy with the classification of sCJD, each gCJD case was given a histotype classification according to histopathological features, PrP^{Sc} type, and *PRNP* codon 129 genotypes. To this purpose the mixed CJD phenotypes were merged with the corresponding "pure" subtype based on the main phenotype, as follows: MM(V)1+ 2C merged with MM(V)1 and VV2 + 1 with VV2.

Table 8. List of *PRNP* haplotypes included in the study cohort.

<i>PRNP</i> haplotype	n	Gender (n)	Codon 129 genotype (n)	Age at onset: range (years)	Disease duration: range (months)
R148H-129M	1	F	MM	82	5.5
D178N-129V	11	F (5), M (6)	MV (5), VV (6)	36-51	11.0-47.0
T183A-129M	2	M (2)	MM (2)	40-41	48.0-108.0
T188K-129M	1	F	MV	57	1.5
E196K-129M	3	F (3)	MM (2), MV (1)	75-79	2.0-30.0
E196K-129V	1	M	VV	71	24.0
E200K-129M	54	F (25), M (29)	MM (46), MV (8)	36-78	1.5-50.0
E200K-129V	5	F (4), M (1)	MV (4), VV (1)	48-67	6.0-13.5
V203I-129M	2	F (1), M (1)	MM (1), MV (1)	76-87	1.0-2.0
R208H-129M ^a	6	F (4), M (2)	MM (4), MV (2)	58-80	2.0-29.0
R208H-129V	1	F	VV	63	28.0
V210I-129M	49	F (19), M (30)	MM (40), MV (9)	44-82	1.0-18.0
E211Q-129M	1	F	MM	40	8.0
E219G-129V	1	F	MV	52	25.0
3OPRIs-129M	1	M	MM	69	Na
4OPRIs-129M	4	F (1), M (3)	MM (4)	53-69	3.5-13.5
5OPRIs-129M	6	F (4), M (2)	MM (4), MV (2)	35-65	48.0-162.0
5OPRIs-129V	6	F (6)	MV (1), VV (5)	62-77	4.0-12.0
6OPRIs-129M	1	F	MV	52	120.0
6OPRIs-129V	1	F	MV	47	18.0

^a Homozygous mutation in one case.

Accordingly, cases were classified as follows:

- MM(V)1 (n=121), including 53 E200K-129M, 49 V210I-129M, 5 3-4OPRIs-129M, 6 R208H-129M, 2 V203I-129M, 3 E196K-129M, 1 R148H-129M, 1 T188K-129M, and 1 E211Q-129M.
- MM(V)2C (n=2), including 1 E200K-129M and 1 5OPRIs-129M.
- MV2 (n=5), including 4 E200K-129V and 1 6OPRIs-129V.
- MV2K (n=1): 6OPRIs-129V.
- VV2 (n=8), including 1 E200K-129V, 1 R208H-129V, E196K-129V, and 5 5OPRIs-129V.
- VV(M)1 (n=11), including 11 D178V-129M.
- Atypical (n=8), including 2 T183A-129M and 6 5-6OPRIs-129M.

To increase the number of cases in each group, subtypes were merged according to the corresponding strain:

- MM(V)1 cases = strain M1
- MM(V)2C cases = strain M2C
- MV2, MV2K and VV2 cases (merged in the VV(M)2 group) = strain V2
- VV(V)1 cases = strain V1

The clinical, neuropathological and biochemical results obtained were compared with those in a large series of sCJD cases from Europe and USA published in Parchi *et al.*, 1999 and 2009b.

3.3 Results

3.3.1 Demographic findings, age at onset and disease duration

Eighty-one subjects were from Italy, 36 from USA (two of them with Slovakian ancestry), 6 from France, 30 from Germany, 2 from Chile, 1 from China, and 1 from the Netherlands.

In the whole study population gender was equally distributed (female 50.3% vs male 47.7%, ratio 1:1). However, some differences were observed in the VV(M)2 group where women were most common (86.6%) and, to a lesser extent, in the MM(V)1 group where men were conversely most frequent (54%). A higher frequency of women within the V2 strain-related subgroup has also been recently reported in sCJD (Rossi *et al.*, 2019b).

The mean age at onset in the whole cohort was 62.7 ± 11.5 years, but with significant differences depending on the specific *PRNP* mutation and the histotype (Table 9). In particular, subjects carrying the D178N-129V, T183A-129M, and 5-6OPRIs-129M variants were the youngest at disease onset. While the latter mutations have been associated with atypical histopathological phenotypes which do not fit with those observed in sCJD (see below), the former showed analogies with the sCJD VV1 phenotype. Interestingly, among the sCJD subtypes, VV1 patients showed the youngest age at onset (see Table 1). Within the D178N-129V group, the age of onset was slightly lower in patients with 129 valine homozygosity than in those 129 heterozygous (mean 40.4 ± 4.5 vs 48.2 ± 3.3 years). When sCJD and gCJD subgroups were compared, the age at onset was similar, indirectly supporting the hypothesis that only some mutations may promote the early appearance of the disease (mean age at onset gCJD vs sCJD: MM(V)1 64.5 vs 65.5 years; VV2 63.6 vs 61.3 years; MV2 58.8 vs 59.4 years; MM2C 69.0 vs 64.3 years; VV1 40.5 vs 39.3 years, sCJD data taken from Parchi *et al.*, 1999).

Overall the mean disease duration was 12.7 ± 24.8 years. As for age at onset, both the specific *PRNP* mutation and the histotype influenced the disease duration (Table 9). MM(V)1 cases had the shortest clinical course (5.2 ± 6.1 months), followed by the VV(M)2 (12.7 ± 8.1 months), VV(M)1 (21.7 ± 10.4 months), and MM(V)2C (96.0 months) groups. These results were similar to those observed in the corresponding sCJD subtype, with minor exceptions. For example, the disease duration was longer in genetic than in sporadic MM(V)2C, but, given the single genetic case available, this result needs to be confirmed in a larger cohort. In the VV(M)2, the VV2 and MV2 cases were merged, although notoriously they differ for disease duration in sCJD (i.e. shorter in VV2, Table 1). Although the mean disease duration in the merged group was similar in sCJD and gCJD, in the latter no differences were found in VV2 and MV2 cases (12.1 ± 9.9 vs 13.3 ± 6.5 months, respectively). This observation may depend on the high prevalence of 5-6OPRIs cases associated with codon 129 valine homozygosity. In these cases the effect of the specific mutation could have overcome that of the histotype; accordingly 5-6OPRIs-129M had significantly longer duration than typical MM(V)1. In the VV(M)1 group the mean disease duration was shorter in the subjects carrying 129VV (17.2 ± 3.7 months) than in those MV (26.2 ± 13.5 months). No differences were found associated with the *PRNP* codon 129 genotype in the other subtypes. Finally, the atypical phenotypes associated with the rare mutation T183A-129M and with the 5-6OPRIs had an extremely long duration, 78.0 ± 42.4 and 106.5 ± 37.9 months, respectively.

Phenotypic heterogeneity of genetic CJD

Table 9. Gender, age at onset and duration of symptoms.

Phenotype	MM(V)1				MM(V)2C	VV(M)2			VV(M)1	Others	
	E200K- 129M	V210I- 129M	3-4OPRIs- 129M	Others ^a	^b	E200K- 129V	5-6OPRIs- 129V	Others ^c	D178N- V129	T183A- 129M	5-6OPRIs- 129M
No. of cases	53	49	5	14	2 [*]	5	7	3	11	2	6
Female (%)	45.3	39.6	20.0	78.6	100.0	80.0	100.0	66.7	45.4	0.0	50.0
Age at onset (yr.)	62.2±9.1	65.2±9.4	63.2±7.0	70.5±1 2.6	69.0±5.9	58.0±7.3	63.6±8.9	62.0±9.5	44.3±5.5	40.5±0.7	41.8±6.0
Duration (mo.)	5.4±6.9	3.7±2.9	8.6±4.9	7.9±9.5	96.0	10.1±3.4	8.5±5.4	25.7±2.1	21.7±10.4	78.0±42.4	106.5±37.9

Age at onset and disease duration were expressed as mean and standard deviation.

^a R208H, V203I, E196K, R148H, T188K, E211Q. ^b E200K, 5OPRIs. ^c Includes E219G, E196K, R208H.

* Disease duration was available in one case only.

3.3.2 Clinical findings

Symptoms and signs at onset

Data were available in 143 cases. In line with previous observations in sCJD (Parchi *et al.*, 1999, 2009b), cognitive dysfunction was the most frequent manifestation at disease onset also in the present series of gCJD cases (62.2%) followed by cerebellar symptoms/signs (58.7%). However, the latter were slightly more common in the present gCJD group compared to a large cohort of sCJD patients (58.7% vs 47%) (Parchi *et al.*, 1999). The distribution of cognitive symptoms at onset in the MM(V)1 subtype was also different between sCJD and gCJD: in detail, while in the former group the cognitive impairment was more common than the cerebellar one (70% and 33%, respectively) (Parchi *et al.*, 1999), in the latter they showed similar frequencies (62.7% and 59.3%). Similarly to sCJD, the gCJD VV(M)2 group showed the highest prevalence of cerebellar symptoms/signs at onset (78.6%) and remarkably within this group symptoms/signs were more frequent in VV2 than in MV2 cases (85.7% vs 71.4%). Conversely, VV2 showed a lower prevalence of cognitive symptoms at onset compared to MV2 (42.9% vs 57.1%). Other similarities with sCJD concern the exclusive association of some manifestations at onset with the MM(V)1 subtype: 22.9% of patient belonging to MM(V)1 presented with visual symptoms, 8.5% with dyskinesia other than myoclonus, and 14.5% with unilateral, focal neurological signs, such as limb weakness. Psychiatric symptoms requiring specialist evaluation/intervention were observed at onset in 10-15% of patients belonging to the MM(V)1, the VV(M)2 and the VV(M)1 subtypes. Finally, it is remarkable that 12.5% of patients carrying the E200K-129M mutation complained of sensory symptoms at onset. Since the percentage of sensory manifestations in the other mutation belonging to the MM(V)1 group was significantly lower, a possible mutation-specific effect cannot be ruled out.

The symptoms/signs at disease onset in the gCJD cohort are summarized in Table 10.

Clinical symptom/signs during evolution

Data were available in 145 cases. Dementia characterized almost all gCJD subjects with the exception of a relatively small group of MM(V)1 (i.e. E200K-129M and V210I-129M) who abruptly lapsed into a stupor/coma and presented neurological signs without dementia at onset, and 1 case E200K-129V with disease duration of 11 months who manifested cerebellar ataxia at onset and did not develop cognitive dysfunction throughout the entire course of the disease. Cerebellar symptoms/signs were highest in the VV(M)2 group virtually affecting all patients belonging to this group; they were also found in about 80% of MM(1) cases and in ~50% of VV(M)1. Visual symptoms and dyskinesia were seen most frequently in the MM(V)1 group (28.9% and 21.5%, respectively) compared to the other subtypes. Myoclonus was observed in 100% of D178N-129M cases and in a significant percentage of cases in the MM(V)1 group (66.9%). It was also reported in 42.9% of VV(M)2 cases in association with very long disease duration (e.g., R208H-129V, 28 months, and E219G-129V, 25 months) or in subjects carrying the 5-6OPRIs-129V mutation. Pyramidal signs and parkinsonism have been reported in association with all the subtypes, and usually, they are observed in a late disease stage. Seizures are also a late manifestation affecting about 20% of gCJD subjects. Although seizures were observed in all the subtypes, they were less frequent in the VV(M)2 group.

The symptoms/signs throughout the entire disease course in the gCJD cohort are summarized in Table 11.

Phenotypic heterogeneity of genetic CJD

Table 9. Symptoms and signs at onset (in %).

Phenotype	MM(V)1				MM(V)2C	VV(M)2			VV(M)1	Others	
	Mutation	E200K- 129M	V210I- 129M	4OPRI- 129M	Others ^a	5OPRI- 129M	E200K- 129V	5-6OPRI- 129V	Others ^b	D178N- V129	T183A- 129M
No. of cases	48	47	4	13	1	5	6	3	7	2	6
Cognitive [^]	62.5	57.4	50.0	69.2	0.0	20.0	66.7	66.7	85.7	100.0	100.0
Aphasia [*]	10.4	8.5	0.0	0.0	0.0	0.0	0.0	33.3	0.0	0.0	0.0
Memory loss [*]	8.3	4.3	0.0	15.4	0.0	20.0	33.3	0.0	14.3	0.0	0.0
Visual [§]	14.6	36.2	0.0	23.1	0.0	0.0	0.0	0.0	0.0	0.0	0.0
Oculomotor	6.3	2.1	0.0	7.7	0.0	20.0	0.0	0.0	0.0	0.0	0.0
Cerebellar	70.8	53.2	25.0	53.8	100.0	100.0	83.3	33.3	28.6	0.0	50.0
Myoclonus	4.2	4.3	0.0	0.0	0.0	0.0	0.0	0.0	0.0	0.0	0.0
Other dyskinesia	8.3	12.8	0.0	0.0	0.0	0.0	0.0	0.0	0.0	0.0	0.0
Parkinsonism	2.1	4.3	0.0	7.7	0.0	0.0	16.7	0.0	0.0	50.0	16.7
Pyramidal	10.4	6.4	0.0	0.0	0.0	0.0	0.0	0.0	0.0	0.0	0.0
Sensory	12.5	6.4	25.0	0.0	0.0	0.0	0.0	0.0	0.0	0.0	0.0
Psychiatric [£]	6.3	17.0	0.0	23.1	100.0	0.0	16.7	0.0	14.1	0.0	0.0
Insomnia	12.5	6.4	0.0	0.0	0.0	0.0	16.7	0.0	0.0	0.0	0.0
Pseudobulbar	2.1	0.0	0.0	0.0	0.0	0.0	0.0	0.0	0.0	0.0	0.0
Unilateral	16.7	19.1	0.0	0.0	0.0	0.0	0.0	0.0	0.0	0.0	0.0

^a R208H V203I, E196K, R148H, T188K, E211Q. ^b E219G, E196K, R208H.

[^] One or more of memory loss, confusion and/or disorientation, intellectual decline.

^{*} Isolated deficit at onset.

[§] One or more of visual loss, visual field defect, visual distortion, abnormal colour vision, cortical blindness.

[£] One or more of depression or anxiety of recent onset requiring psychiatric evaluation, delusions, hallucinations, panic attacks, psychosis.

Phenotypic heterogeneity of genetic CJD

Table 10. Symptoms and signs throughout the entire course of the illness (in %).

Phenotype	MM(V)1				MM(V)2C	VV(M)2			VV(M)1	Others	
	E200K- 129M	V210I- 129M	4OPRIs- 129M	Others ^a	5OPRIs- 129M	E200K- 129V	5-6OPRIs- 129V	Others ^b	D178N- V129	T183A- 129M	5-6OPRIs- 129M
No. of cases	49	49	4	13	1	5	6	3	7	2	6
Cognitive [^]	93.9	89.8	100.0	100.0	100.0	80.0	100.0	100.0	100.0	100.0	100.0
Visual [§]	26.5	36.7	0.0	23.1	0.0	20.0	16.7	0.0	28.6	0.0	33.3
Oculomotor	18.4	12.2	0.0	7.7	0.0	40.0	0.0	0.0	0.0	0.0	16.7
Cerebellar	81.6	81.6	100.0	84.6	100.0	100.0	100.0	66.7	57.1	50.0	100.0
Myoclonus	77.6	57.1	75.0	69.2	0.0	0.0	66.7	66.7	100.0	0.0	50.0
Seizures	28.6	14.3	25.0	0.0	100.0	0.0	0.0	33.3	28.6	0.0	50.0
Other dyskinesia	20.4	28.6	0.0	0.0	0.0	0.0	0.0	0.0	42.9	0.0	33.3
Parkinsonism	24.5	26.5	75.0	15.4	100.0	20.0	66.7	33.3	85.7	50.0	33.3
Pyramidal	61.2	55.1	75.5	23.1	100.0	20.0	33.3	66.7	71.4	0.0	50.0
Sensory	18.4	12.2	25.0	7.7	0.0	0.0	0.0	33.3	0.0	0.0	0.0
Psychiatric [£]	20.4	34.7	50.0	53.8	100.0	80.0	33.3	0.0	14.1	50.0	33.3
Pseudobulbar	14.3	6.1	0.0	23.1	0.0	40.0	0.0	0.0	0.0	0.0	16.7

^a R208H, V203I, E196K, R148H, T188K, E211Q. ^b E219G, E196K, R208H.

[^] One or more of memory loss, confusion and/or disorientation, intellectual decline.

[§] One or more of visual loss, visual field defect, visual distortion, abnormal colour vision, cortical blindness.

[£] One or more of depression or anxiety of recent onset requiring psychiatric evaluation, delusions, hallucinations, panic attacks, psychosis.

Phenotypic heterogeneity of genetic CJD

Diagnostic investigations

EEG results were available in 129 cases. Electroencephalographic recordings showed typical PSWCs in 60% of gCJD cases. As in sCJD (Parchi *et al.*, 1999), this finding was most frequent in the MM(V)1 subtype (about 68.2% of cases), than in the others (MM(V)2C 50%, VV(M)2 23.1%, VV(M)1 20.0%). PSWCs were also found in 40% of 5-6OPRIs-129M patients. Within the MM(V)1 group, PSWCs were less common in the E200K-129M compared to V210I-129M and other missense mutations (59.2% vs 79.5% vs 83.3%); this finding may account for PSWCs slightly lower frequency in the genetic compared to sporadic MM(V)1 group (68.2% vs 80%). The mean time of appearance of PSWCs was significantly earlier in the patients belonging to the MM(V)1 subtype than to the others (2.3 ± 1.8 vs 7.0 ± 2.6 months). Paroxysmal electroencephalographic activities (i.e. ictal and not-ictal discharges) were also slightly most common in MM(V)1 patients compared to VV(M)2 (15% vs 7.7%), while they were not found in the MM(V)2C and VV(M)1 groups. Finally, diffuse unspecific slowing was the unique finding in about 25% of gCJD cases, being especially observed in the VV(M)2 (69.2%) and VV(M)1 (80%) subjects (Table 11).

MRI including FLAIR and/or DWI sequences was available in a subgroup of 51 subjects. According to (Zerr *et al.*, 2009), “typical” cortical and/or basal ganglia hyperintensities were found in 74.5% of these cases. Abnormal MRI findings involved the striatum in 81.6% of cases, the cortical ribbon in 50%, and thalamus in 13.2%. Although the prevalence of typical MRI findings in the present gCJD cohort was only slightly lower than that originally reported by (Zerr *et al.*, 2009) in a large series of sCJD cases (80.9%), more recent studies have demonstrated that MRI has a sensitivity up to 92% (Rudge *et al.*, 2018). Some factors may be responsible for this divergence including: 1) the MR images were analysed in various medical centers by different physicians with variable expertise in CJD, 2) MRIs were performed within a broad range of years during which MR technology has progressively improved its accuracy. Although the comparison of MRI findings in the various subtypes between gCJD and sCJD is limited by the small samples evaluated in the former group, the most striking difference is the significantly lower prevalence of typical imaging alterations within the VV(M)2 group in gCJD (66.7%) than in sCJD (87.5%-96.7%) (Baiardi *et al.*, 2017; Franceschini *et al.*, 2017). Notably, among the sCJD subtypes, FLAIR/DW MRI has the highest sensitivity in VV2 and MV2K (Baiardi *et al.*, 2017; Foutz *et al.*, 2017; Franceschini *et al.*, 2017). MRI findings in gCJD are summarized in Table 12.

CSF 14-3-3 protein was tested positive in 68 out of 81 cases (83.9%); more specifically, it was positive in 81.4% of MM(V)1 subjects and in all those belonging to the gCJD VV(M)2 group, namely 6 VV2 and 4 MV2 cases. In sCJD while CSF 14-3-3 protein is virtually found positive in all VV2 cases (i.e. 100% sensitivity) according to (Baiardi *et al.*, 2017; Foutz *et al.*, 2017; Franceschini *et al.*, 2017; Lattanzio *et al.*, 2017), it showed suboptimal sensitivity in MV2K (i.e. 11.1%-87.5%) (Zerr *et al.*, 2009; Foutz *et al.*, 2017; Franceschini *et al.*, 2017). CSF t-tau protein was >1250 pg/ml in 95.5% of cases (29 out of 31) revealing a diagnostic sensitivity higher than 14-3-3 protein. The two subjects, both carrying the E200K-129V variant, who tested negative belonged to MV2 subtype (overall sensitivity in this subgroup 50%), paralleling the findings in sCJD of a suboptimal sensitivity in MV2K cases. Finally, CSF prion RT-QuIC was positive in all 21 cases tested irrespective of the mutation, subtype and type of recombinant hamster prion protein (23-231 full-length PrP or IQ; 90-231 truncated PrP or PQ). Results of CSF analyses are summarized in Table 13.

Phenotypic heterogeneity of genetic CJD

Table 11. Electroencephalographic findings (in %).

Phenotype	MM(V)1				MM(V)2C ^b	VV(M)2			VV(M)1	Others	
	E200K-129M	V210I-129M	4OPRI-129M	Others ^a 12		E200K-129V	5-6OPRI-129V	Others ^c		D178N-V129	T183A-129M
Mutation											
No. of cases	49	39	2		2	5	6	2	5	2	5
Typical	59.2	79.5	50.0	83.3	50.0	0.0	33.3	50.0	20.0	0.0	40.0
PSWCs [^]											
Paroxysmal discharges [§]	16.3	15.4	0.0	8.3	0.0	0.0	16.7	0.0	0.0	0.0	20.0
Slowing only	24.5	5.1	50.0	8.3	50.0	100.0	50.0	50.0	80.0	100.0	40.0

^a R208H, V203I, E196K, R148H, E211Q. ^b E200K, 5OPRI. ^c E196K, R208H.

[^] Periodic sharp-waves complexes. [§] Paroxysmal discharges without periodism.

Table 12. Magnetic resonance imaging findings (in %).

Phenotype	MM(V)1				VV(M)2			Others	
	E200K-129M	V210I-129M	4OPRI-129M	Others ^a	E200K-129V	5OPRI-129V	E219G-129V	T183A-129M	5-6OPRI-129M
Mutation									
No. of cases	19	17	1	4	4	1	1	2	2
Typical [^]	84.2	88.2	0.0	50.0	50.0	100.0	100.0	0.0	0.0
Cerebral cortex	56.3	53.3	-	50.0	0.0	0.0	100.0	-	-
Striatum	93.8	73.3	-	50.0	100.0	100.0	100.0	-	-
Thalamus	12.2	13.3	-	0.0	50.0	0.0	0.0	-	-

Typical MRI findings were defined according to (Zerr *et al.*, 2009). Only cases with at least one exam performed with diffusion weighted (DW) imaging or fluid attenuated inversion recovery (FLAIR) sequences were included in the analysis. ^a R208H, E196K.

Phenotypic heterogeneity of genetic CJD

Table 13. Cerebrospinal fluid findings (in %).

Phenotype	MM(V)1				MM(V)2C	VV(M)2			VV(M)1	Others	
	E200K- 129M	V210I- 129M	4OPRIs- 129M	Others ^a	E200K- 129M	E200K- 129V	5-6OPRIs- 129V	Others ^b	D178N- V129	T183A- 129M	5-6OPRIs- 129M
Positive 14-3-3	80.9 (21)	75.8 (33)	100.0 (3)	100.0 (11)	100.0 (1)	100.0 (4)	100.0 (3)	100.0 (3)	-	-	50.0 (2)
T-tau >1250 pg/ml	100.0 (10)	100.0 (9)	100.0 (3)	100.0 (4)	100.0 (1)	33.3 (3)	-	100.0 (1)	-	-	-
Positive RT- QuIC assay	100.0 (7)	100.0 (7)	100.0 (2)	100.0 (2)	100.0 (2)	-	-	100.0 (1)	-	-	-
IQ [^]	100.0 (7)	100.0 (6)	100.0 (2)	100.0 (1)	100.0 (2)			100.0 (1)			
PQ [§]	100.0 (6)	100.0 (5)	100.0 (1)	100.0 (1)	100.0 (1)			100.0 (1)			

The number of cases available for each CSF analysis is shown in brackets.

^a Include R208H, V203I, E196K, R148H, T188K, E211Q.

^b Include E219G, E196K, R208H.

[^] First generation RT-QuIC assay with full-length (23-231) hamster recombinant prion protein.

[§] Second generation RT-QuIC assay with truncated (90-231) hamster recombinant prion protein.

3.3.3 Neuropathological findings

Lesion profiles

A comprehensive neuropathological evaluation allowing the analysis of the regional distribution of pathological changes throughout the brain structures and the construction of the “lesion profiles” was available in 138 cases. Results of the present analysis in gCJD were compared with those in a cohort of 300 sCJD previously described (Parchi *et al.*, 1999).

The lesion profile of the MM(V)1 subtype was identical in gCJD and sCJD. All the neocortical areas were variably affected with neuropathological change usually most severe in the occipital neocortex, as well as striatum, thalamus, entorhinal cortex, and cerebellum; hippocampus and brainstem nuclei were usually spared (i.e. in several cases, especially in those of shorter disease duration, the latter regions were virtually spared). Within the MM(V)1 group no differences were documented among the different mutations. Notably, despite the significant longer disease duration and the peculiar different type of PrP^{Sc} deposits on immunochemistry (see below), 5-6OPRIs-129M mutation displayed a regional distribution of neuropathological change indistinguishable from the genetic variants belonging to the MM(V)1 group (Figure 8).

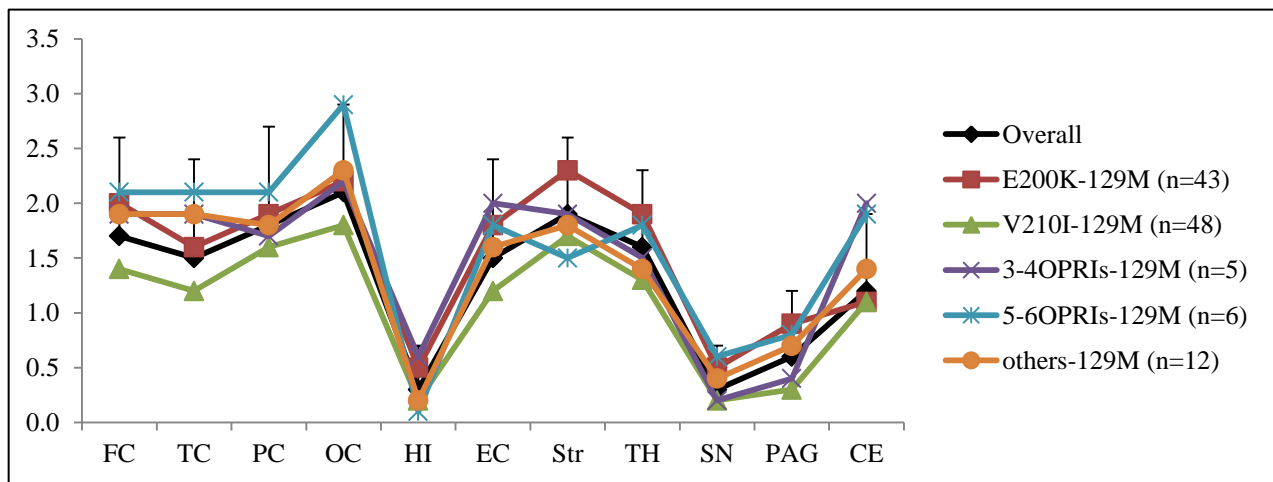


Figure 8. Lesion profile of the MM(V)1 subgroup and of 5-6OPRIs-129M mutation. Others include R208H-129M, V203I-129M, E196K-129M, T188K-129M, E211Q-129M.

The lesion profile gCJD VV(M)2 group was also consistent with the observation in sCJD VV2 and MV2K, with minor exceptions. It recapitulates the typical subcortical tropism of the strain V2: neuropathological changes were more severe in the striatum, thalamus, midbrain and cerebellum than in neocortical areas (Figure 9).

However, at variance with sCJD, when VV(M)2 cases were further divided into the MV2 and VV2, no differences were found in the lesion profiles, which were reminiscent of sCJD MV2K (Figure 10). This finding is likely related to the inclusion of two panencephalopathic sCJD cases in the VV2 subgroup. Indeed, it is well known that neuropathological change affects the neocortical region of VV2 in a time-dependent manner (i.e. the longer the disease duration is, the more severely the neocortices are affected) (Baiardi *et al.*, 2017). Once these cases are excluded from the analysis, the gCJD VV2 lesion profile matches that of sCJD and is clearly recognizable that also the hippocampus is significantly more affected than the neocortices (Figure 10).

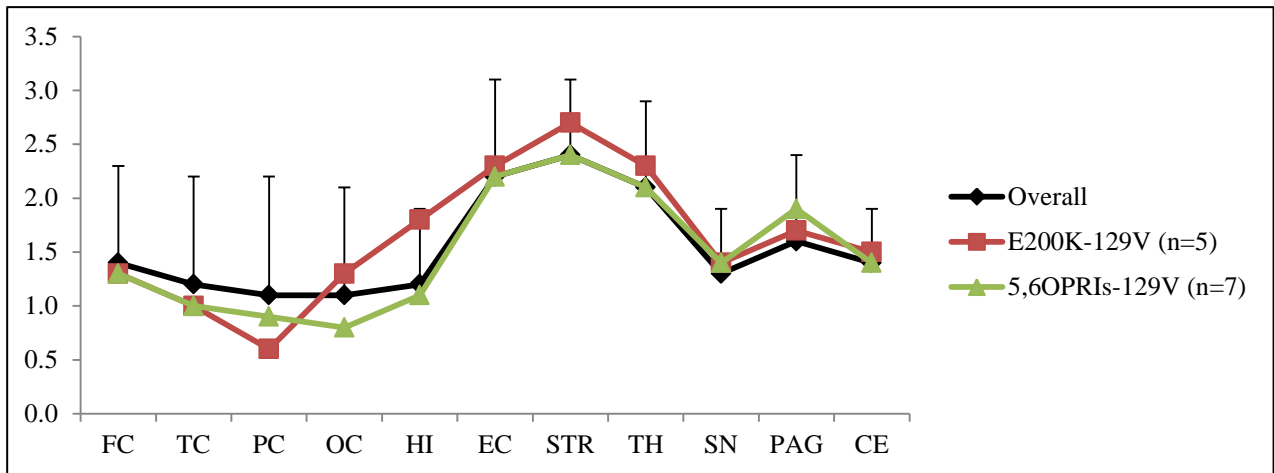


Figure 9. Lesion profile of the VV(M)2 subgroup.

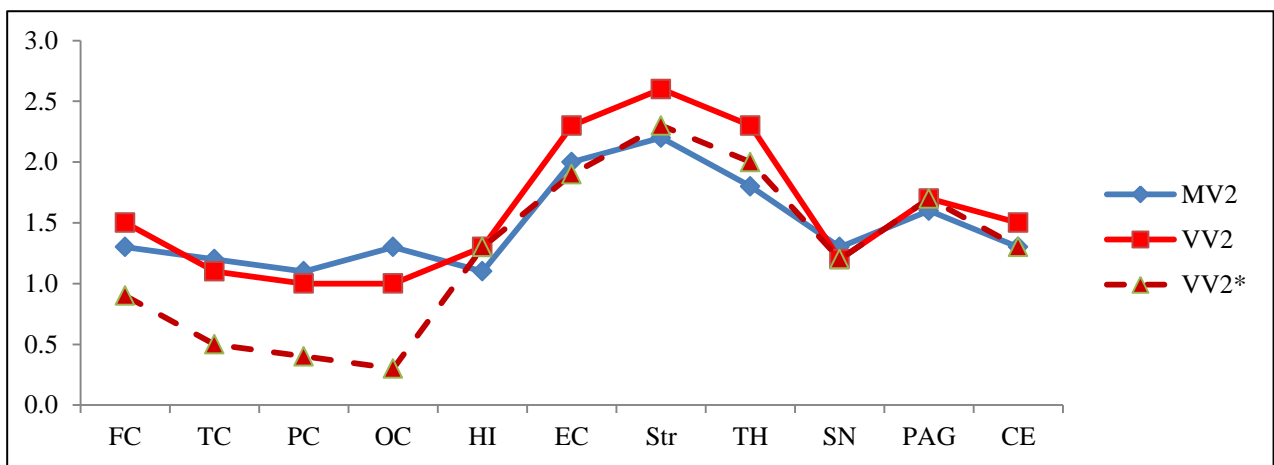


Figure 10. Lesion profile of gCJD VV2 and MV2 subtypes. *VV2 cases without panencephalopathic.

Despite the very small number of cases available which does not allow us to draw definite conclusions, the gCJD MM(V)2C also showed similarities with the corresponding sCJD subtype. The cortical regions (neocortices and entorhinal) were most significantly affected, while the hippocampus, the brainstem nuclei and the cerebellum were relatively spared. At variance with sCJD, striatum and thalamus were only mildly affected (Figure 11).

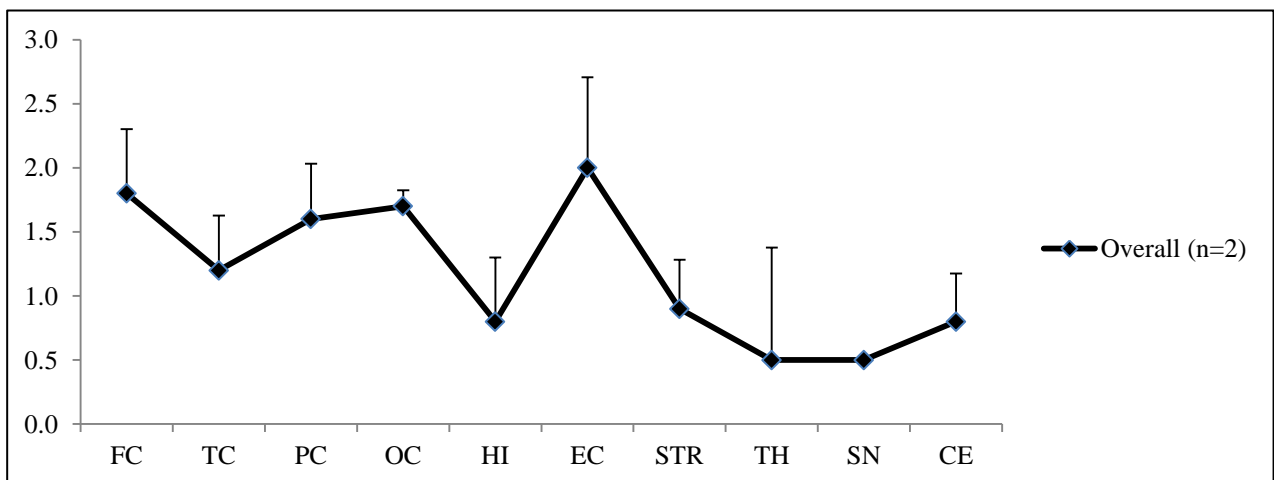


Figure 11. Lesion profile of the MM(V)2C subgroup.

Phenotypic heterogeneity of genetic CJD

The lesion profile of D178V-129V cases (=VV(M)1 group) is highly comparable to that of sCJD VV1: the neocortices (i.e. the occipital lobe showed the mildest neuropathological change among the cortical areas), the entorhinal cortex and the striatum were severely affected, while the thalamus revealed only moderate pathological change. Conversely, hippocampus, midbrain and cerebellum were virtually spared (Figure 12).

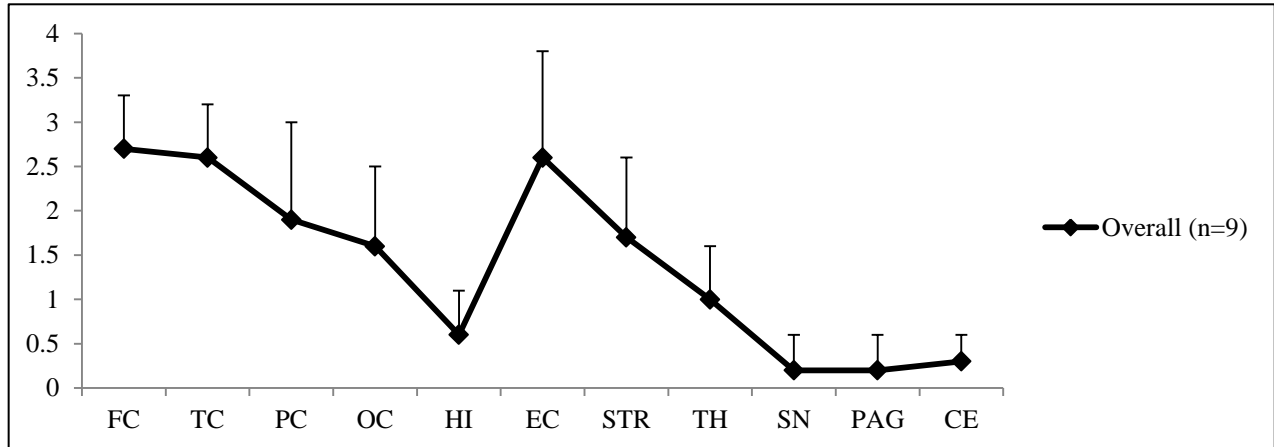


Figure 12. Lesion profile of the VV(M)1 subgroup.

Finally, the lesion profile of atypical T183A-129M cases did not share any features neither with subgroups carrying the mutation in *cis* with 129M nor with those accumulating PrP^{Sc} type 2. The neocortices and the striatum were the most severely affected regions, while the thalamus, the hippocampus and the cerebellum showed only mild neuropathological change. The brainstem nuclei were spared (Figure 13). Overall these findings were vaguely reminiscent of those in gCJD VV(M)1.

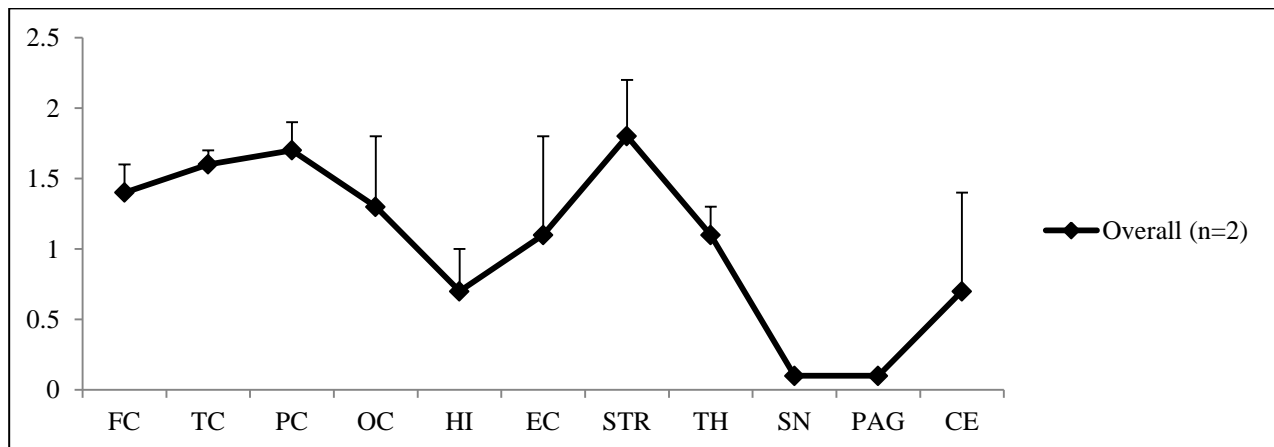


Figure 13. Lesion profile of the T183A-129M mutation.

Phenotypic heterogeneity of genetic CJD

Immunohistochemical findings

The pattern of PrP^{Sc} deposition at immunohistochemistry, which was performed in 126 gCJD cases representative of all the subtypes described above, largely overlapped that of the corresponding sCJD subtypes (Table 14, Figure 14). All the subtypes showed the synaptic pattern of PrP^{Sc} deposition in the cerebellum and/or cerebral cortex, but the MM(V)2C group in which PrP^{Sc} accumulated uniquely in the form of coarse perivacuolar deposits. Cerebellar plaque-like deposits were detected in all cases belonging to the VV(M)2 group, in about 30% of 5-6OPRIs-129M and occasionally in 4-OPRIs-129M (n=1) and D178V-129V (n=1). Moreover, the T183A-129M cases were characterized by both the synaptic and the cerebellar plaque-like patterns of PrP^{Sc} deposition. Punctate perineuronal PrP^{Sc} staining was most frequently found in association with the VV(M)2 subtype and to a lesser extent with the MM(V)1 one.

Remarkably, the coarse perivacuolar pattern was also found in 36.1% of MM(V)1 cases, and largely co-localized with large, confluent vacuoles, and in most cases was most evident in the occipital cortex. Similarly to sCJD, this finding is indirectly indicative of the coexistence of PrP^{Sc} type 1 and 2 within the same brain (i.e. mixed phenotype, see below).

A major difference with sCJD was found. Indeed, while the strain V2 in sCJD subjects carrying 129MV leads invariably to PrP^{Sc} deposition in the form of cerebellar kuru plaques (i.e. MV2K subtype), in gCJD they were observed only in one patient with the 6OPRIs-129V (codon 129 MV) mutation (1 out of 4 MV2 cases, 25%). Conversely, in sCJD VV2 cerebellar kuru plaques were never found, but one gCJD VV2 patient carrying the R208H-129V mutation with long disease duration (i.e. 28 months). Although the long duration may somehow promote the aggregation of PrP^{Sc} in the form of amyloid plaques, a mutation-specific effect is corroborated by similar findings in another case carrying the same mutation (Basset-Leobon *et al.*, 2006; Tiple *et al.*, 2019).

Other unusual patterns of PrP^{Sc} deposition in gCJD were detected in association with some mutations, rather than with the subtype. They include:

- a) About 35% of cases carrying the E200K-129M variant showed a peculiar patchy “dense”/fine granular synaptic PrP^{Sc} deposition, which is most evident in the molecular layer of the cerebellum (Figure 14). Sometimes, especially at lower microscopic magnification, these deposits may have a “cotton-wool” or “bushes” aspects.
- b) The OPRIs-129M mutations, independently of the number of octarepeat insertion showed linear PrP^{Sc} accumulations perpendicular to the surface in the molecular layer of the cerebellum (Figure 14).
- c) Intraneuronal deposition of PrP^{Sc} was found in E200K-129V cases (Figure 14).

Phenotypic heterogeneity of genetic CJD

Table 14. Patterns of PrP^{Sc} deposition (in %).

Mutation	MM(V)1				MM(V)2C	VV(M)2			VV(M)1	Others	
	E200K-	V210I-	3-4OPRI-	Others ^a	^b	E200K-	5OPRI-	Others ^c	D178N-	T183A-	5-6OPRI-
	129M	129M	129M			129V	129V		V129	129M	129M
No. of cases	38	42	5	12	2	3	7	2	7	2	6
Cerebellar or cortical synaptic	100.0	100.0	100.0	100.0	0.0	100.0	100.0	100.0	100.0	100.0	100.0
Cortical coarse perivacuolar	26.3	50.0	0.0	25.0	100.0	0.0	0.0	0.0	0.0	0.0	16.7
Punctate pericellular	10.5	11.9	20.0	16.7	0.0	100.0	42.9	50.0	0.0	0.0	0.0
Cerebellar plaque-like	0.0	0.0	20.0	0.0	0.0	100.0	100.0	100.0	14.3	100.0	33.3
Cerebellar kuru plaques	0.0	0.0	0.0	0.0	0.0	0.0	14.3	50.0	0.0	0.0	0.0
Dense synaptic	36.8	0.0	0.0	16.7	0.0	0.0	0.0	0.0	0.0	0.0	16.7
Cerebellar tract-like	0.0	0.0	80.0	0.0	0.0	0.0	0.0	0.0	0.0	0.0	50.0

^a Include R208H, V203I, E196K, R148H, E211Q.

^b Include E200K, 5OPRI.

^c Include E196K, R208H.

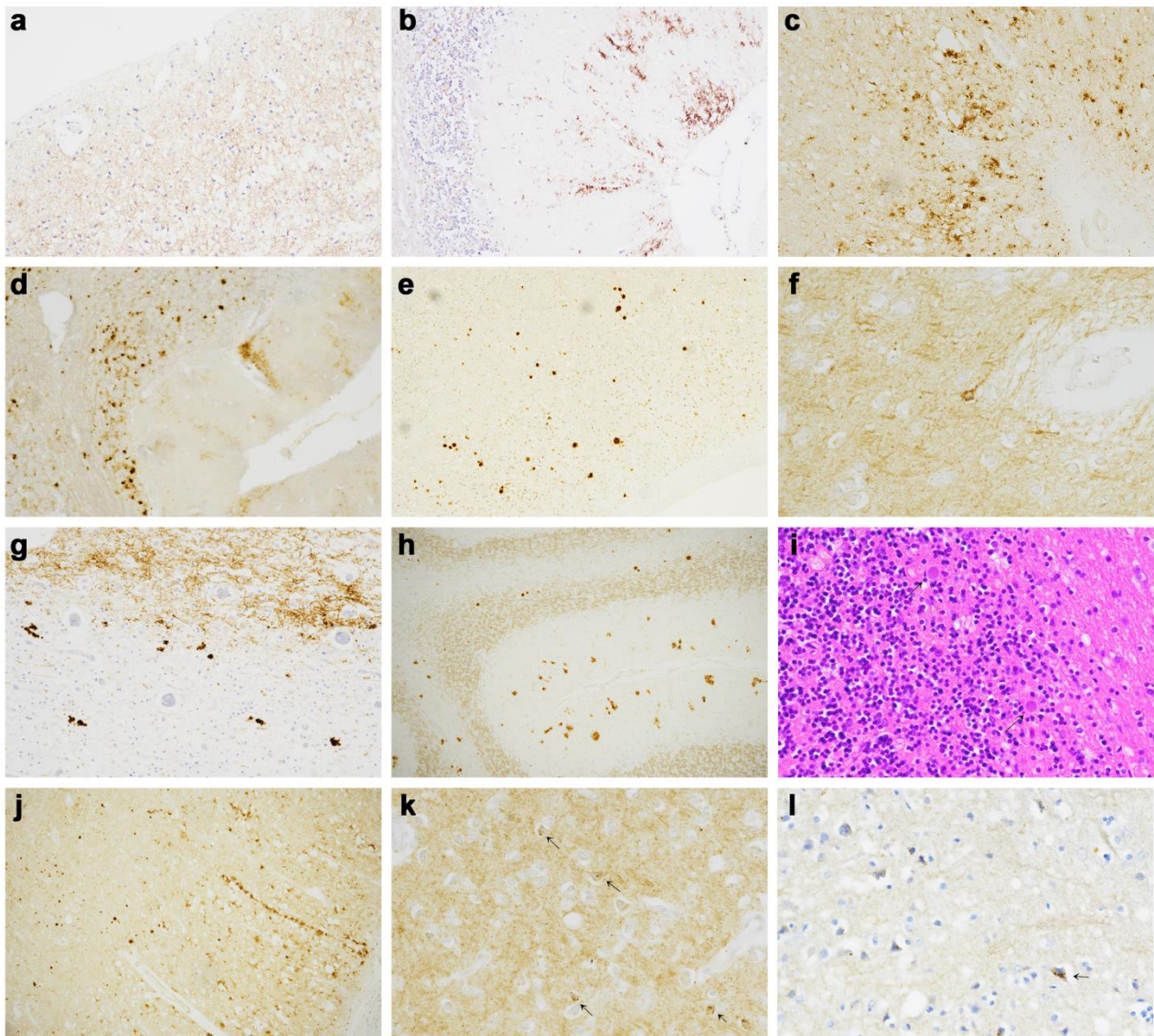


Figure 14. Patterns of PrP^{Sc} deposition in gCJD. (a) Synaptic deposition in the occipital cortex (x20). (b) Patchy “dense” synaptic deposits in the molecular layer of cerebellum in E200K-129M (x20). Coarse perivacuolar PrP^{Sc} aggregates co-localizing with large and confluent vacuoles in the occipital cortex (x20). (d-e) Plaque-like deposits in cerebellum (x20) and occipital cortex (x10). (f) Perineuronal deposits in the deep layer of temporal cortex (x40). (g-h) Amyloid PrP^{Sc} plaques in the white matter of the temporal lobe (x20) and cerebellum (x10); plaque-like deposits are evident in the molecular layer of cerebellum. (i) Unilocentric kuru plaques (arrows) at the transition between the molecular and granular layers of cerebellum (x40). (j) Linear PrP^{Sc} accumulations perpendicular to the surface in the molecular layer of the cerebellum in 5OPRI-129M (x10). (k-j) Intraneuronal PrP^{Sc} deposition in form of small granules in E200K-129V (x40). Immunohistochemistry of PrP with mAb 3F4 (a-h, j-l). Haematoxylin and eosin staining (i).

Phenotypic heterogeneity of genetic CJD

Alzheimer's disease/primary AD/PART pathology in genetic CJD

In a subgroup of 64 gCJD cases the relative level of AD pathology was assessed according to Thal's phases (A β) (Thal *et al.*, 2002), Braak's stages (tau) (Braak *et al.*, 2006) and ABC score (Montine *et al.*, 2012) and then compared to that in a cohort of 386 sCJD cases. No significant differences were found between the two groups. A similar result was obtained when the analysis was limited to the two most frequent mutations (i.e., E200K-129M and V210I-129M) compared to 270 sCJD cases belonging to the MM(V)1 subgroup (Table 15).

Table 15. Alzheimer's disease-related neuropathological changes in sCJD and gCJD.

No. of cases		sCJD 386 (%)	gCJD ^a 61 (%)	sCJDMM(V)1 270 (%)	V210I-129M 30 (%)	E200K-129M 20 (%)
ABC Score	Not	144 (37.3)	27 (44.3)	93 (34.4)	9 (30.0)	11 (55.0)
	Low	210 (54.4)	29 (47.5)	152 (56.3)	17 (56.7)	8 (40.0)
	Intermediate-High	32 (8.3)	5 (8.2)	25 (9.3)	4 (13.3)	1 (5.0)
Thal Phase	0	144 (37.3)	27 (44.3)	93 (34.4)	9 (30.0)	11 (55.0)
	1-2	118 (30.6)	15 (24.6)	84 (31.1)	8 (26.7)	4 (20.0)
	3	76 (19.7)	13 (21.3)	56 (20.7)	8 (26.7)	4 (20.0)
	4-5	48 (12.4)	6 (9.8)	37 (13.7)	5 (16.7)	1 (5.0)
Braak Stage	0	208 (53.9)	33 (54.1)	133 (49.3)	11 (36.7)	13 (65.0)
	I-II	133 (34.5)	25 (40.9)	102 (37.8)	15 (50.0)	6 (30.0)
	>III	45 (11.7)	5 (8.2)	35 (13.0)	4 (13.3)	1 (5.0)

^a Genetic CJD cases include the following mutations: V210I-129M (n=30), E200K-129M (n=20), E200K-129V (n=2), R208H-129M (n=4), V203I (n=2), 4-5OPRIs-129M (n=3).

3.3.4 PrP^{Sc} typing

As in sCJD we detected PrP^{Sc} Type 1 and type 2 in gCJD cases. Paralleling the distribution of PrP^{Sc} type among codon 129 genotypes in sCJD, also in gCJD the majority of MM subjects showed PrP^{Sc} type 1, whereas the VV predominantly displayed type 2. However, at variance with sCJD, in the present gCJD cohort, MV cases were found most frequently associated with PrP^{Sc} type 1 than with type 2, a finding best explained by overrepresentation of the MM(V)1 subtype relatively to the very small number of VV(M)2 cases.

Given the possible co-occurrence of both PrP^{Sc} types and their heterogeneous distribution within the brain, PrP^{Sc} typing was performed in 6 areas, namely frontal, temporal and occipital neocortices, striatum, thalamus and cerebellum, in 92 subjects for whom sufficient tissues were available. PrP^{Sc} type 1 and 2 co-occurrence was found in only 8.7% of cases (Table 16).

As previously described, the electrophoretic profile of E200K and D178N mutated PrP^{Sc} showed an overrepresentation of the diglycosylated band, whereas on the contrary, the same band was markedly under-represented in the T183A variant. In all the remaining *PRNP* mutations the western blot pattern was indistinguishable from that seen in sCJD.

Table 16. *PRNP* genotype and PrP^{Sc} type in 92 gCJD cases.

Type ^a	MM	MV	VV	Total
Type 1	58 (87.9)	14 (66.7)	1 (20.0)	73 (79.3)
Type 1+2 concurrence	5 (7.6)	2 (9.5)	1 (20.0)	8 (8.7)
Type 2	3 (4.5)	5 (23.8)	3 (60.0)	11 (11.9)
Total	66	21	5	92

^a Based on WB analysis (3F4 mAb) of at least 6 regions (frontal, temporal and occipital cortices, putamen, thalamus, and cerebellum). % are expressed in brackets and refer to each single column.

3.3.5 Mixed phenotypes in gCJD

Although we demonstrated the occurrence of both PrP^{Sc} types by Western blotting in less than 10% of gCJD, a significant number of cases (25.6%) showed mixed histopathological features, which indirectly suggest the PrP^{Sc} types 1+2 coexistence. Since the non-dominant phenotype may occur very focally, PrP^{Sc} typing based on western blotting may underestimate the extent of 1+2 coexistence as a consequence of inadequate brain sampling or more unlikely the use of only one antibody (i.e., mAb 3F4). To increase the accuracy of the identification of mixed phenotypes, we performed the analysis only in gCJD cases studied in detail by both PrP^{Sc} immunohistochemistry (at least 6 regions from cerebrum and cerebellum) and PrP^{Sc} typing (n=133). The results are summarized in Table 17.

Both the prevalence and the histopathological features of mixed phenotypes in gCJD largely overlapped those of sCJD. Among them, the most frequent MM(V)1+2C phenotype (94.1%) displayed varying relative amounts of the pure MM(V)1 (dominant) and MM(V)2C (non-dominant) subtypes. In this group, the typical histopathological features of the non-dominant phenotype (i.e. large confluent vacuoles and perivacuolar pattern of PrP^{Sc} accumulation) were found in the occipital (96.9%), parietal (46.9%), temporal (46.9%), and frontal (18.7%) cortices. Interestingly, this mixed phenotype was significantly more frequent in V210I-129M than in E200K-129M carriers (44.7% vs 18.4%), indicating a potential mutation-specific influence on PrP^{Sc} structural conversion. The MV2C+1 and VV2+1 were only found in one patient each (2.9%), carrying 5OPRIs-129M and 5OPRIs-respectively.

Table 17. Histotype based on IHC findings and PrP^{Sc} typing.

	MM(V)1	MM(V)1+2C	MV2C	MV2C+1	MV2/MV2K	VV(M)1	VV2	VV2+1	Atypical	Total
R148H	1	-	-	-	-/-	-	-	-	-	1
D178V	-	-	-	-	-/-	6	-	-	-	6
T183A	-	-	-	-	-	-	-	-	2	2
T188K	1	-	-	-	-/-	-	-	-	-	1
E196K	3	-	-	-	-/-	-	1	-	-	4
E200K	31	7	1	-	4/-	-	1	-	-	44
V203I	1	1	-	-	-/-	-	-	-	-	2
R208H	3	1	-	-	-/-	-	1*	-	-	5
V210I	26	21	-	-	-/-	-	-	-	-	47
E211Q	1	-	-	-	-/-	-	-	-	-	1
E219G	-	-	-	-	1/-	-	-	-	-	1
3,4OPRIs	2	-	-	-	-/-	-	-	-	3	5
5,6OPRIs	2	2	-	1	1/1	-	4	1	2	14
Total	71	32	1	1	6/1	6	7	1	7	133

Legend: *with cerebellar kuru plaques

3.4 Discussion

The results of the present study demonstrate, in the largest gCJD cohort examined to date, that the phenotypic spectrum of gCJD largely reproduces that of sCJD subtypes, although specific mutation also accounts for phenotypic variations in some cases.

Similarly to sCJD, the methionine at codon 129 of *PRNP* (129M) in *cis* with the mutation was most frequently associated with PrP^{Sc} type 1, and the valine codon (129V) to PrP^{Sc} type 2. As the only exception, D178N-129V haplotype has been linked to PrP^{Sc} type 1 rather than type 2. Accordingly, the main genetic determinant of the gCJD phenotype is not the *PRNP* variant itself, but the genotype at codon 129 in *cis* with the mutation, as confirmed by the divergent phenotypes found in subjects carrying the same mutation, but a distinct codon 129 genotype in *cis* with the mutation. However, only the E200K, R208H, E196K and OPRIs mutations have been found in *cis* either with 129M or 129V, while all the other variants were invariably in *cis* with 129M.

Despite the dominant role played by the 129 genotype in *cis* with the mutation, sometimes also the wild type allele may modify the disease phenotype. Within the VV(M)1 subgroup (i.e. gCJD D178N-129V), for example, subjects carrying 129VV showed a younger age at onset and a shorter disease duration than those carrying 129MV. Since in all subjects carrying the D178N mutation, PrP^{Sc} is only expressed by the mutant allele (Chen *et al.*, 1997), the allelic origin of PrP^{Sc} cannot explain this finding. The atypical glycoform is also unlikely responsible for that observation, given that in subjects carrying the E200K variant, which similarly to D178N showed both overexpression of the diglycosylated PrP^{Sc} isoform and selective conversion of mutant allele (Cardone *et al.*, 1999, Capellari *et al.*, 2000a), the wild type allele seems not to influence the disease phenotype. Intriguingly, FFI linked to the D178N-129M mutation is characterized by an analogous phenotypical heterogeneity associated with codon 129 homozygosity and heterozygosity

Phenotypic heterogeneity of genetic CJD

(Parchi *et al.*, 1998), suggesting that a genetic variant involving this specific *PRNP* codon might modulate the interaction between the mutant and the wild type alleles (e.g. changes in the tertiary or quaternary PrP^{Sc} structure).

Although demographic data largely overlaps between gCJD and sCJD, a significant younger age at onset and a longer disease duration characterize the “atypical” phenotypes linked to the 5-6OPRIs-129M and T183A-129M haplotypes, as previously reported (Goldfarb *et al.*, 1991; Nitrini *et al.*, 1997; Grasbon-Frodl *et al.*, 2004; Mead *et al.*, 2006). According to Croes *et al.*, in OPRIs mutations these demographic parameters relate to the number of *PRNP* octarepeat insertions, given that both age at onset and disease duration of subjects carrying 3-4OPRI-129M match those of sCJD MM(V)1s (Croes *et al.*, 2004). Notably, the same correlation in subjects carrying an OPRI expansion in *cis* with 129V, given that in 5-6OPRIs-129V, age at onset and disease duration are similar to those of the corresponding sCJD subtype.

Overall, clinical symptoms at onset and during the disease course in gCJD largely matched those of sCJD patients. Nevertheless, we also confirmed previous reports of a relative higher prevalence of sensory symptoms at onset in gCJD E200K-129M in comparison to sCJD MM(V)1 (Schelzke *et al.*, 2012; Feketeová *et al.*, 2018). Since PNS is most frequently involved at onset in the V2 strain-related subtypes, the sensory symptoms in E200K-129M may originate from a dysfunction of corticospinal somatosensory pathways rather than peripherally. In support of this hypothesis are the findings of an early PrP^{Sc} deposition in the spinal cord of a mouse model of gCJD-E200K (Friedman-Levi *et al.*, 2011).

The diagnostic test findings in gCJD were also qualitatively indistinguishable from those reported in sCJD; moreover, they matched the frequency distribution reported in the sCJD subtypes. As a minor difference, the sensitivity of MRI detection of the “typical” hyperintensities on DWI and FLAIR sequences in the VV(M)2 gCJD group was slightly lower than those previously reported in sCJD cohorts (Rudge *et al.*, 2018). The difference may also depend on the retrospective nature of the study, the broad variety of technical instruments adopted for image collection and the different expertise of neuroradiologists who evaluated the sequences.

Among CSF surrogate biomarkers of neurodegeneration, t-tau >1250 pg/ml had better sensitivity than 14-3-3 protein detection, as previously reported in sCJD (Lattanzio *et al.*, 2017). Finally, prion CSF RT-QuIC was tested positive in all the analysed cases providing the basis for a very accurate diagnosis *in vivo*. Of interest, gCJD linked to the E200K-129M mutation showed a higher ThT max mean value and a shorter lag phase in comparison to the other tested gCJD haplotypes (Franceschini *et al.*, 2017), indirectly indicating that mutant PrP^{Sc} associated with this genetic variant is more prone to conversion and aggregation.

With the significant exception of the “atypical” phenotype associated with the T183A-129M mutation, the lesion profiles of all the other haplotype largely overlapped those of the corresponding sCJD subtype. Additional histopathological differences concerned the presence of kuru plaques and the pattern of PrP^{Sc} deposition. Regarding the former aspect, kuru plaques were absent in the cerebellum of E200K-129V cases heterozygotes at codon 129 (i.e., with 129M in the wild-type allele), which might be attributed to the selective origin of PrP^{Sc} from the mutant allele. Indeed, sCJD cases with 129MV and belonging to the strain V2 are invariably associated with cerebellar kuru plaques (i.e. MV2K subtype) and the unglycosylated PrP^{Sc} isoforms show a “doublet” at western blot analysis, comprising one band migrating at 19 kDa (PrP^{Sc} type 2) and one at 20 kDa (i.e. intermediate between type 1 and 2, PrP^{Sc} type “i”) (Parchi *et al.*, 1999, 2009b). In contrast, in gCJD-E200K MV2 cases we only detected PrP^{Sc} type 2. Recent observations on iCJD in humans carrying MM and the characterization of their transmission properties provided critical information for the interpretation of these findings. While most iCJD-129MM cases are indistinguishable from sCJD MM(V)1, a subgroup shows the widespread occurrence of kuru plaques and plaque-like deposits, and PrP^{Sc} type “i” instead of type 1

Phenotypic heterogeneity of genetic CJD

(Kobayashi *et al.*, 2007). The latter iCJD group transmitted most efficiently the disease in knock-in mice expressing human PrP with 129VV, in analogies with the sCJD subtypes associated with V2 prions. Moreover, while PrP^{Sc} type “i” reproduced itself in 129MM mice, it shifted to PrP^{Sc} type 2 in the 129VV mice (Kobayashi *et al.*, 2007). The transmission of sCJD VV2 into 129MM mice (Kobayashi *et al.*, 2010), provided the final demonstration that both the kuru plaques and PrP^{Sc} “i” represent the hallmarks of the conversion of the codon 129M allele by V2 prions. In view of these findings, the lack of conversion of the wild-type 129M allele provides the best explanation for the absence of kuru plaques and of PrP^{Sc} type “i” in gCJD-E200K MV2. At variance, we found cerebellar kuru plaques in one case carrying the 6OPRIs-129V (129MV), which is consistent with the notion that both mutant and wild type allele are converted to PrP^{Sc} in OPRIs (Chen *et al.*, 1997).

Another exception to the findings in sCJD is the occurrence of kuru plaques in two subjects carrying the R208H-129VV genotype. This observation together with the notion that kuru plaques never occur in sCJD VV2 raised the possibility of a mutation-specific effect.

Additional phenotypic variations at PrP immunohistochemistry with respect to the findings in sCJD, which can also be attributed to mutation specific effects include the following: 1) OPRIs-129M showed linear PrP^{Sc} deposits, perpendicular to the surface of molecular layer of the cerebellum; 2) E200K-129M displayed a “dense” synaptic pattern of PrP^{Sc} accumulation in the molecular layer of cerebellum; 3) E200K-129V showed intraneuronal PrP^{Sc} deposits.

As stated above the T183A-129M showed an “atypical” histotype not fitting the general molecular rules of sCJD classification. Indeed, PrP^{Sc} type 2 in combination with 129M should lead to a MM2C or MM2T phenotype. While the lesion profile of T183A-129M might fit that of sCJDMM2C both the pattern of deposition (synaptic and plaque-like) and the type of vacuolation (intermediate without large confluent vacuoles) were significantly different. The known profound effects of the mutation on the processing of the mutated protein which lead to its intracellular accumulation of the mutated protein and the block of the addition of the first glycan to the Asp residue 181 (Capellari *et al.*, 2000b; Grasbon-Frodl *et al.*, 2004), resulting in the marked under-representation of the diglycosylated isoform, may be responsible of these histopathological differences. Future studies will be critical to demonstrate whether this gCJD variant also generates a specific prion strain upon serial transmission.

With regard to MM2 phenotype it is also noteworthy to underline the relative rarity of this variant in gCJD in comparison to sCJD. Indeed, we detected this histotype only in two subjects carrying E200K-129M and 5OPRIs-129M with heterozygosity at codon 129. Accordingly, the E200K and 5-OPRIs mutations are the only ones we found associated with three different prion strains, namely M1, V2 and M2C.

The spectrum of mixed phenotypes in gCJD reproduced the most common variants previously described in sCJD, namely the MM(V)1+2C, by far the most frequent, MM2C+1 and VV2+1 subtypes. However, Their overall frequency was slightly lower than in sCJD (25% vs 35%). The relative rarity of the mixed phenotypes in the large E200K-129M group may explain this difference. In contrast, the MM(V)1+2C phenotype had a prevalence of ~50% in subjects carrying V210I-129M, although a dominant 2C MM(V)2C phenotype (i.e., MM(V)2C+1) was never observed in this genetic variant. Altogether these findings may indicate that certain *PRNP* mutations may modulate the frequency of strain specific PrP^{Sc} conversion. In particular, the predominant representation of the diglycosylated isoform in the mutated PrP E200K could, at least partially, prevent the M2C strain conversion through a reduced PrP^C recruitment (Baskakov *et al.*, 2018). This hypothesis is also supported by the relative rarity of the M2C phenotype in gCJD variant linked to the D178N-129M haplotype (i.e. FFI).

In conclusion, the results of the present study confirm that, despite the presence of the *PRNP* mutations, which play a major role in determining disease susceptibility, the clinicopathological spectrum of gCJD largely overlap with

Phenotypic heterogeneity of genetic CJD

that of sCJD, supporting the view that both the disease forms are linked to the same prion strains. Nevertheless, besides conferring susceptibility to develop the disease, specific mutations may cause some minor modifications of the disease phenotype, including age at onset, disease duration, clinical presentation, the pattern of PrP^{Sc} deposition, and the prevalence of mixed phenotypes. The atypical gCJD phenotype linked to the T183A-129M haplotype represents the most significant example of a mutation specific effect and of the divergence from sporadic and genetic CJD. However, whether this atypical phenotype may lead to the demonstration of the “first” specific “genetic” CJD strain upon serial transmission remains to be seen.

REFERENCES

- Abu-Rumeileh S, Redaelli V, Baiardi S, Mackenzie G, Windl O, Ritchie DL, et al. Sporadic Fatal Insomnia in Europe: Phenotypic Features and Diagnostic Challenges. *Ann Neurol* 2018
- Aguzzi A. Recent developments in the pathogenesis, diagnosis, and therapy of prion diseases. *Dialogues Clin Neurosci* 2001; 3: 25–36.
- Aguzzi A, Heikenwalder M, Polymenidou M. Insights into prion strains and neurotoxicity. *Nat Rev Mol Cell Biol* 2007; 8: 552–561.
- Angus-Leppan H, Rudge P, Mead S, Collinge J, Vincent A. Autoantibodies in sporadic Creutzfeldt-Jakob disease. *JAMA Neurol* 2013; 70: 919–922.
- Asante EA, Gowland I, Grimshaw A, Linehan JM, Smidak M, Houghton R, et al. Absence of spontaneous disease and comparative prion susceptibility of transgenic mice expressing mutant human prion proteins. *J Gen Virol* 2009; 90: 546–558.
- Atarashi R, Moore RA, Sim VL, Hughson AG, Dorward DW, Onwubiko HA, et al. Ultrasensitive detection of scrapie prion protein using seeded conversion of recombinant prion protein. *Nat Methods* 2007; 4: 645–650.
- Atarashi R, Sano K, Satoh K, Nishida N. Real-time quaking-induced conversion: a highly sensitive assay for prion detection. *Prion* 2011; 5: 150–153.
- Babelhadj B, Di Bari MA, Pirisinu L, Chiappini B, Gaouar SBS, Riccardi G, et al. Prion Disease in Dromedary Camels, Algeria. *Emerging Infect Dis* 2018; 24: 1029–1036.
- Baiardi S, Capellari S, Bartoletti Stella A, Parchi P. Unusual Clinical Presentations Challenging the Early Clinical Diagnosis of Creutzfeldt-Jakob Disease. *J Alzheimers Dis* 2018; 64: 1051–1065.
- Baiardi S, Capellari S, Ladogana A, Strumia S, Santangelo M, Pocchiari M, et al. Revisiting the Heidenhain Variant of Creutzfeldt-Jakob Disease: Evidence for Prion Type Variability Influencing Clinical Course and Laboratory Findings. *J Alzheimers Dis* 2016; 50: 465–476.
- Baiardi S, Magherini A, Capellari S, Redaelli V, Ladogana A, Rossi M, et al. Towards an early clinical diagnosis of sporadic CJD VV2 (ataxic type). *J Neurol Neurosurg Psychiatry* 2017; 88: 764–772.
- Baiardi S, Redaelli V, Ripellino P, Rossi M, Franceschini A, Moggio M, et al. Prion-related peripheral neuropathy in sporadic Creutzfeldt-Jakob disease. *J Neurol Neurosurg Psychiatry* 2018
- Baiardi S, Rossi M, Capellari S, Parchi P. Recent advances in the histo-molecular pathology of human prion disease. *Brain Pathol* 2018
- Baron GS, Wehrly K, Dorward DW, Chesebro B, Caughey B. Conversion of raft associated prion protein to the protease-resistant state requires insertion of PrP-res (PrP(Sc)) into contiguous membranes. *EMBO J* 2002; 21: 1031–1040.
- Bartz JC. Prion Strain Diversity. *Cold Spring Harb Perspect Med* 2016; 6
- Baskakov IV, Katorcha E, Makarava N. Prion Strain-Specific Structure and Pathology: A View from the Perspective of Glycobiology. *Viruses* 2018; 10
- Basset-Leobon C, Uro-Coste E, Peoc'h K, Haik S, Sazdovitch V, Rigal M, et al. Familial Creutzfeldt-Jakob disease with an R208H-129V haplotype and Kuru plaques. *Arch Neurol* 2006; 63: 449–452.
- Bishop MT, Will RG, Manson JC. Defining sporadic Creutzfeldt-Jakob disease strains and their transmission properties. *Proc Natl Acad Sci USA* 2010; 107: 12005–12010.

References

- Bongianni M, Orrù C, Groveman BR, Sacchetto L, Fiorini M, Tonoli G, et al. Diagnosis of Human Prion Disease Using Real-Time Quaking-Induced Conversion Testing of Olfactory Mucosa and Cerebrospinal Fluid Samples. *JAMA Neurol* 2017; 74: 155–162.
- Bougard D, Brandel J-P, B elondrade M, B eringue V, Segarra C, Fleury H, et al. Detection of prions in the plasma of presymptomatic and symptomatic patients with variant Creutzfeldt-Jakob disease. *Sci Transl Med* 2016; 8: 370ra182.
- Braak H, Alafuzoff I, Arzberger T, Kretschmar H, Del Tredici K. Staging of Alzheimer disease-associated neurofibrillary pathology using paraffin sections and immunocytochemistry. *Acta Neuropathol* 2006; 112: 389–404.
- Brandner S, Isenmann S, Raeber A, Fischer M, Sailer A, Kobayashi Y, et al. Normal host prion protein necessary for scrapie-induced neurotoxicity. *Nature* 1996; 379: 339–343.
- Bremer J, Baumann F, Tiberi C, Wessig C, Fischer H, Schwarz P, et al. Axonal prion protein is required for peripheral myelin maintenance. *Nat Neurosci* 2010; 13: 310–318.
- Bruce ME. TSE strain variation. *Br Med Bull* 2003; 66: 99–108.
- B ueler H, Aguzzi A, Sailer A, Greiner RA, Autenried P, Aguet M, et al. Mice devoid of PrP are resistant to scrapie. *Cell* 1993; 73: 1339–1347.
- Calzolari L, Lysek DA, P erez DR, G untert P, W uthrich K. Prion protein NMR structures of chickens, turtles, and frogs. *Proc Natl Acad Sci USA* 2005; 102: 651–655.
- Campana V, Caputo A, Sarnataro D, Paladino S, Tivodar S, Zurzolo C. Characterization of the properties and trafficking of an anchorless form of the prion protein. *J Biol Chem* 2007; 282: 22747–22756.
- Capellari S, Parchi P, Russo CM, Sanford J, Sy MS, Gambetti P, et al. Effect of the E200K mutation on prion protein metabolism. Comparative study of a cell model and human brain. *Am J Pathol* 2000; 157: 613–622.
- Capellari S, Strammiello R, Saverioni D, Kretschmar H, Parchi P. Genetic Creutzfeldt-Jakob disease and fatal familial insomnia: insights into phenotypic variability and disease pathogenesis. *Acta Neuropathol* 2011; 121: 21–37.
- Capellari S, Zaidi SIA, Long AC, Kwon EE, Petersen RB. The Thr183Ala Mutation, Not the Loss of the First Glycosylation Site, Alters the Physical Properties of the Prion Protein. *J Alzheimers Dis* 2000; 2: 27–35.
- Cardone F, Liu QG, Petraroli R, Ladogana A, D’Alessandro M, Arpino C, et al. Prion protein glycoform analysis in familial and sporadic Creutzfeldt-Jakob disease patients. *Brain Res Bull* 1999; 49: 429–433.
- Caughey B, Baron GS, Chesebro B, Jeffrey M. Getting a grip on prions: oligomers, amyloids, and pathological membrane interactions. *Annu Rev Biochem* 2009; 78: 177–204.
- Caughey B, Lansbury PT. Protofibrils, pores, fibrils, and neurodegeneration: separating the responsible protein aggregates from the innocent bystanders. *Annu Rev Neurosci* 2003; 26: 267–298.
- Caughey B, Raymond GJ. The scrapie-associated form of PrP is made from a cell surface precursor that is both protease- and phospholipase-sensitive. *J Biol Chem* 1991; 266: 18217–18223.
- Chapman J, Ben-Israel J, Goldhammer Y, Korczyn AD. The risk of developing Creutzfeldt-Jakob disease in subjects with the PRNP gene codon 200 point mutation. *Neurology* 1994; 44: 1683–1686.
- Chapuis J, Moudjou M, Reine F, Herzog L, Jaumain E, Chapuis C, et al. Emergence of two prion subtypes in ovine PrP transgenic mice infected with human MM2-cortical Creutzfeldt-Jakob disease prions. *Acta Neuropathol Commun* 2016; 4: 10.
- Chasseigneaux S, Haik S, Laffont-Proust I, De Marco O, Lenne M, Brandel J-P, et al. V180I mutation of the prion protein gene associated with atypical PrP^{Sc} glycosylation. *Neurosci Lett* 2006; 408: 165–169.
- Chen SG, Parchi P, Brown P, Capellari S, Zou W, Cochran EJ, et al. Allelic origin of the abnormal prion protein isoform in familial prion diseases. *Nat Med* 1997; 3: 1009–1015.

References

- Chesebro B, Race B, Meade-White K, Lacasse R, Race R, Klingeborn M, et al. Fatal transmissible amyloid encephalopathy: a new type of prion disease associated with lack of prion protein membrane anchoring. *PLoS Pathog* 2010; 6: e1000800.
- Chesebro B, Trifilo M, Race R, Meade-White K, Teng C, LaCasse R, et al. Anchorless prion protein results in infectious amyloid disease without clinical scrapie. *Science* 2005; 308: 1435–1439.
- Choi YP, Gröner A, Ironside JW, Head MW. Comparison of the level, distribution and form of disease-associated prion protein in variant and sporadic Creutzfeldt-Jakob diseased brain using conformation-dependent immunoassay and Western blot. *J Gen Virol* 2011; 92: 727–732.
- Collinge J, Palmer MS, Sidle KC, Gowland I, Medori R, Ironside J, et al. Transmission of fatal familial insomnia to laboratory animals. *Lancet* 1995; 346: 569–570.
- Collins SJ, Sanchez-Juan P, Masters CL, Klug GM, van Duijn C, Pologgi A, et al. Determinants of diagnostic investigation sensitivities across the clinical spectrum of sporadic Creutzfeldt-Jakob disease. *Brain* 2006; 129: 2278–2287.
- Colombo R. Age and origin of the PRNP E200K mutation causing familial Creutzfeldt-Jacob disease in Libyan Jews. *Am J Hum Genet* 2000; 67: 528–531.
- Concha-Marambio L, Pritzkow S, Moda F, Tagliavini F, Ironside JW, Schulz PE, et al. Detection of prions in blood from patients with variant Creutzfeldt-Jakob disease. *Sci Transl Med* 2016; 8: 370ra183.
- Cramm M, Schmitz M, Karch A, Zafar S, Varges D, Mitrova E, et al. Characteristic CSF prion seeding efficiency in humans with prion diseases. *Mol Neurobiol* 2015; 51: 396–405.
- Croes EA, Theuns J, Houwing-Duistermaat JJ, Dermaut B, Slegers K, Roks G, et al. Octapeptide repeat insertions in the prion protein gene and early onset dementia. *J Neurol Neurosurg Psychiatry* 2004; 75: 1166–1170.
- D'Alessandro M, Petraroli R, Ladogana A, Pocchiari M. High incidence of Creutzfeldt-Jakob disease in rural Calabria, Italy. *Lancet* 1998; 352: 1989–1990.
- Deiningner MH, Bekure-Nemariam K, Trautmann K, Morgalla M, Meyermann R, Schluessener HJ. Cyclooxygenase-1 and -2 in brains of patients who died with sporadic Creutzfeldt-Jakob disease. *J Mol Neurosci* 2003; 20: 25–30.
- Douglas PM, Treusch S, Ren H-Y, Halfmann R, Duennwald ML, Lindquist S, et al. Chaperone-dependent amyloid assembly protects cells from prion toxicity. *Proc Natl Acad Sci USA* 2008; 105: 7206–7211.
- Esiri MM, Gordon WI, Collinge J, Patten JS. Peripheral neuropathy in Creutzfeldt-Jakob disease. *Neurology* 1997; 48: 784.
- Favereaux A, Quadrio I, Vital C, Perret-Liaudet A, Anne O, Laplanche J-L, et al. Pathologic prion protein spreading in the peripheral nervous system of a patient with sporadic Creutzfeldt-Jakob disease. *Arch Neurol* 2004; 61: 747–750.
- Feketeová E, Jarčušková D, Janáková A, Rozprávková E, Cifráková Z, Farkašová-Inaccione S, et al. Creutzfeldt-Jakob disease surveillance in Eastern Slovakia from 2004 to 2016. *Cent Eur J Public Health* 2018; 26 Suppl: S37–S41.
- Ferrer I, Armstrong J, Capellari S, Parchi P, Arzberger T, Bell J, et al. Effects of formalin fixation, paraffin embedding, and time of storage on DNA preservation in brain tissue: a BrainNet Europe study. *Brain Pathol* 2007; 17: 297–303.
- Foutz A, Appleby BS, Hamlin C, Liu X, Yang S, Cohen Y, et al. Diagnostic and prognostic value of human prion detection in cerebrospinal fluid. *Ann Neurol* 2017; 81: 79–92.
- Franceschini A, Baiardi S, Hughson AG, McKenzie N, Moda F, Rossi M, et al. High diagnostic value of second generation CSF RT-QuIC across the wide spectrum of CJD prions. *Sci Rep* 2017; 7: 10655.
- Franceschini A, Strammiello R, Capellari S, Giese A, Parchi P. Regional pattern of microgliosis in sporadic Creutzfeldt-Jakob disease in relation to phenotypic variants and disease progression. *Neuropathol Appl Neurobiol* 2018; 44: 574–589.

References

- Franz M, Eiden M, Balkema-Buschmann A, Greenlee J, Schatzl H, Fast C, et al. Detection of PrP(Sc) in peripheral tissues of clinically affected cattle after oral challenge with bovine spongiform encephalopathy. *J Gen Virol* 2012; 93: 2740–2748.
- Friedman-Levi Y, Meiner Z, Canello T, Frid K, Kovacs GG, Budka H, et al. Fatal prion disease in a mouse model of genetic E200K Creutzfeldt-Jakob disease. *PLoS Pathog* 2011; 7: e1002350.
- Gill AC, Castle AR. The cellular and pathologic prion protein. *Handb Clin Neurol* 2018; 153: 21–44.
- Glatzel M, Abela E, Maissen M, Aguzzi A. Extraneural pathologic prion protein in sporadic Creutzfeldt-Jakob disease. *N Engl J Med* 2003; 349: 1812–1820.
- Goldfarb LG, Brown P, Haltia M, Cathala F, McCombie WR, Kovanen J, et al. Creutzfeldt-Jakob disease cosegregates with the codon 178Asn PRNP mutation in families of European origin. *Ann Neurol* 1992; 31: 274–281.
- Goldfarb LG, Brown P, McCombie WR, Goldgaber D, Swergold GD, Wills PR, et al. Transmissible familial Creutzfeldt-Jakob disease associated with five, seven, and eight extra octapeptide coding repeats in the PRNP gene. *Proc Natl Acad Sci USA* 1991; 88: 10926–10930.
- Goldfarb LG, Petersen RB, Tabaton M, Brown P, LeBlanc AC, Montagna P, et al. Fatal familial insomnia and familial Creutzfeldt-Jakob disease: disease phenotype determined by a DNA polymorphism. *Science* 1992; 258: 806–808.
- Goldgaber D, Goldfarb LG, Brown P, Asher DM, Brown WT, Lin S, et al. Mutations in familial Creutzfeldt-Jakob disease and Gerstmann-Sträussler-Scheinker's syndrome. *Exp Neurol* 1989; 106: 204–206.
- Grasbon-Frodl E, Lorenz H, Mann U, Nitsch RM, Windl O, Kretzschmar HA. Loss of glycosylation associated with the T183A mutation in human prion disease. *Acta Neuropathol* 2004; 108: 476–484.
- Groschup MH, Beekes M, McBride PA, Hardt M, Hainfellner JA, Budka H. Deposition of disease-associated prion protein involves the peripheral nervous system in experimental scrapie. *Acta Neuropathol* 1999; 98: 453–457.
- Groschup MH, Weiland F, Straub OC, Pfaff E. Detection of scrapie agent in the peripheral nervous system of a diseased sheep. *Neurobiol Dis* 1996; 3: 191–195.
- Guiroy DC, Shankar SK, Gibbs CJ, Messenheimer JA, Das S, Gajdusek DC. Neuronal degeneration and neurofilament accumulation in the trigeminal ganglia in Creutzfeldt-Jakob disease. *Ann Neurol* 1989; 25: 102–106.
- Hainfellner JA, Budka H. Disease associated prion protein may deposit in the peripheral nervous system in human transmissible spongiform encephalopathies. *Acta Neuropathol* 1999; 98: 458–460.
- Head MW, Ritchie D, Smith N, McLoughlin V, Nailon W, Samad S, et al. Peripheral tissue involvement in sporadic, iatrogenic, and variant Creutzfeldt-Jakob disease: an immunohistochemical, quantitative, and biochemical study. *Am J Pathol* 2004; 164: 143–153.
- Horiuchi M, Caughey B. Prion protein interconversions and the transmissible spongiform encephalopathies. *Structure* 1999; 7: R231-240.
- Houston F, Andréoletti O. Animal prion diseases: the risks to human health. *Brain Pathol* 2019; 29: 248–262.
- Ishida C, Okino S, Kitamoto T, Yamada M. Involvement of the peripheral nervous system in human prion diseases including dural graft associated Creutzfeldt-Jakob disease. *J Neurol Neurosurg Psychiatry* 2005; 76: 325–329.
- Jaumain E, Quadrio I, Herzog L, Reine F, Rezaei H, Andréoletti O, et al. Absence of Evidence for a Causal Link between Bovine Spongiform Encephalopathy Strain Variant L-BSE and Known Forms of Sporadic Creutzfeldt-Jakob Disease in Human PrP Transgenic Mice. *J Virol* 2016; 90: 10867–10874.
- Jeong B-H, Kim Y-S. Genetic studies in human prion diseases. *J Korean Med Sci* 2014; 29: 623–632.
- Jones M, Peden AH, Prowse CV, Gröner A, Manson JC, Turner ML, et al. In vitro amplification and detection of variant Creutzfeldt-Jakob disease PrPSc. *J Pathol* 2007; 213: 21–26.

References

- Kimberlin RH, Hall SM, Walker CA. Pathogenesis of mouse scrapie. Evidence for direct neural spread of infection to the CNS after injection of sciatic nerve. *J Neurol Sci* 1983; 61: 315–325.
- Kobayashi A, Asano M, Mohri S, Kitamoto T. Cross-sequence transmission of sporadic Creutzfeldt-Jakob disease creates a new prion strain. *J Biol Chem* 2007; 282: 30022–30028.
- Kobayashi A, Iwasaki Y, Otsuka H, Yamada M, Yoshida M, Matsuura Y, et al. Deciphering the pathogenesis of sporadic Creutzfeldt-Jakob disease with codon 129 M/V and type 2 abnormal prion protein. *Acta Neuropathol Commun* 2013; 1: 74.
- Kobayashi A, Sakuma N, Matsuura Y, Mohri S, Aguzzi A, Kitamoto T. Experimental verification of a traceback phenomenon in prion infection. *J Virol* 2010; 84: 3230–3238.
- Korth C, Kaneko K, Groth D, Heye N, Telling G, Mastrianni J, et al. Abbreviated incubation times for human prions in mice expressing a chimeric mouse-human prion protein transgene. *Proc Natl Acad Sci USA* 2003; 100: 4784–4789.
- Kovács GG, Puopolo M, Ladogana A, Pocchiari M, Budka H, van Duijn C, et al. Genetic prion disease: the EURO-CJD experience. *Hum Genet* 2005; 118: 166–174.
- Kovács T, Arányi Z, Szirmai I, Lantos PL. Creutzfeldt-Jakob disease with amyotrophy and demyelinating polyneuropathy. *Arch Neurol* 2002; 59: 1811–1814.
- Küffer A, Lakkaraju AKK, Mogha A, Petersen SC, Airich K, Doucerain C, et al. The prion protein is an agonistic ligand of the G protein-coupled receptor Adgrg6. *Nature* 2016; 536: 464–468.
- Ladogana A, Kovacs GG. Genetic Creutzfeldt-Jakob disease. *Handb Clin Neurol* 2018; 153: 219–242.
- Ladogana A, Puopolo M, Croes EA, Budka H, Jarius C, Collins S, et al. Mortality from Creutzfeldt-Jakob disease and related disorders in Europe, Australia, and Canada. *Neurology* 2005; 64: 1586–1591.
- Ladogana A, Puopolo M, Poggi A, Almonti S, Mellina V, Equestre M, et al. High incidence of genetic human transmissible spongiform encephalopathies in Italy. *Neurology* 2005; 64: 1592–1597.
- Laplanche JL, Delasnerie-Lauprêtre N, Brandel JP, Chatelain J, Beaudry P, Alperovitch A, et al. Molecular genetics of prion diseases in France. French Research Group on Epidemiology of Human Spongiform Encephalopathies. *Neurology* 1994; 44: 2347–2351.
- Lattanzio F, Abu-Rumeileh S, Franceschini A, Kai H, Amore G, Poggiolini I, et al. Prion-specific and surrogate CSF biomarkers in Creutzfeldt-Jakob disease: diagnostic accuracy in relation to molecular subtypes and analysis of neuropathological correlates of p-tau and A β 42 levels. *Acta Neuropathol* 2017; 133: 559–578.
- Le NTT, Wu B, Harris DA. Prion neurotoxicity. *Brain Pathol* 2019; 29: 263–277.
- Lee AM, Paulsson JF, Cruite J, Andaya AA, Trifilo MJ, Oldstone MBA. Extraneural manifestations of prion infection in GPI-anchorless transgenic mice. *Virology* 2011; 411: 1–8.
- Lee C-CM, Kuo LT, Wang CH, Scaravilli F, An SF. Accumulation of prion protein in the peripheral nervous system in human prion diseases. *J Neuropathol Exp Neurol* 2005; 64: 716–721.
- Lee HS, Sambuughin N, Cervenakova L, Chapman J, Pocchiari M, Litvak S, et al. Ancestral origins and worldwide distribution of the PRNP 200K mutation causing familial Creutzfeldt-Jakob disease. *Am J Hum Genet* 1999; 64: 1063–1070.
- Llorens F, López-González I, Thüne K, Carmona M, Zafar S, Andréoletti O, et al. Subtype and regional-specific neuroinflammation in sporadic creutzfeldt-jakob disease. *Front Aging Neurosci* 2014; 6: 198.
- Lloyd SE, Mead S, Collinge J. Genetics of prion diseases. *Curr Opin Genet Dev* 2013; 23: 345–351.
- Macleod M-A, Stewart GE, Zeidler M, Will R, Knight R. Sensory features of variant Creutzfeldt-Jakob disease. *J Neurol* 2002; 249: 706–711.

References

- Mallucci G, Dickinson A, Linehan J, Klöhn P-C, Brandner S, Collinge J. Depleting neuronal PrP in prion infection prevents disease and reverses spongiosis. *Science* 2003; 302: 871–874.
- Mastrianni JA, Nixon R, Layzer R, Telling GC, Han D, DeArmond SJ, et al. Prion protein conformation in a patient with sporadic fatal insomnia. *N Engl J Med* 1999; 340: 1630–1638.
- Masujin K, Matthews D, Wells GAH, Mohri S, Yokoyama T. Prions in the peripheral nerves of bovine spongiform encephalopathy-affected cattle. *J Gen Virol* 2007; 88: 1850–1858.
- McBride PA, Beekes M. Pathological PrP is abundant in sympathetic and sensory ganglia of hamsters fed with scrapie. *Neurosci Lett* 1999; 265: 135–138.
- McGuire LI, Peden AH, Orrú CD, Wilham JM, Appleford NE, Mallinson G, et al. Real time quaking-induced conversion analysis of cerebrospinal fluid in sporadic Creutzfeldt-Jakob disease. *Ann Neurol* 2012; 72: 278–285.
- McGuire LI, Poggioli A, Poggiolini I, Suardi S, Grznarova K, Shi S, et al. Cerebrospinal fluid real-time quaking-induced conversion is a robust and reliable test for sporadic creutzfeldt-jakob disease: An international study. *Ann Neurol* 2016; 80: 160–165.
- Mead S, Poulter M, Beck J, Webb TEF, Campbell TA, Linehan JM, et al. Inherited prion disease with six octapeptide repeat insertional mutation--molecular analysis of phenotypic heterogeneity. *Brain* 2006; 129: 2297–2317.
- Minikel EV, Vallabh SM, Lek M, Estrada K, Samocha KE, Sathirapongsasuti JF, et al. Quantifying prion disease penetrance using large population control cohorts. *Sci Transl Med* 2016; 8: 322ra9.
- Mitrová E, Belay G. Creutzfeldt-Jakob disease with E200K mutation in Slovakia: characterization and development. *Acta Virol* 2002; 46: 31–39.
- Moda F, Suardi S, Di Fede G, Indaco A, Limido L, Vimercati C, et al. MM2-thalamic Creutzfeldt-Jakob disease: neuropathological, biochemical and transmission studies identify a distinctive prion strain. *Brain Pathol* 2012; 22: 662–669.
- Montine TJ, Phelps CH, Beach TG, Bigio EH, Cairns NJ, Dickson DW, et al. National Institute on Aging-Alzheimer's Association guidelines for the neuropathologic assessment of Alzheimer's disease: a practical approach. *Acta Neuropathol* 2012; 123: 1–11.
- Morales R. Prion strains in mammals: Different conformations leading to disease. *PLoS Pathog* 2017; 13: e1006323.
- Nitrini R, Rosemberg S, Passos-Bueno MR, da Silva LS, Iughetti P, Papadopoulos M, et al. Familial spongiform encephalopathy associated with a novel prion protein gene mutation. *Ann Neurol* 1997; 42: 138–146.
- Nonno R, Di Bari MA, Cardone F, Vaccari G, Fazzi P, Dell'Omo G, et al. Efficient transmission and characterization of Creutzfeldt-Jakob disease strains in bank voles. *PLoS Pathog* 2006; 2: e12.
- Notari S, Xiao X, Espinosa JC, Cohen Y, Qing L, Aguilar-Calvo P, et al. Transmission characteristics of variably protease-sensitive prionopathy. *Emerging Infect Dis* 2014; 20: 2006–2014.
- Ong CJ, Al-Lozi M, Cimino PJ, Bucelli R. Peripheral nervous system hyperexcitability in VV2 sporadic Creutzfeldt-Jakob disease. *Neurol Clin Pract* 2015; 5: 326–332.
- Orrú CD, Bongiani M, Tonoli G, Ferrari S, Hughson AG, Groveman BR, et al. A test for Creutzfeldt-Jakob disease using nasal brushings. *N Engl J Med* 2014; 371: 519–529.
- Orrú CD, Wilham JM, Hughson AG, Raymond LD, McNally KL, Bossers A, et al. Human variant Creutzfeldt-Jakob disease and sheep scrapie PrP(res) detection using seeded conversion of recombinant prion protein. *Protein Eng Des Sel* 2009; 22: 515–521.
- Orrú CD, Yuan J, Appleby BS, Li B, Li Y, Winner D, et al. Prion seeding activity and infectivity in skin samples from patients with sporadic Creutzfeldt-Jakob disease. *Sci Transl Med* 2017; 9

References

- Owen F, Poulter M, Lofthouse R, Collinge J, Crow TJ, Risby D, et al. Insertion in prion protein gene in familial Creutzfeldt-Jakob disease. *Lancet* 1989; 1: 51–52.
- Palmer MS, Dryden AJ, Hughes JT, Collinge J. Homozygous prion protein genotype predisposes to sporadic Creutzfeldt-Jakob disease. *Nature* 1991; 352: 340–342.
- Parchi P, de Boni L, Saverioni D, Cohen ML, Ferrer I, Gambetti P, et al. Consensus classification of human prion disease histotypes allows reliable identification of molecular subtypes: an inter-rater study among surveillance centres in Europe and USA. *Acta Neuropathol* 2012; 124: 517–529.
- Parchi P, Capellari S, Chen SG, Petersen RB, Gambetti P, Kopp N, et al. Typing prion isoforms. *Nature* 1997; 386: 232–234.
- Parchi P, Cescatti M, Notari S, Schulz-Schaeffer WJ, Capellari S, Giese A, et al. Agent strain variation in human prion disease: insights from a molecular and pathological review of the National Institutes of Health series of experimentally transmitted disease. *Brain* 2010; 133: 3030–3042.
- Parchi P, Giese A, Capellari S, Brown P, Schulz-Schaeffer W, Windl O, et al. Classification of sporadic Creutzfeldt-Jakob disease based on molecular and phenotypic analysis of 300 subjects. *Ann Neurol* 1999; 46: 224–233.
- Parchi P, Notari S, Weber P, Schimmel H, Budka H, Ferrer I, et al. Inter-laboratory assessment of PrPSc typing in creutzfeldt-jakob disease: a Western blot study within the NeuroPrion Consortium. *Brain Pathol* 2009; 19: 384–391.
- Parchi P, Petersen RB, Chen SG, Autilio-Gambetti L, Capellari S, Monari L, et al. Molecular pathology of fatal familial insomnia. *Brain Pathol* 1998; 8: 539–548.
- Parchi P, Strammiello R, Giese A, Kretzschmar H. Phenotypic variability of sporadic human prion disease and its molecular basis: past, present, and future. *Acta Neuropathol* 2011; 121: 91–112.
- Parchi P, Strammiello R, Notari S, Giese A, Langeveld JPM, Ladogana A, et al. Incidence and spectrum of sporadic Creutzfeldt-Jakob disease variants with mixed phenotype and co-occurrence of PrPSc types: an updated classification. *Acta Neuropathol* 2009; 118: 659–671.
- Parchi P, Zou W, Wang W, Brown P, Capellari S, Ghetti B, et al. Genetic influence on the structural variations of the abnormal prion protein. *Proc Natl Acad Sci USA* 2000; 97: 10168–10172.
- Peden AH, Ritchie DL, Head MW, Ironside JW. Detection and localization of PrPSc in the skeletal muscle of patients with variant, iatrogenic, and sporadic forms of Creutzfeldt-Jakob disease. *Am J Pathol* 2006; 168: 927–935.
- Peggion C, Bertoli A, Sorgato MC. Almost a century of prion protein(s): From pathology to physiology, and back to pathology. *Biochem Biophys Res Commun* 2017; 483: 1148–1155.
- Poggiolini I, Saverioni D, Parchi P. Prion protein misfolding, strains, and neurotoxicity: an update from studies on Mammalian prions. *Int J Cell Biol* 2013; 2013: 910314.
- Prusiner SB. Prions. *Proc Natl Acad Sci USA* 1998; 95: 13363–13383.
- Rangel A, Race B, Klingeborn M, Striebel J, Chesebro B. Unusual cerebral vascular prion protein amyloid distribution in scrapie-infected transgenic mice expressing anchorless prion protein. *Acta Neuropathol Commun* 2013; 1: 25.
- Rangel A, Race B, Striebel J, Chesebro B. Non-amyloid and amyloid prion protein deposits in prion-infected mice differ in blockage of interstitial brain fluid. *Neuropathol Appl Neurobiol* 2013; 39: 217–230.
- Rodríguez-Martínez AB, Barreau C, Coupry I, Yagüe J, Sánchez-Valle R, Galdós-Alcelay L, et al. Ancestral origins of the prion protein gene D178N mutation in the Basque Country. *Hum Genet* 2005; 117: 61–69.
- Rossi M, Baiardi S, Parchi P. Understanding Prion Strains: Evidence from Studies of the Disease Forms Affecting Humans. *Viruses* 2019; 11

References

- Rossi M, Kai H, Baiardi S, Bartoletti-Stella A, Carlà B, Zenesini C, et al. The characterization of AD/PART co-pathology in CJD suggests independent pathogenic mechanisms and no cross-seeding between misfolded A β and prion proteins. *Acta Neuropathol Commun* 2019; 7: 53.
- Rossi M, Saverioni D, Di Bari M, Baiardi S, Lemstra AW, Pirisinu L, et al. Atypical Creutzfeldt-Jakob disease with PrP-amyloid plaques in white matter: molecular characterization and transmission to bank voles show the M1 strain signature. *Acta Neuropathol Commun* 2017; 5: 87.
- Rudge P, Hyare H, Green A, Collinge J, Mead S. Imaging and CSF analyses effectively distinguish CJD from its mimics. *J Neurol Neurosurg Psychiatry* 2018; 89: 461–466.
- Safar J, Roller PP, Gajdusek DC, Gibbs CJ. Conformational transitions, dissociation, and unfolding of scrapie amyloid (prion) protein. *J Biol Chem* 1993; 268: 20276–20284.
- Safar JG, Geschwind MD, Deering C, Didorenko S, Sattavat M, Sanchez H, et al. Diagnosis of human prion disease. *Proc Natl Acad Sci USA* 2005; 102: 3501–3506.
- Salvatore M, Genuardi M, Petraroli R, Masullo C, D'Alessandro M, Pocchiari M. Polymorphisms of the prion protein gene in Italian patients with Creutzfeldt-Jakob disease. *Hum Genet* 1994; 94: 375–379.
- Samman I, Schulz-Schaeffer WJ, Wöhrl JC, Sommer A, Kretschmar HA, Hennerici M. Clinical range and MRI in Creutzfeldt-Jakob disease with heterozygosity at codon 129 and prion protein type 2. *J Neurol Neurosurg Psychiatry* 1999; 67: 678–681.
- Saverioni D, Notari S, Capellari S, Poggiolini I, Giese A, Kretschmar HA, et al. Analyses of protease resistance and aggregation state of abnormal prion protein across the spectrum of human prions. *J Biol Chem* 2013; 288: 27972–27985.
- Scheckel C, Aguzzi A. Prions, prionoids and protein misfolding disorders. *Nat Rev Genet* 2018; 19: 405–418.
- Scholz G, Kretschmar HA, Zerr I. Clinical aspects of common genetic Creutzfeldt-Jakob disease. *Eur J Epidemiol* 2012; 27: 147–149.
- Simoneau S, Rezaei H, Salès N, Kaiser-Schulz G, Lefebvre-Roque M, Vidal C, et al. In vitro and in vivo neurotoxicity of prion protein oligomers. *PLoS Pathog* 2007; 3: e125.
- Soto C, Anderes L, Suardi S, Cardone F, Castilla J, Frossard M-J, et al. Pre-symptomatic detection of prions by cyclic amplification of protein misfolding. *FEBS Lett* 2005; 579: 638–642.
- Stöhr J, Watts JC, Legname G, Oehler A, Lemus A, Nguyen H-OB, et al. Spontaneous generation of anchorless prions in transgenic mice. *Proc Natl Acad Sci USA* 2011; 108: 21223–21228.
- Tateishi J, Brown P, Kitamoto T, Hoque ZM, Roos R, Wollman R, et al. First experimental transmission of fatal familial insomnia. *Nature* 1995; 376: 434–435.
- Telling GC, Parchi P, DeArmond SJ, Cortelli P, Montagna P, Gabizon R, et al. Evidence for the conformation of the pathologic isoform of the prion protein enciphering and propagating prion diversity. *Science* 1996; 274: 2079–2082.
- Thal DR, Rüb U, Orantes M, Braak H. Phases of A beta-deposition in the human brain and its relevance for the development of AD. *Neurology* 2002; 58: 1791–1800.
- Tiple D, Poleggi A, Mellina V, Morocutti A, Brusa L, Iani C, et al. Clinicopathological features of the rare form of Creutzfeldt-Jakob disease in R208H-V129V PRNP carrier. *Acta Neuropathol Commun* 2019; 7: 47.
- Trifilo MJ, Yajima T, Gu Y, Dalton N, Peterson KL, Race RE, et al. Prion-induced amyloid heart disease with high blood infectivity in transgenic mice. *Science* 2006; 313: 94–97.
- Walker LC, Jucker M. Neurodegenerative diseases: expanding the prion concept. *Annu Rev Neurosci* 2015; 38: 87–103.

References

- Watts JC, Bourkas MEC, Arshad H. The function of the cellular prion protein in health and disease. *Acta Neuropathol* 2018; 135: 159–178.
- Watts JC, Giles K, Serban A, Patel S, Oehler A, Bhardwaj S, et al. Modulation of Creutzfeldt-Jakob disease prion propagation by the A224V mutation. *Ann Neurol* 2015; 78: 540–553.
- Windl O, Dempster M, Estibeiro JP, Lathe R, de Silva R, Esmonde T, et al. Genetic basis of Creutzfeldt-Jakob disease in the United Kingdom: a systematic analysis of predisposing mutations and allelic variation in the PRNP gene. *Hum Genet* 1996; 98: 259–264.
- Wopfner F, Weidenhöfer G, Schneider R, von Brunn A, Gilch S, Schwarz TF, et al. Analysis of 27 mammalian and 9 avian PrPs reveals high conservation of flexible regions of the prion protein. *J Mol Biol* 1999; 289: 1163–1178.
- Worrall BB, Rowland LP, Chin SS, Mastrianni JA. Amyotrophy in prion diseases. *Arch Neurol* 2000; 57: 33–38.
- Wulf M-A, Senatore A, Aguzzi A. The biological function of the cellular prion protein: an update. *BMC Biol* 2017; 15: 34.
- Yokoyama T, Takeuchi A, Yamamoto M, Kitamoto T, Ironside JW, Morita M. Heparin enhances the cell-protein misfolding cyclic amplification efficiency of variant Creutzfeldt-Jakob disease. *Neurosci Lett* 2011; 498: 119–123.
- Zeidler M, Stewart GE, Barraclough CR, Bateman DE, Bates D, Burn DJ, et al. New variant Creutzfeldt-Jakob disease: neurological features and diagnostic tests. *Lancet* 1997; 350: 903–907.
- Zéphir H, Stojkovic T, de Seze J, Muraige C-A, Peoc'h K, Haïk S, et al. Severe and rapidly evolving peripheral neuropathy revealing sporadic Creutzfeldt-Jakob disease. *J Neurol* 2009; 256: 134–136.
- Zerr I, Kallenberg K, Summers DM, Romero C, Taratuto A, Heinemann U, et al. Updated clinical diagnostic criteria for sporadic Creutzfeldt-Jakob disease. *Brain* 2009; 132: 2659–2668.
- Zerr I, Parchi P. Sporadic Creutzfeldt-Jakob disease. *Handb Clin Neurol* 2018; 153: 155–174.
- WHO | WHO infection control guidelines for transmissible spongiform encephalopathies. Report of a WHO consultation, Geneva, Switzerland, 23-26 March 1999 [Internet]. WHO[cited 2019 Jun 16] Available from: https://www.who.int/csr/resources/publications/bse/WHO_CDS_CSR_APH_2000_3/en/